การส่งเสริมเชิงเคมีไฟฟ้าของโพรเพนออกซิเดชันบนตัวเร่งปฏิกิริยาแพลเลเดียม อิริเดียม รูเทเนียม และคอปเปอร์ และการดัดแปรตัวเร่งปฏิกิริยาเคมีไฟฟ้าแพลเลเดียมด้วยแมงกานีสออกไซด์ เพื่อปรับปรุงการส่งเสริมเชิงเคมีไฟฟ้า

นางสาวศรันยา เพ็งอ้น

วิทยานิพนธ์นี้เป็นส่วนหนึ่งของการศึกษาตามหลักสูตรปริญญาวิศวกรรมศาสตรดุษฎีบัณฑิต
สาขาวิชาวิศวกรรมเคมี ภาควิชาวิศวกรรมเคมี
คณะวิศวกรรมศาสตร์ จุฬาลงกรณ์มหาวิทยาลัย
ปีการศึกษา 2555
ลิขสิทธิ์ของจุฬาลงกรณ์มหาวิทยาลัย

ELECTROPROMOTED PROPANE OXIDATION ON SPUTTER-DEPOSITED Pd, Ir, Ru, AND Cu CATALYST-ELECTRODES ON YSZ AND MODIFICATION OF Pd CATALYST WITH Mn_xO_y INTERLAYER FOR FURTHER IMPROVEMENT

Miss Saranya Peng-ont

A Dissertation Submitted in Partial Fulfillment of the Requirements
for the Degree of Doctor of Engineering Program in Chemical Engineering
Department of Chemical Engineering
Faculty of Engineering
Chulalongkorn University
Academic Year 2012

Thesis Title	ELECTROPROMOTED PROPANE OXIDATION ON SPUTTER-DEPOSITED Pd, Ir, Ru, AND Cu CATALYST-ELECTRODES ON YSZ AND MODIFICATION OF Pd CATALYST WITH Mn_xO_y INTERLAYER FOR FURTHER IMPROVEMENT
By	Miss Saranya Peng-ont
Field of Study	Chemical Engineering
Thesis Advisor	Professor Piyasan Praserthdam Dr.Ing.
Thesis Co-advisor	Professor Suttichai Assabumrungrat, Ph.D. Professor Constantinos G. Vayenas, Ph.D.

Accepted by the Faculty of Engineering, Chulalongkorn University in Partial Fulfillment of the Requirements for the Doctoral Degree

.....Dean of the Faculty of Engineering
(Associate Professor Boonsom Lerdhirunwong, Dr.Ing.)

THESIS COMMITTEE

.....Chairman
(Associate Professor Bunjerd Jongsomjit, Ph.D.)

.....Thesis Advisor
(Professor Piyasan Praserthdam, Dr.Ing.)

.....Thesis Co-advisor
(Professor Suttichai Assabumrungrat, Ph.D.)

.....Thesis Co-advisor
(Professor Constantinos G. Vayenas, Ph.D.)

.....Examiner
(Associate Professor Joongjai Panpranot, Ph.D.)

.....Examiner
(Parichatr Vanalabhpatana, Ph.D.)

.....External Examiner
(Peangpit Wongmaneenil, D.Eng.)

ศรันยา เพ็งอ้น : การส่งเสริมเชิงเคมีไฟฟ้าของโพรเพนออกซิเดชันบนตัวเร่งปฏิกิริยาแพลเลเดียม อิริเดียม รูเทเนียม และคอปเปอร์ และการดัดแปรตัวเร่งปฏิกิริยาเคมีไฟฟ้าแพลเลเดียมด้วยแมงกานีสออกไซด์เพื่อปรับปรุงการส่งเสริมเชิงเคมีไฟฟ้า (ELECTROPROMOTED PROPANE OXIDATION ON SPUTTER-DEPOSITED Pd, Ir, Ru, AND Cu CATALYST-ELECTRODES ON YSZ AND MODIFICATION OF Pd CATALYST WITH Mn_xO_y INTERLAYER FOR FURTHER IMPROVEMENT) อ.ที่ปรึกษาวิทยานิพนธ์หลัก: ศ.ดร.ปิยะสาร ประเสริฐธรรม, อ.ที่ปรึกษาวิทยานิพนธ์ร่วม: ศ.ดร.สุทธิชัย อัสสะบำรุงรัตน์, PROF. CONSTANTINOS G. VAYENAS, 132 หน้า.

งานวิจัยนี้ได้ศึกษาการส่งเสริมเชิงเคมีไฟฟ้าของเอทิลีนและโพรเพนออกซิเดชัน โดยมีการเปรียบเทียบตัวเร่งปฏิกิริยาที่แตกต่างกัน ในกรณีของการส่งเสริมเชิงเคมีไฟฟ้าของเอทิลีนด้วยตัวเร่งปฏิกิริยาแพลทินัมบนวายเอสแซด เป็นครั้งแรกที่มีการค้นพบการเกิดปฏิกิริยาสามแบบจากทั้งหมดสี่แบบ ประกอบด้วยอิเล็กโทรโฟบิค อิเล็กโทรฟิลลิค และ โวลเคโน ที่มาจากปฏิกิริยาเดียวเท่านั้น ซึ่งการเกิดปฏิกิริยานี้ขึ้นอยู่กับภาวะที่ทำการทดลอง คืออุณหภูมิและความเข้มข้นของแก๊ส จากการศึกษาพบว่าภายใต้ภาวะที่มีออกซิเจนมากเกินพอ ปฏิกิริยาที่เกิดขึ้นนั้นจะเป็นแบบอิเล็กโทรโฟบิคซึ่งก็คืออัตราการเกิดปฏิกิริยาจะเพิ่มมากขึ้นเมื่อมีการให้ศักย์ไฟฟ้าที่เป็นบวก ในขณะที่ปฏิกิริยาจะเปลี่ยนไปเป็นแบบอิเล็กโทรฟิลลิค คืออัตราการเกิดปฏิกิริยาจะเพิ่มมากขึ้นเมื่อมีการให้ศักย์ไฟฟ้าที่เป็นลบ เมื่อภาวะความเข้มข้นของแก๊สที่ป้อนเปลี่ยนไป เข้าใกล้กับสัดส่วนที่เหมาะสมที่ทำให้เกิดการเผาไหม้ที่สมบูรณ์ ในส่วนของตัวเร่งปฏิกิริยาแพลเลเดียม อิริเดียม รูเทเนียม และคอปเปอร์ ได้ทำการศึกษาในปฏิกิริยาโพรเพนออกซิเดชัน ภายใต้ภาวะการเผาไหม้ที่มีออกซิเจนเกินพอ โดยอุณหภูมิที่ทำการบันทึกข้อมูลอยู่ในช่วง 250-450 องศาเซลเซียส ณ ความดันบรรยากาศ โดยพบว่าตัวเร่งปฏิกิริยาทั้งหมดนี้ เกิดปฏิกิริยาแบบอิเล็กโทรโฟบิคซึ่งก็คือการที่อัตราการเกิดปฏิกิริยาเพิ่มมากขึ้น เมื่อมีการให้ศักย์ไฟฟ้าที่เป็นบวก และยังพบอีกว่าอัตราการเกิดปฏิกิริยาลดลงเล็กน้อย เมื่อมีการให้ค่าศักย์ไฟฟ้ามีค่าเป็นลบ สำหรับโพรเพนออกซิเดชันนั้น ค่าโรหรือการเพิ่มขึ้นของอัตราการเกิดปฏิกิริยาในระบบปิด (มีการให้กระแสไฟฟ้าหรือศักย์ไฟฟ้า) เมื่อเทียบกับอัตราการเกิดปฏิกิริยาในระบบเปิด (ไม่มีการให้กระแสไฟฟ้าหรือศักย์ไฟฟ้า) พบว่ามีค่ามากที่สุดประมาณ 3 แต่อย่างไรก็ตามอัตราการเกิดปฏิกิริยาที่เปลี่ยนไป เทียบกับอัตราการเคลื่อนที่ของไอออน (กระแสต่อประจุไอออนคูณกับค่าคงที่ของฟาราเดย์) มีค่าสูงสุดถึงค่า 250 สำหรับตัวเร่งปฏิกิริยาแพลเลเดียม 125 สำหรับตัวเร่งปฏิกิริยาอิริเดียม และ 15 สำหรับตัวเร่งปฏิกิริยารูเทเนียมในฝั่งที่มีการให้ค่าศักย์ไฟฟ้าเป็นลบ แต่พบว่าตัวเร่งปฏิกิริยาเหล่านี้เสื่อมสภาพลงอย่างรวดเร็ว เนื่องจากขนาดของผลึกที่มีขนาดเพิ่มขึ้น ดังที่มีการวิเคราะห์โดยกล้องจุลทรรศน์อิเล็กตรอนแบบส่องกราดและเทคนิคการเลี้ยวเบนของรังสีเอ็กซ์ และจากการศึกษาพบว่าประสิทธิภาพของตัวเร่งปฏิกิริยาแพลเลเดียมที่มีแมงกานีสออกไซด์เป็นชั้นที่อยู่ระหว่างแพลเลเดียมและวายเอสแซดดีกว่าตัวเร่งปฏิกิริยาแพลเลเดียมเพียงอย่างเดียว ซึ่งยืนยันโดยการศึกษาด้านจลนพลศาสตร์ พบว่าอัตราการเกิดปฏิกิริยาสูงสุดนั้นเปลี่ยนไป ณ ความดันย่อยของออกซิเจนที่สูงขึ้น จากการศึกษาเปรียบเทียบโพรเพนออกซิเดชันของตัวเร่งปฏิกิริยาแพลเลเดียมและตัวเร่งปฏิกิริยาแพลเลเดียมร่วมกับแมงกานีสออกไซด์ พบว่าตัวเร่งปฏิกิริยาแพลเลเดียมสามารถผันกลับได้ โดยมีค่าอัตราการเกิดปฏิกิริยาที่เปลี่ยนไปเทียบกับอัตราการเคลื่อนที่ของไอออนเท่ากับ 1000 เท่า ในขณะที่ตัวเร่งปฏิกิริยาแพลเลเดียมร่วมกับแมงกานีสออกไซด์นั้นไม่เกิดการส่งเสริมเชิงเคมีไฟฟ้า

ภาควิชา	วิศวกรรมเคมี	ลายมือชื่อนิสิต	
สาขาวิชา	วิศวกรรมเคมี	ลายมือชื่อ อ.ที่ปรึกษาวิทยานิพนธ์หลัก	
ปีการศึกษา	2555	ลายมือชื่อ อ.ที่ปรึกษาวิทยานิพนธ์ร่วม	
		ลายมือชื่อ อ.ที่ปรึกษาวิทยานิพนธ์ร่วม	

5271828621 : MAJOR CHEMICAL ENGINEERING
KEYWORDS : ELECTROCHEMICAL PROMOTION / PROMOTION RULE / CATALYTIC KINETICS / ETHYLENE OXIDAITON / PROPANE OXIDATION / PASTED CATALYST-ELECTRODE / SPUTTERED CATALYST-ELECTRODE / YSZ

SARANYA PENG-ONT : ELECTROPROMOTED PROPANE OXIDATION ON SPUTTER-DEPOSITED Pd, Ir, Ru, AND Cu CATALYST-ELECTRODES ON YSZ AND MODIFICATION OF Pd CATALYST WITH Mn_xO_y INTERLAYER FOR FURTHER IMPROVEMENT. ADVISOR : PROF. PIYASAN PRASERTHDAM, Dr.Ing., CO-ADVISOR : PROF. SUTTICHAI ASSABUMRUNGRAT, Ph.D., PROF. CONSTANTINOS G. VAYENAS, Ph.D., 132 pp.

The electrochemical promotion of ethylene and propane oxidation has been investigated in comparison upon different catalyst-electrodes. Depending on experimental conditions (temperature and gas composition), in the case of the electrochemical promotion of C_2H_4 oxidation over Pt/YSZ, this is the first time to demonstrate three out of four promotion behaviours, i.e. here for electrophobic, electrophilic, and volcano types by the use of single catalytic reaction. It was found that under mildly oxidizing conditions the reaction exhibits an electrophobic behavior, i.e. rate increase by anodic polarization, while it shifts to electrophilic, i.e. rate increase by cathodic polarization, under near stoichiometric feed conditions. The different metal catalyst-electrodes, i.e. Pd, Ru, Ir, and Cu were tested on deep propane oxidation under lean burn condition and at temperature range of 250-450^{o}C. All of these catalyst-electrodes exhibit electrophobic behavior, where the rate increases during anodic polarization and slightly decreases with negative polarization. The increase in the catalytic rate, Δr, is reached to the maximum ρ values of 3, however, it is significantly higher than the rate of ion transport, *I/2F,* Λ, taking values up to 250 for Pd, 125 for Ir, and 15 for Ru catalyst-electrode under anodic polarization. Fast catalyst deactivation is observed due to increased particle size as observed by SEM and XRD. The better catalytic performance of Pd with Mn_xO_y in comparison on Pd deposited on YSZ is observed and confirmed by the kinetic studies exhibiting the shift of rate maximum at higher oxygen partial pressure. Propane oxidation can be reversibly enhanced by the Pd metallic phase via the application of current or potential up to 1000, whereas the interlayer of Mn_xO_y hinders the electrochemical promotion of propane oxidation in excess of oxygen.

Department :	Chemical Engineering	Student's Signature	
Field of Study :	Chemical Engineering	Advisor's Signature	
Academic Year :	2012	Co-advisor's Signature	
		Co-advisor's Signature	

ACKNOWLEDEGEMENTS

I would like to express my sincerest gratitude and deep appreciation to my advisor, Professor Piyasan Praserthdam and my co-advisor, Professor Suttichai Assabumrungrat for his valuable guidance, encouragement, supports and suggestion throughout the course of my research as well as life attitude in non-thesis field. Moreover, I would also be grateful to my another co-advisor Professor Constantinos G. Vayenas for his kind assistance, valuable advice, and encouragement as he allowed me to use his equipment to complete my experiments together with livelihood in non-thesis area in Greece for one year. Additionally, I am most deeply indebted to Dr. Susanne Brosda for her continuous support, plentiful ideas, and valuable discussion that we have sharing during this work together with her help and kind advise me relating to life in Greece in non-thesis part. I would also be grateful to Dr. Parichatr Vanalabhpatana for her useful suggestions and great support. Finally, I would be grateful to Associate Professor Bunjerd Jongsomjit as the chairman, Associate Professor Joongjai Panpranot and Dr. Peangpit Wongmaneenil as the members of my thesis committee.

I would like to acknowledge the Royal Golden Jubilee Ph.D. program under Thailand Research Fund and Chulalongkorn University for supporting and offering me to study abroad. I had earned so much great experience during one year in Greece.

I would like to give a special acknowledgement to my friends in Greece, especially Dr. Souentie Stamatios for his kindness particularly in discussion and solution for the problem during experimental. Moreover, I would like to thank the other members of the Department of Chemical Engineering, University of Patras, Greece for their kindly and friendly assistance. Finally, I would like to thank the member of Centre of Excellence on Catalysis and Catalytic Reaction Engineering, Department of Chemical Engineering, Chulalongkorn University for their supports.

Finally, I would like to thank my beloved family including mother, father, grandmother, and aunt, who generous supported and encouraged me though the time spent on this study. I can say that I could not achieve my degree on time without their encouragements.

CONTENTS

Page

ABSTRACT (THAI) iv
ABSTRACT (ENGLISH) v
ACKNOWLEDGEMENTS vi
CONTENTS vii
LIST OF TABLES x
LIST OF FIGURES xi
NOMENCLATURE xvii

CHAPTER

I INTRODUCTION 1
1.1 Inspiration 1
1.2 Objectives 3
1.3 Scopes of work 4
1.4 The structure of this dissertation 4
II THEORY 6
2.1 Non-Faradaic electrochemical modification of catalytic activity (NEMCA) or electrochemical promotion of catalysis (EPOC) 6
2.1.1 Fundamental principle 6
2.1.2 Solid electrolyte 11
2.1.3 Rules of chemical promotion 12
2.1.4 The basic experiment set up for ethylene and propane oxidation 17
2.1.5 Reactor configuration for electrochemical promotion experiment 18
2.1.6 Status of NEMCA in commercial system 19
2.2 Ethylene and propane oxidation 21
III LITERATURE REVIEWS 23
3.1 Hydrocarbon oxidation by conventional catalyst 23

CHAPTER page

3.2 Non-Faradaic electrochemical modification of catalytic activity (NEMCA) or electrochemical promotion of catalysis (EPOC) 25
3.2.1 Non-Faradaic electrochemical modification of catalytic activity (NEMCA) for hydrocarbon oxidation 25
3.2.2 The electrochemical promotion for other reactions 31
IV EXPERIMENTAL 35
4.1 Material and Catalyst preparation 35
4.1.1 Pasted catalyst-electrode preparation 35
4.1.2 Sputtered catalyst electrodes preparation 36
4.1.3 Mn_xO_y interlayer preparation 38
4.2 The catalytic activity measurement 38
4.3 Catalyst characterization 39
V RESULTS AND DISCUSSIONS 41
5.1 The electrochemical promotion of deep ethylene oxidation on Pt/YSZ catalyst deposited on yttria-stabilized zirconia catalyst 41
5.1.1 Catalyst Characterization 41
5.1.2 Steady state measurement 42
5.2 The electrochemical promotion of deep propane oxidation on Pd, Ir, Ru, and Cu catalyst deposited on yttria-stabilized zirconia catalyst 56
5.2.1 Catalyst Characterization 56
5.2.2 Catalytic activity measurement 61
5.3 The role of MnxOy interlayer for Pd catalysts deposited on yttria-stabilized zirconia in the deep propane oxidation 82
5.3.1 Catalyst Characterization 82
5.3.2 Catalytic activity measurement 86
VI CONCLUSIONS AND RECOMMENDATIONS 97
6.1 Conclusions 97
6.2 Recommendations 98
REFERENCES 99

CHAPTER page

APPENDICES 112
APPENDIX A CALCULATION FOR ETHYLENE AND PROPANE OXIDATION CONVERSION 113
APPENDIX B RATE OF CO_2 FORMATION CALCUALTION 114
APPENDIX C OVERPOTENTIAL CALCUALTION 116
APPENDIX D THE RATE ENHANCEMENT RATIO CALCULATION 117
APPENDIX E THE FARADAIC EFFICIENCY CALCULATION 119
APPENDIX F THE SURFACE METAL CATALYST CALCULATION 121
APPENDIX G ACTIVATION ENERGY CALCUALTION 124
APPENDIX H SOLID ELECTROLYTE CONDUCTIVITY CALCULATION 126
APPENDIX I CALCULATION FOR MANGANESE OXIDE PREPARATION 128
APPENDIX J CONDITION OF GAS CHROMATROGRAPHY 129
APPENDIX K LIST OF PUBLICATIONS 130
VITA 132

LIST OF TABLES

TABLE page

2.1 Classification of electrochemical promotion 13

3.1 Kinetic data from isothermal studies of ethylene oxidation on Pt/YSZ 26

4.1 Sputtering deposition thickness for the catalyst-electrodes (Pd, Ir, Ru, Cu and Au) 37

5.1 Apparent activation energy of the C_2H_4 oxidation reaction on Pt/YSZ under open circuit state and positive and negative potential application at three different feed compositions compositions (i) $P_{O_2}/P_{C_2H_4} = 40$, (ii) $P_{O_2}/P_{C_2H_4} = 10$, (iii) $P_{O_2}/P_{C_2H_4} = 3$ 54

5.2 Apparent activation energy values for Pd, Ir, and Ru catalyst-electrodes under open circuit and positive and negative potential application conditions. $P_{C_3H_8} = 1.2$ kPa, $P_{O_2} = 10$ kPa 82

J.1 GC analysis condition for ethylene and propane oxidation 125

LIST OF FIGURES

FIGURE page

2.1 Three possible pathways of oxygen-adsorbed species at three-phase boundary by current/potential application (a) desorption, (b) reaction, (c) backspillover 8

2.2 Schematic of the effective double layer and double layer on the solid electrolyte both YSZ and β''-Al_2O_3 9

2.3 Example for four types of electrochemical promotion behavior 13

2.4 Fundamental experimental set up for electrochemical promotion study (a) ethylene oxidation and (b) propane oxidation on the metal catalyst electrode deposited on Yttria-stabilized zirconia 17

2.5 Reactor configuration (a) fuel-cell type configuration, (b) single-pellet design configuration 18

2.6 NEMCA interface to heterogeneous catalysis, fuel cells, electrolysis, and battery 19

2.7 NEMCA road map from researcher's point of view 20

2.8 General pattern between conversion and temperature of catalytic combustion 22

3.1 Schematic of the oxygen storage (1) at the Pt/YSZ interface (2) the gas expose the gas surface via backspillover (3) in bulk platinum via solid state diffusion (4) leaving to the gas phase 28

3.2 Schematic of the pathway of reappearance of the anodic generated hidden Pt-O promoters during open-circuit after current interruption 29

4.1 Single pellet design reactor configuration 40

5.1 Surface image for the on top of the fresh Pt catalyst electrode deposited over YSZ 42

FIGURE page

5.2 Steady-state effect of temperature on the CO_2 formation catalytic rate and on the corresponding ethylene conversion under open-circuit state and positive and negative (± 1V) potential application conditions. Feed condition: (a) $P_{C_2H_4}$ = 0.2 kPa, P_{O_2} = 8 kPa, (b) $P_{C_2H_4}$ = 0.5 kPa, P_{O_2} = 5 kPa, (c) $P_{C_2H_4}$= 1 kPa, P_{O_2} = 3 kPa, F_v = 400 cm^3 min^{-1}(STP) 43

5.3 Steady-state effect of $P_{C_2H_4}$ on the CO_2 formation catalytic rate under open-circuit state and positive and negative (± 1V) potential application. Feed condition: (a) P_{O_2} = 5 kPa, (b) P_{O_2} = 8 kPa, (c) P_{O_2} = 12 kPa at T= 310°C 46

5.4 Steady-state effect of P_{O_2} on the CO_2 formation catalytic rate under open- circuit state and positive and negative (± 1V) potential application. Feed condition: $P_{C_2H_4}$ = 0.2 kPa at T= 310°C 47

5.5 Steady-state effect of applied overpotential (bottom) on the CO_2 formation rate, (middle) on the current and (top) on the rate enhancement ratio, ρ, under different $P_{C_2H_4}$ feed. Feed condition: (a) P_{O_2} = 8 kPa and (b) P_{O_2} = 12 kPa, Fv = 600-800 cm^3min^{-1}(STP) 49

5.6 Effect of O^{2-} supply (I>0) or remove rate (I<0) to/form the Pt catalyst-electrode, on the rate change of CO_2, Δr_{CO_2}, under (a) P_{O_2} = 8 kPa and (b) P_{O_2} = 12 kPa. T = 310°C 51

5.7 Open-circuit catalytic CO_2 formation rate as a function of exchange current rate i_0/2F under P_{O_2} =8 (top) and 12 kPa (bottom). T = 310°C 52

5.8 Steady-state effect of the applied overpotential on the apparent activation energy, E_{act}, of the C_2H_4 oxidation reaction, at different feed compositions 53

FIGURE page

5.9 Comparison of the observed EPOC-type behavior with the observed kinetic order in electron donor (D, C_2H_4) and in electron acceptor (A, O_2) at 330°C, 350°C and 390°C, under three different feed compositions: mildly oxidizing ($P_{O_2}/P_{C_2H_4}$ = 40), slightly oxidizing ($P_{O_2}/P_{C_2H_4}$ = 10) and stoichiometric ($P_{O_2}/P_{C_2H_4}$ = 3) conditions 55

5.10 SEM micrographs of fresh and used catalyst-electrodes; (a) and (b) for Pd, (b) and (c) Ir, (c) and (d) Ru catalyst-electrodes 57

5.11 XRD spectra for sputtered Pd/YSZ, Ir/YSZ, and Ru/YSZ catalyst-electrode; (a) as prepared sputtered metal catalyst electrodes and (b) spent sputtered metal catalyst electrodes 59

5.12 XRD spectra for sputtered Ru/YSZ catalyst-electrode electrodes for fresh and after exposed to various operating conditions 60

5.13 The first light-off propane oxidation upon different catalyst electrodes: sputtered- Pd, Ir, Ru, and Cu deposited on YSZ;(top) CO_2 formation rate and propane conversion (bottom) open circuit potential as a function of temperature 62

5.14 The second light-off propane oxidation upon different catalyst-electrodes: sputtered-Pd, Ir, Ru, and Cu deposited on YSZ;(top) CO_2 formation rate and propane conversion (bottom) open circuit potential as a function of temperature 63

5.15 Effect of temperature on propane conversion and rate of CO_2 formation (TPR experiments) under (open symbol) open circuit and upon different catalyst potential (filled symbol) U_{WR} = 1 V and (half-filled symbol) U_{WR} = -1 V. Catalyst electrode: (a) sputtered-Pd/YSZ, (b) sputtered-Ir/YSZ, and (c) sputtered-Ru/YSZ. Feed condition: $P_{C_3H_8}$ = 1.2 kPa, P_{O_2} = 10 kPa, F_v = 170 cm^3min^{-1} (STP) 66

FIGURE page

5.16 Effect of temperature and feed conditions on propane conversion and rate of CO_2 formation for Cu/YSZ (transient experiments) under (open symbol) open circuit and upon different catalyst potential (filled symbol) U_{WR} = 1 V and (half-filled symbol) U_{WR} = -1 V. Feed condition: (a) $P_{C_3H_8}$ = 1.2 kPa, P_{O_2} = 10 kPa, (b) $P_{C_3H_8}$ = 1.0 kPa, P_{O_2} = 5 kPa, (c) $P_{C_3H_8}$ = 1.2 kPa, P_{O_2} = 3 kPa, F_v = 170 cm^3min^{-1} (STP) 69

5.17 Rate of CO_2 formation, r_{CO_2}, and catalyst potential, U_{WR}, corresponds to a step change in an applied positive current of 1 mA at T = 350°C, (a) $P_{C_3H_8}$ = 1.2 kPa, P_{O_2} = 10 kPa, F_v = 170 cm^3min^{-1} (STP). Catalyst: Sputtered Pd catalyst-electrode deposited on YSZ 70

5.18 Steady-state effect of applied potential, U_{WR}, on (a) current, (b) rate enhancement ratio, ρ, and (C) the apparent Faradaic efficiency, Λ on Pd and Ir catalyst-electrodes at 350°C and 450°C. Condition: $P_{C_3H_8}$ = 1.2 kPa, P_{O2} = 10 kPa, F_v = 170 cm^3min^{-1} (STP). Catalyst: Sputtered Pd catalyst-electrode deposited on YSZ 73

5.19 Temperature dependence of the ionic conductivity for YSZ solid electrode under $P_{C_3H_8}$= 1.2 kPa, P_{O_2} = 10 kPa, F_v = 170 cm^3min^{-1} 75

5.20 Steady-state effect of propane and oxygen partial pressure ratio on the open circuit potential, E_0 at a constant volumetric gas flow rate and temperature, T= 380°C 76

5.21 Dependence of open circuit and positive and negative potential application of sputtered Pd catalyst-electrode deposited YSZ for on propane oxidation of (a) at constant P_{O_2} (P_{O_2}= 5 kPa) and (b) at constant $P_{C_3H_8}$ ($P_{C_3H_8}$= 0.5 kPa) under T = 350°C 78

5.22 Dependence of open circuit and positive and negative potential application of sputtered Ir catalyst-electrode deposited on propane oxidation of (a) at constant P_{O_2} (P_{O_2}= 3 kPa) and (b) at constant $P_{C_3H_8}$ ($P_{C_3H_8}$= 1.2 kPa) under T = 380°C 80

FIGURE page

5.23 Arrhenius plots for CO_2 formation rate over Pd/YSZ, Ir/YSZ and Ru/YSZ catalysts electrodes under open circuit conditions. $P_{C_3H_8}$ = 1.2 kPa, P_{O_2} = 10 kPa. F_v = 170 cm^3min^{-1} (STP) 81

5.24 SEM micrographs of fresh and used catalyst electrodes; (a) and (b) Mn_xO_y catalyst electrode over YSZ and (c) and (d) Pd/ Mn_xO_y catalyst electrode over YSZ 83

5.25 XRD spectra for Mn_xO_y /YSZ and Pd/ Mn_xO_y/YSZ catalyst-electrode; (a) fresh and (b) used catalyst electrodes 85

5.26 Steady-state effect of temperature on the CO_2 formation rate and propane conversion under open circuit condition. Open symbols represent as prepared catalyst results. Closed symbols represent spent catalyst results. Conditions: $P_{C_3H_8}$ = 1.2 kPa, P_{O_2} = 10 kPa, F_v = 170 cm^3min^{-1} (STP) 86

5.27 Steady-state effect of oxygen partial pressure on the CO_2 formation rate under open circuit condition comparing Pd and Pd/Mn_xO_y catalyst electrodes. Conditions: $P_{C_3H_8}$ = 0.5 kPa, F_v = 170 cm^3min^{-1}(STP) 87

5.28 Steady-state effect of propane partial pressure on the CO_2 formation rate under open circuit condition comparing Pd and Pd/Mn_xO_y catalyst electrodes. Conditions: P_{O_2} = 5 kPa, F_v = 170 cm^3min^{-1}(STP) 88

5.29 Steady-state effect of gas reactant partial pressure on the CO_2 formation rate under open circuit condition for Pd/Mn_xO_y catalyst electrodes upon different temperatures (a) at fixed $P_{C_3H_8}$ = 0.5 kPa, (b) at fixed P_{O_2} = 5 kPa under F_v = 170 cm^3min^{-1}(STP) 90

5.30 Steady-state effect of applied potential as a function of current on Pd and Pd/Mn_xO_y catalyst electrode at 350°C 91

5.31 Steady-state effect of the applied overpotential on rate of reaction in comparision of Pd and Pd/Mn_xO_y catalyst-electrodes at 350°C under $P_{C_3H_8}$ = 1.2 kPa and P_{O_2} = 10 kPa, flow rate = 170 $cm^3 min^{-1}$ (STP) 92

FIGURE page

5.32 Series of AC impedance spectra as a function of time under open circuit condition at T = 450°C, $P_{C_3H_8}$ = 1.2 kPa and P_{O_2} = 10 kPa, volumetric flow rate = 170 cm^3 min^{-1} (STP) 93

5.33 High frequency intersect (Ohmic resistance, Rcell) as a function of exposure time at 450°C, $P_{C_3H_8}$ = 1.2 kPa and P_{O_2} = 10 kPa, volumetric flow rate = 170 cm^3 min^{-1} (STP) and at open circuit conditions 94

5.34 Series of AC impedance spectra at open circuit conditions and as a function of temperature. $P_{C_3H_8}$ = 1.2 kPa and P_{O_2} = 10 kPa, volumetric flow rate = 170 cm^3 min^{-1} (STP) 95

5.35 Arrhenius plots of R_{cell} for the Pd/YSZ and Pd/MnxOy/YSZ cell under reaction conditions and at open circuit 96

D1 Steady-state effect of applied potential on the electrochemically promoted propane oxidation at 350°C on the rate enhancement ratio, ρ. Operating conditions as shown in figure 113

E1 Steady-state effect of applied potential on the electrochemically promoted propane oxidation at 350°C on the Faradaic efficiency, Λ. Operating conditions as shown in figure 115

F1 Rate of CO_2 formation, r_{CO_2}, and catalyst potential, U_{WR}, corresponds to in an applied positive current of 1 mA at T = 350°C, (a) $P_{C_3H_8}$ = 1.2 kPa, P_{O_2} = 10 kPa, F_v = 170 $cm^3 min^{-1}$ (STP). Catalyst: Sputtered Pd catalyst-electrode deposited on YSZ 117

G1 Steady-state effect of temperature on rate of CO_2 formation under closed and open circuit conditions for Pd/YSZ. Condition: $P_{C_3H_8}$ = 1.2 kPa, P_{O_2} = 10 kPa, and F_v = 170 $cm^3 min^{-1}$ (STP) 120

H1 A cylindrical shape 122

NOMENCLATURE

List of acronyms

G/P	Galvanostat/Potentiostat
IR	Infra red spectroscopy
MIS	Metal-support interaction
NEMCA	Non-faradaic Electrochemical Modification of Catalytic Activity
SEP	Solid Electrolyte Potentiometry
SOFC	Solid Oxide Fuel Cell
STP	Standard Temperature and Pressure
STM	Scanning Tunneling Microscopy
TOF	Turnover Frequency
XPS	X-ray Photoelectron Spectroscopy
YSZ	Yttria-stabilized zirconia
ac, AC	alternating current
dc, DC	direct current
o.c.	open circuit condition, I=0
tpb	three phase boundaries

List of symbols

Symbol	**Meaning**	**Units**
a	denotes adsorbed species	
A	electron acceptor adsorbate	
C	capacitance	F
D	electron donor adsorbate	
E_A	activation energy	kJ/mol
e	electron charge	$1.6 \cdot 10^{-19}$ C
F	Faraday constant	96484.6 C
I	current	A

Symbol	Meaning	Units
I_o	exchange current	A
i_o	exchange current density	A/m^2
N_G	surface area of catalyst in mol	mol
n	number of electrons taking part in the overall reaction	
O(a)	adsorbed oxygen	
O^{2-}	oxygen ion	
O^{s-}	backspillover oxygen ion	
PI_i	promotion index	
P	partial pressure	Pa
P_A	partial pressure of electron acceptor A	Pa
P_D	partial pressure of electron donor D	Pa
R	resistance	Ohm
r	catalytic rate	mol/s
r_0	catalytic rate under open circuit	mol/s
T	temperature	K, ^oC
t	time	s
U_{wc}	cell potential	V
U_{WR}	catalytic potential	V
ΔU_{WR}	change in catalyst potential	V
W	index for working electrode	
X	conversion	
Z	impedance	Ohm
Z_{Im}	imaginary part of impedance Z	Ohm
Z_{Re}	real part of impedance Z	Ohm

List of Greek symbols

Symbol	Meaning	Units
γ	permanent rate enhancement ratio	
$\delta+$	positive image charge, index for partially positive charged species	
$\delta-$	negative image charge, index for partially negative charged species	
η	overpotential ($=U_{WR} - U^{o}_{WR} = \Delta U_{WR}$)	V
ρ	rate enhancement ratio	
σ	conductivity	S/m
τ	NEMCA time constant	

Subscripts

i	index for promoter species, e.g. $O^{\delta-}$, $Na^{\delta+}$
A	electron acceptor adsorbate
CE	counter electrode
D	electron donor adsorbate
E	denotes electrode/electrolyte interface
RE	reference electrode
WE	working electrode
WC	index for potential or resistance between working and counter electrode
WR	index for potential or resistance between working and reference electrode
$^{\circ}$	Index for open circuit conditions, I=0

CHAPTER I
INTRODUCTION

1.1 Inspiration

The catalytic combustion of hydrocarbons is necessary for the energy technology to reduce emission of pollutants. At present, there are lots of concern in the environmental crisis, especially air pollution from the exhaust gas emitted by many sources such as automobile sources, fuel plant, and so on. In particular, mobile source discharges many air pollutants that cause harm to human being and damage to the natural environment. The cost of this effect in the reduction of resource is loss productivity, thus cleaning up or improving polluted environment are deeply of concern. The components of automotive emissions consist of suspended particle matter, carbon monoxide (CO), nitric oxide (NO), and unburnt hydrocarbons (HC) [1-3].

Many researchers have paid attention on the controlling pollutant emission, for example, the reduction of nitric oxide, CO oxidation, and hydrocarbon oxidation. To remove hydrocarbons, there are several elimination methods including adsorption, thermal, and catalytic methods. Normally, the main disadvantages of the adsorption processes are the loss of adsorbent and low temperature conditions that are not appropriated with commercial application due to the high temperature hydrocarbon output either stationary or mobile source. On the other hand, thermal methods have to use high temperature operation; hence it requires high loss of energy consumption. In the case of catalytic technology, most researchers have studied in many aspects, e.g. developing catalysts, hydrocarbon combustion mechanisms, and so on. The noble metal catalysts are recognized as the most active catalytic systems for volatile organic compounds (VOCs), carbon monoxide, and light hydrocarbon oxidation, i.e. methane or propane oxidation, even at low temperature operating conditions and in excess of oxygen. Among of these classical metals, Pd is known as the best catalyst for light hydrocarbon oxidation, whereas Pt is recognized as the highest catalytic activity for propane oxidation [4-8]. According to high material cost and limitation of noble metal, many efforts have been paid to the modification and development of catalyst

systems. In addition, there are still drawbacks in the case of classical catalyst including the short life time (due to the catalyst deactivation) and the weakness to control their activity during the catalytic process. Methane and propane are representatives of unburnt hydrocarbons from combustion process. A large number of studies have focused on the methane and propane combustion with not only metal, metal oxide supported catalysts but also in electrochemical membrane reactor. However, the higher alkane like propane requires quite high temperature for complete oxidation. Previous studies concerning either hydrocarbon oxidation or combustion had focused on the nature of catalyst, e.g. support material, particle support and metal size, additive promoter, catalyst dispersion, and so on.

An interesting alteration for hydrocarbon oxidation is electrochemical promotion of catalysis. The control of modification and development of catalyst on metal or metal oxide deposited on solid electrolyte, i.e. yttria-stabilized zirconia (YSZ), β'' – Al_2O_3, etc. is a well-known study. It is clear that a wide range of catalyst, electrolyte and varieties of reaction can be found in this effect. The phenomenon of electrochemical promotion of catalysis (EPOC), for which the catalytic rate enhancement is reversible, leading to a short time activated state and the innovation concept is improving catalytic efficiency by controlling work function of catalyst. A key parameter of electrochemical promotion studies is an applied potential, U_{WR}, applied between catalyst working electrode and reference electrode. The rate change was observed when applied current or potential, under a wide range of operating conditions [9, 10]. There are efforts carried out via several surface and electrochemical techniques for the monitoring reaction behavior. The deep oxidation of light hydrocarbon on the noble metal deposited on YSZ under various conditions has been studies for many years. Recently, the electrochemical promotion of catalysis has been investigated on Pt, Pd, and Rh catalyst deposited on YSZ for light hydrocarbon oxidation including methane, ethane, and propane oxidation. The rate of CO_2 formation for these catalyst-electrodes can be further increased via application of potential or current. Additionally, the electrochemical promotion of propane oxidation has also been successfully on Pt and Rh catalysts deposited on YSZ electrolyte support; however, the Pt was found much more active than Rh catalyst-electrode [11]. In addition, there are some groups of researchers focusing on Pt, Pd, and Ag for

propane oxidation. The different behaviour had been found among of them, i.e. electrophobic and inverted-volcano behavior. While Pt and Ag catalyst electrodes exhibited the increase in catalytic activity, Pd cannot be further electrochemically promoted under the reducing condition upon different temperatures [12]. In addition, Pt catalyst electrode exhibited both electrophobic and inverted-volcano behavior [13-15]. Recently, Pt was still used as the catalyst working electrode film in the propane oxidation process in order to study in more detail on permanent electrochemical promotion of catalyst and catalyst film morphology [16]. It was found that Pt catalyst electrode deposited on YSZ exhibited a good activity for propane oxidation and the inverted-volcano behavior was still obtained [15]; however, there is no study in metal oxide catalyst for propane oxidation. Moreover, metal oxides, both RuO_2 and IrO_2, are really high conductive for ethylene oxidation [17, 18] as well as they are low cost materials comparing to Pt and Pd. From all mentioned above, there are lack of information relating to comparison of behavior of all catalysts and the use of low cost material for propane oxidation. Furthermore, there are some researches employing Mn_2O_3 as oxide catalyst for propane oxidation. It exhibited quite high temperature for complete conversion; however, it have been identified in the terms of low cost material catalyst for oxidation reactions of carbon monoxide and organic compounds and hydrocarbons as well as it is also considered as an environmental material [19-21].

According to many reasons that mentioned above, so this work is focused on electrochemical promotion of catalysis on different catalyst-electrode for deep ethylene and propane oxidation together with the combination of manganese oxide interlayer with Pd deposited on YSZ.

1.2 Objectives

1. To investigate the electrochemical promotion of catalysis (EPOC) for deep ethylene oxidation on Pt deposited on yttria-stabilized zirconia (YSZ).
2. To investigate the electrochemical promotion of catalysis (EPOC) for deep propane oxidation on four different metal catalyst-electrodes deposited on yttria-stabilized zirconia (YSZ), i.e. Pd, Ru, Ir, and Cu.

3. To observe the role of manganese oxide interlayer for Pd catalysts deposited on yttria-stabilized zirconia (YSZ) on the deep propane oxidation.

1.3 Scopes of work

1. To observe details of catalysts under open circuit conditions and under polarization.
2. To conduct the experiment for examining the effect of oxide inter layer between catalyst film and electrolyte.
3. To monitor additional mechanistic information and catalytic behavior via electrochemical techniques e.g. AC Impedance, cyclic voltammetry, and so on.

1.4 The structure of this dissertation

This dissertation is involved with the electrochemical promotion of light hydrocarbon oxidation, here for ethylene and propane oxidation on noble metal catalyst electrodes. The entire of this book has been organized as follows,

Chapter II presents the principle of non-Faradaic electrochemical promotion of catalytic activity (NEMCA) or electrochemical promotion of catalysis (EPOC). The fundamental concept, rule of electrochemical promotion, basic experimental set up, and the trend of electrochemical promotion of catalysis in economic point of view are included. Moreover, light hydrocarbon oxidation consists of ethylene and propane oxidation is also explained.

Chapter III reviews the relating study on the classical catalyst and also the electrochemical promotion of catalysis for light hydrocarbon oxidation and other reactions. The conventional catalyst is reviewed as the first part with the work up to present. Non-Faradaic electrochemical promotion of catalytic activity (NEMCA) for light hydrocarbon oxidation and other relating reaction together with the background of this phenomenon is reviewed for more understanding of this effect.

Chapter IV describes the material and catalyst-electrode preparation including pasted, sputtering, and impregnation method upon the different raw materials. The catalytic activity measurement, i.e. light-off experiment, transient, kinetics study etc.,

with the experimental set up is included. Finally, the catalyst characterization techniques, i.e. XRD and SEM are explained in detail for this present study.

Chapter V presents the results of the electrochemical promotion effect upon different catalyst-electrode for ethylene and propane oxidation. The electrochemical promotion for ethylene oxidation on pasted Pt catalyst-electrode over YSZ is investigated. Moreover, the electrochemical promotion of deep propane oxidation on Pd, Ir, Ru, and Cu catalyst-electrode deposited on YSZ together with the role of Mn_xO_y interlayer of sputtered Pd catalyst-electrode are included in the following section.

Chapter VI presents the conclusion of this research, which is all relating to the electrochemical promotion effect, given based on the different catalyst-electrodes and recommendations for further development.

CHAPTER II
THEORY

This chapter provides the fundamental concepts of non-Faradaic electrochemical of catalytic activity (NEMCA) or electrochemical promotion of catalysis (EPOC), i.e. the principle concept of this phenomena, the solid electrolyte for EPOC system, the rule of electrochemical promotion, the basic experimental set up, the reactor design, and the status of electrochemical promotion of catalysis in commercial systems. Finally, the ethylene and propane oxidations are described based on the literature reviews.

2.1 Non-Faradaic electrochemical modification of catalytic activity (NEMCA) or electrochemical promotion of catalysis (EPOC)

2.1.1 Fundamental principle

Professor C.G. Vayenas and his group were the first group who discovered the catalytic activity and selectivity alteration by applying a small current ($1\text{-}10^4$ $\mu A/cm^2$) and potential (± 2 V) between working and counter catalyst-electrode. It was first reported in 1981 relating to non-Faradaic enhancement in heterogeneous catalysis for the case of ethylene epioxidation on Ag catalyst-electrodes, but the term "electrochemical promotion" was realized in 1988. The term of non-Faradaic electrochemical modification of catalytic activity (NEMCA) can be so called in several synonyms, i.e. electrochemical promotion (EP), electrochemical promotion of catalysis (EPOC), and *in situ* controlled promotion (ICP) [9, 22].

The electrochemical reaction is involved in the reaction, which charges transfer across the interface between the electrode and electrolyte. Therefore, the electrode acts as the heterogeneous catalyst and enhances even the catalytic activity or selectivity of reaction. If this phenomenon relates to the net charge transfer between electrolyte and catalyst electrode, it is electrocatalysis. While, the electrochemical promotion of catalysis or non-Faradaic electrochemical modification of catalytic

activity (NEMCA) has no net charge transfer, hence this is the main distinguish of this phenomena that break the Faraday's law [22].

The phenomenon of non-Faradaic electrochemical of catalytic activity (NEMCA) or electrochemical promotion of catalysis (EPOC) is related to electrochemically controlled back spillover of ion or ion migration over the metal catalyst surface with an application of a little current (1-10^4 μA/cm^2) or potential (± 2 V) on the catalyst surface (between the conductive catalyst film and a second metal film, and thus the back spillover of ion served as "sacrificial promoter"($O^{\delta-}$ in the case of O^{2-} conductors such as yttria-stabilized zirconia, $Na^{\delta+}$ in the case of Na^+ conductors such as β"-Al_2O_3). This phenomenon has led to the modification of chemical catalyst surface properties according to the change of catalytic activity and selectivity. Generally, this phenomenon is not limited on a few of reactions and kinds of solid electrolyte. More than 80 catalytic reactions including oxidations, hydrogenation, dehydrogenation, isomerization, and decompositions and many classes of electrolyte supports have been achieved by electrochemical promotion [9, 11, 23-30].

The origin of this phenomena has been investigated by several *in situ* techniques including (i) surface science techniques, e.g. X-ray photoelectron spectroscopy (XPS) [31-34], ultraviolet photoelectron spectroscopy (UPS) [9], temperature programmed desorption (TPD) [28, 35-39], photoelectron emission microscopy (PEEM) [40], and scanning tunneling microscopy (STM) [41, 42], (ii) electrochemical technique, e.g. cyclic voltammetry [9, 35] and AC impedance spectroscopy [43], (iii) conventional catalyst technique, e.g. rate transient technique [9] and work function measurement [9, 44, 45] as well as theoretical ab initio quantum mechanical calculation [46, 47].

As shown in Figure 2.1, the typical metal film thickness is approximately 2-5 μm deposited on electrolyte support and ion movement under potential or current application at the three phase boundaries, which is the catalyst/solid electrolyte/gas. There are three possible pathways, as follows

(a) Desorption to the gas phase

(b) Reaction with a co-adsorbed species

(c) Migration over gas-exposed catalyst electrode surface

In the two former cases (a and b), there are no evidence of NEMCA or EPOC effect. In the case b, the rate change, Δr, equals to I/nF. Even in this case, if the product remains at the surface and has some catalytic property it will be NEMCA. In last case, it is NEMCA phenomena, where the new species is pumped onto the catalyst surface, thus these ion species can interact with co-adsorbed reactant led to form an oxygen molecule form over metal catalyst surface as illustrated in Figure 2.1c.

(a)

(b)

(c)

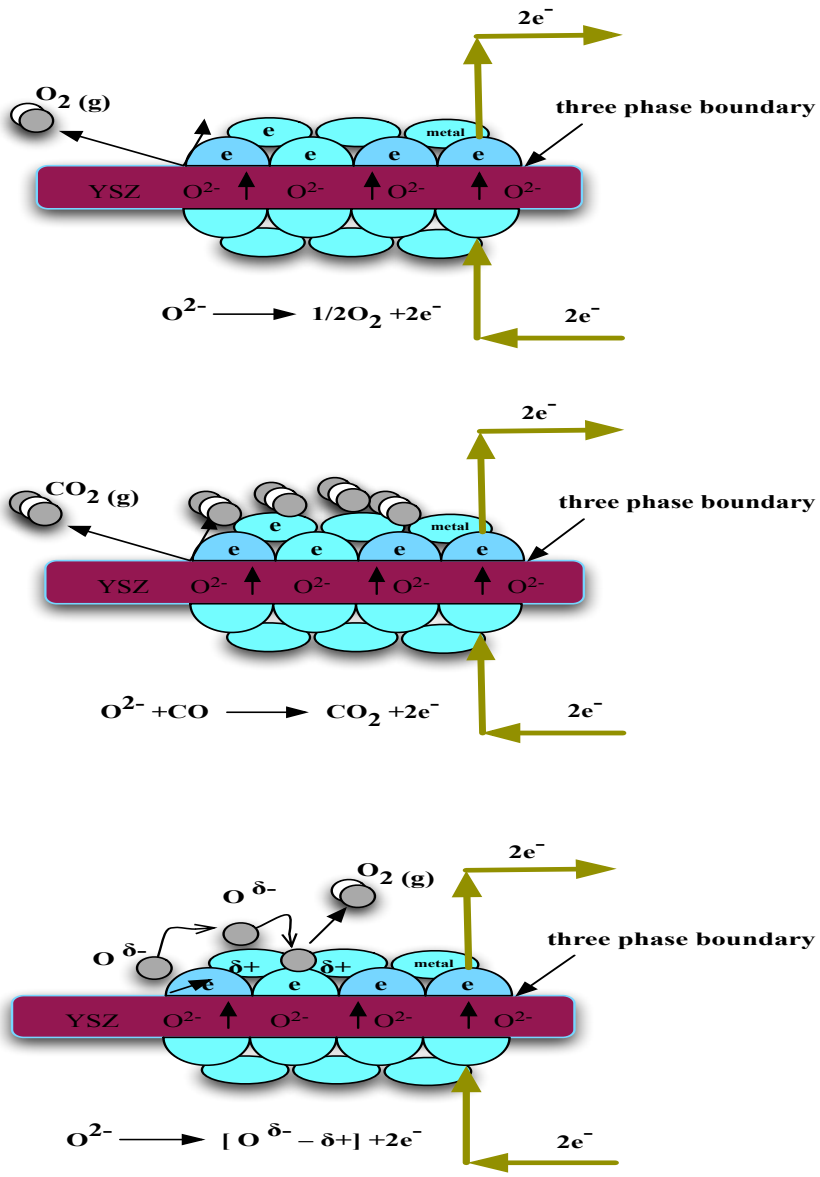

Figure 2.1 Three possible pathways of oxygen-adsorbed species at three-phase boundary by current/potential application (a) desorption, (b) reaction, (c) backspillover [9]

The basic concept of the electrochemical promotion is shown in Figure 2.2.

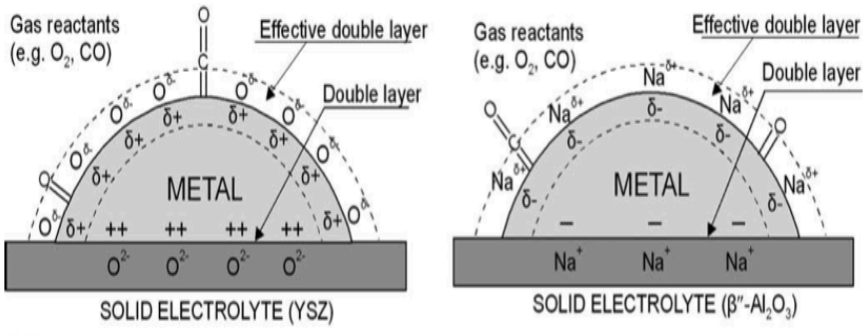

Figure 2.2 Schematic of the effective double layer and double layer on the solid electrolyte both YSZ and β"-Al_2O_3 [22].

This figure presents a common scheme of a catalyst-electrode supported on solid electrolyte, i.e. YSZ and β"-Al_2O_3 under electrochemical promotion conditions, where promoting ion with their compensating image charge on the metal, ($O^{\delta-}$ - δ^+ and $Na^{\delta+}$ - δ^-), migrate over the entire gas exposed surface after polarization. Therefore, the current or potential that control promoting species like $O^{\delta-}$ or $Na^{\delta+}$ transported from solid electrolyte to catalyst surface is the key parameter of the electrochemical promotion leading to the formation of effective double layer. The promoting species (e.g. $O^{\delta-}$ and $Na^{\delta+}$), is in general, consumed during the catalytic reaction, then the promoter is termed sacrificial promoter. The density of effective double layer varies during the varied potential. It has an effect on both work function of the surface and the chemisorptive bond strength of reactant and intermediates, hence the catalyst activity and selectivity was modified.

There are three common parameters for measuring the magnitude of electrochemical promotion of catalysis [9, 13, 15, 48-50], defined as,

1. The rate enhancement ratio, defined as

$$\rho = r/r_0 \qquad (2.1)$$

Where r_0 is the catalytic rate under open circuit condition (I=0)

r is the catalytic rate under closed circuit condition

2. The faradaic efficiency or enhancement factor, defined as

$$\Lambda=\Delta r/(I/nF) \tag{2.2}$$

Where Δr is the change in faradaic reaction rate

I is the applied current

n is the ion charge that can be up to 3×10^5 or down to -10^4

The expected magnitude of enhancement factor, defined as

$$|\Lambda| = 2Fr_0/I_0 \tag{2.3}$$

Where r_0 is the catalytic rate at open-circuit condition (I=0)

I_0 is an exchange current from IU curve or Tafel plot

one can easily show that

$$\tau_{PR}/\tau_R=\Lambda \tag{2.4}$$

which shows that the Faradaic efficiency, Λ, of electrochemically promoted reactions expresses the ratio of the average lifetimes of promoting species ($O^{\delta-}$, $Na^{\delta+}$) and of the key reactants on the catalyst surface [9].

3. The promotion index, PI_j, in the case of O^{2-}

$$PI_j = (\Delta r/r_0)/\Delta\theta_i \tag{2.5}$$

Where i is the promoting ion

r_0 is the catalytic rate under open-circuit condition (I=0)

r is the catalytic rate

$\Delta\theta_i$ is the ion coverage on the catalyst surface during the transient (It/FN_G)

t is the time of current application

N_G is the metal surface area (mol metal)

F is Faraday's constant, 96500 s ·A /mol

A reaction is electrochemically promoted, or exhibits the NEMCA effect, when $|\Lambda|>1$. In the case $\Lambda>1$, i.e. when the reaction rate is enhanced with positive current and increasing catalyst potential U_{WR} the reaction is termed electrophobic, while $\Lambda<-1$, i.e. when the rate is enhanced with negative current and decreasing catalyst potential, the reaction is termed electrophilic.

2.1.2 Solid electrolyte

The solid electrolyte is one kind of conductor that can be the ionic conductor or the mixed conductor (ionic and electronic conductor). Michael Faraday first discovered solid PbF_2 in 1834 [51]. The categorization of solid electrolyte is depended on the ion type for conducting.

There are several kinds of solid electrolyte as follows [9],

1. Oxygen ion conductors, for example, calcia- or yittria-stabilized zirconia (YSZ) typically used in sensor technology under the temperature range of 400-1200^{o}C.
2. H^+ and Li^+ conductors: good cationic conductors exhibit in varieties of alkali and salt solution such as $CsHSO_4$, nafion that normally used in the proton exchange membrane (PEMs), and so on.
3. Na^+ conductors: It is common in β and β"-Al_2O_3 that used in temperature range of 150-300^{o}C.
4. K^+, Cs^+, Rb^+, Ti^+ conductors: they are also in β and β"-Al_2O_3 used in the temperature range of 200-400^{o}C.
5. Ag^+ conductors, e.g. AgI, $RbAg_4I_5$ and Ag_2HgI_4 commonly used in the temperature range of 150-350^{o}C.
6. Cu^+ conductors, e.g. Cu_2Se and KCu_4I_5. They are usually used in the temperature range of 250-400^{o}C.
7. F^- conductors, including PbF_2 and CaF_2 are conductive above temperature of 500 and 600^{o}C, respectively.

The solid electrolytes commonly used in the electrochemical promotion are as follows,

1 Yittria-stabilized-zirconia (YSZ), oxygen ion conductors with the temperature range of 280-650^{o}C.

2 β"-Al_2O_3 and Na^+ conductor at temperature range of 130-140^{o}C

3 $CsHSO_4$ and nafion, a proton conductor at temperature of 150^{o}C and 25^{o}C, respectively.

4 CaF_2 an F^- conductor at temperature range of 550-700^{o}C.

5 Aqueoua KOH solutions (0.01-0.2 M) at temperatures range of 25-60^{o}C.

2.1.3 Rules of chemical promotion

The catalyst potential (U_{WR}), which is the applied potential between working and reference electrode, is the key parameter in electrochemical promotion. The subscribe "WR" stands for the potential difference between working electrode (W) and reference electrode (R). It should be noted that the varying potentials at a given temperature and gas composition has effects on the catalytic rate, r, [52]. The large variation of the catalytic rate, r was observed in comparison to unpromoted rate of reaction, r_0 under open circuit condition. Simple and rigorous rules [10, 52, 53] have been found for electrochemical promotion, which allow one to predict the type of catalytic rate dependence on catalyst potential on the basis of the unpromoted kinetics, i.e. on the basis of the catalytic rate dependence on the reactants partial pressures. These rules were established by making the following four observations:

(1) All electrophobic reactions ($\partial r/\partial U_{WR} > 0$) are positive order in the electron donor (D) reactant (e.g. C_2H_4, C_6H_6) and zero or negative order in the electron acceptor (A) reactant (e.g. O_2, NO).
(2) All electrophilic reactions are negative or zero order in the electron donor reactant and positive order in the electron acceptor reactant.
(3) In all volcano reactions, the rate vs P_A (partial pressure of electron acceptor) and rate vs P_D (partial pressure of electron donor) curves also pass through a maximum.
(4) All inverted volcano reactions are positive order in both reactants.

These observations form the rules of electrochemical promotion, and are summarized schematically in Figure 2.3, in terms of the catalytic reaction rate orders with respect to the electron acceptor (A) reactant (α_A) and with respect to the electron donor (D) reactant (α_D). The reaction orders α_A and α_D are defined, as usually, from:

$$\alpha_A = (\partial \ln r/\partial \ln P_A)_{P_D} \quad (2.6)$$

$$\alpha_D = (\partial \ln r/\partial \ln P_D)_{P_A} \quad (2.7)$$

Equivalently one can express the above four electrochemical promotion rules in terms of the chemisorptive propensity of the electron acceptor and electron donor reactants. Therefore, there are four global electrochemical rules that expressed in the term of global electrochemical rule, G1-G4 as follows,

G1: Reaction is called electrophobic referred to the electron acceptor reactant is strongly adsorbed on the catalyst surface.

G2: Reaction is called electrophilic with respect to the electron donor reactant is strongly adsorbed on the catalyst surface.

G3: Reaction is volcano-type, which both reactants are strongly adsorbed on the catalyst surface.

G4: Reaction is inverted volcano-type, which both reactants are weakly, adsorbed on the catalyst surface.

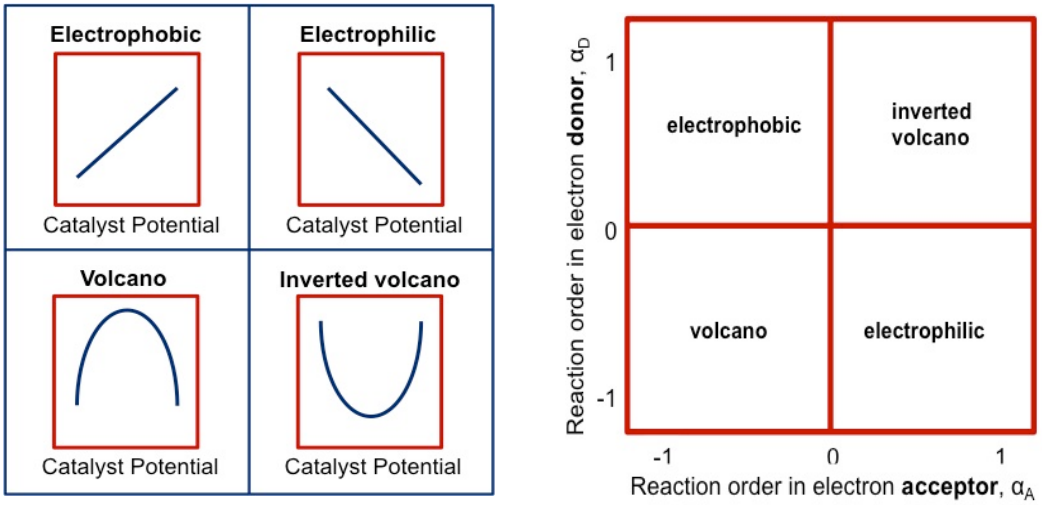

Figure 2.3 Examples for four types of electrochemical promotion behavior [52-54]

Table 2.1 Classification of electrochemical promotion [52]

Reactants		Catalyst	Solid electrolyte	P_A/P_D	T/°C	Rule
D	A					
Purely electrophobic reactions						
C_2H_4	O_2	Pt	ZrO_2 (Y_2O_3)	12- 16	260-450	G1
C_2H_4	O_2	Pt	β"-Al_2O_3	238	180-300	G1
C_2H_4	O_2	Pt	TiO_2	3.5-12	450-600	G1

Table 2.1 (continue)

Reactants		Catalyst	Solid electrolyte	P_A/P_D	T/°C	Rule
D	A					
C_2H_4	O_2	Rh	$ZrO_2(Y_2O_3)$	0.05-2.6	250-400	G1
C_2H_4	O_2	Ag	$ZrO_2(Y_2O_3)$	0.2-1.1	320-470	G1
C_2H_4	O_2	IrO_2	$ZrO_2(Y_2O_3)$	300	350-400	G1
C_2H_4	O_2	RuO_2	$ZrO_2(Y_2O_3)$	155	240-500	G1
CO	O_2	Pt	CaF_2	11-17	500-700	G1
CO	O_2	Pd	$ZrO_2(Y_2O_3)$	500	400-550	?
CH_4	O_2	Pd	$ZrO_2(Y_2O_3)$	0.2-4.8	380-440	G1
C_3H_6	O_2	Ag	$ZrO_2(Y_2O_3)$	20-120	320-420	G1
CH_4	O_2	Ag	$ZrO_2(Y_2O_3)$	0.02-2	650-850	G1
CO	NO	Pd	$ZrO_2(Y_2O_3)$	0.5-6.5	320-480	G2
C_6H_6	H_2	Pt	β''-Al_2O_3	0.02-0.12	100-150	G1
C_2H_2	H_2	Pt	β''-Al_2O_3	1.7-9	100-300	?
H_2	CO_2	Rh	$ZrO_2(Y_2O_3)$	0.03-0.7	300-450	G1
H_2	C_2H_2, C_2H_4	Pd	β''-Al_2O_3	0.1-5.9[a]	70-100	G1
H_2S	-	Pt	$ZrO_2(Y_2O_3)$	-	600-750	?
CH_4	-	Ag	$SrCe_{0.95}Yb_{0.05}O_3$	-	750	?
NH_3	-	Fe	$CaZr_{0.9}In_{0.1}O_{3-\alpha}$	4-12 kPa	530-600	G1
NH_3	-	Fe	$K_2YZr(PO_4)_3$	4-12 kPa	500-700	G1
CH_4	H_2O	Ni	$ZrO_2(Y_2O_3)$	0.05-3.5	600-900	G1
Purely electrophilic reactions						
C_2H_4	O_2	Pt	$CaZr_{0.9}In_{0.1}O_{3-\alpha}$	4.8	385-470	G2
C_2H_4	O_2	Pt	CeO_2	1.6-3.7	500	G2
C_2H_4	O_2	Pt	ZYTi10	3	400-475	?
C_2H_4	O_2	Ag	β''-Al_2O_3	0.3-0.4	240-280	G2
CO	O_2	Ag	β''-Al_2O_3	0.1-10	360-420	G2
C_3H_6	O_2	Pt	$ZrO_2(Y_2O_3)$	0.9-55	350-480	G2
CH_3OH	O_2	Ag	$ZrO_2(Y_2O_3)$	0-2	500	G2

Table 2.1 (continue)

Reactants		Catalyst	Solid electrolyte	P_A/P_D	T/°C	Rule
D	A					
CH_4	O_2	Au	$ZrO_2(Y_2O_3)$	0.1-0.7	700-750	G2
H_2	N_2	Fe	$CaZr_{0.9}In_{0.1}O_{3-\alpha}$	0-3	440	?
H_2	C_2H_4	Ni	$CaHSO_4$	1	150-170	?
	CH_3OH	Pt	$ZrO_2(Y_2O_3)$	-	400-500	?
	CH_3OH	Ag	$ZrO_2(Y_2O_3)$	0.6 kPa	550-750	G2
C_2H_4	NO	Pt	$ZrO_2(Y_2O_3)$	0.2-10	380-500	G2
C_2H_4	NO	Pt	β"-Al_2O_3	0.1-1.1	280-400	?
CO	NO	Pt	β"-Al_2O_3	0.3-5	320-400	G2
CO	NO	Pd	$ZrO_2(Y_2O_3)$	0.5-6.5	320-480	G2
CO	N_2O	Pd	$ZrO_2(Y_2O_3)$	2-50	440	G2
	1-C_4H_8	Pd	Nafion	-	70	G2
Volcano-type reaction						
C_2H_4	O_2	Pt	$NaZr_2Si_2PO_{12}$	1.3-3.8	430	G3
CO	O_2	Pt	$ZrO_2(Y_2O_3)$	0.2-5	468-558	G3
CO	O_2	Pt	β"-Al_2O_3	0.5-20	300-450	G3
H_2	O_2	Pt	H_2O-0.1N KOH	0.3-3	25-50	G1
H_2	O_2	Pt	Nafion	0.2-5	25	G3
SO_2	O_2	Pt	V_2O_5	1.8	350-450	?
C_3H_6	NO	Pt	β"-Al_2O_3	2-70	375	G3
H_2	NO	Pt	β"-Al_2O_3	0.3-6	360-400	G3
Inverted volcano reactions						
	O_2	Pt	TiO_2	0.2-0.3[b]	450-600	G4
	O_2	Pt	YSTi10	5	400-500	?
	O_2	Ag	$ZrO_2(Y_2O_3)$	0.6-14	350-450	G4
	O_2	Ag-Pd alloy	$ZrO_2(Y_2O_3)$	3.5-12.5	450-500	G4
	O_2	Au	$ZrO_2(Y_2O_3)$	3-53	450-600	G4
	O_2	Pt	$ZrO_2(Y_2O_3)$	0.06-7	270-500	G4
	O_2	Pt	$ZrO_2(Y_2O_3)$	0.02-7	600-750	G4

Table 2.1 (continue)

Reactants		Catalyst	Solid electrolyte	P_A/P_D	T/^oC	Rule
D	A					
	O_2	Pt	$ZrO_2(Y_2O_3)$	3-45	300-500	?
	CO_2	Pd	$ZrO_2(Y_2O_3)$	0.2-1.1	500-590	G4
	NO, O_2	Rh	$ZrO_2(Y_2O_3)$	0.08-8[c]	250-450	G4
	NO, O_2	Rh	$ZrO_2(Y_2O_3)$	0.33[c]	250-450	G4

"A" respects to the electron acceptor

"D" respects to the electron donor

"G1" respect to electrophobic reaction

"G2" respect to electrophilic reaction

"G3" respect to volcano-type reaction

"G4" respect to inverted volcano-type reaction

"?" respect to no data available

"a" respect to $P_D = P_{C_2H_2}/P_{C_2H_4}$

"b" respect to low P_A, P_D region

"c" respect to P_A/P_D is the ratio $P_{NO}/P_{C_3H_6}$ and P_{NO}/P_{CO}. The P_{O_2} range is between 0 and 6 kPa

2.1.4 The basic experiment set up for ethylene and propane oxidation

(a)

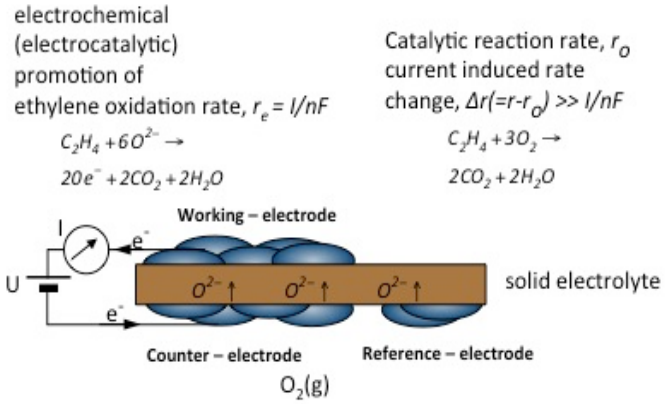

(b)

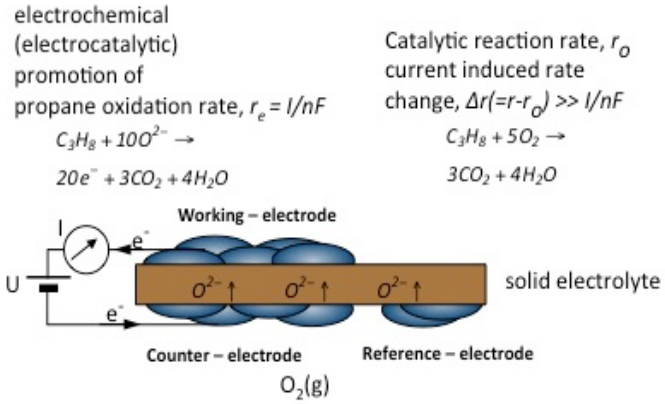

Figure 2.4 Fundamental experimental set up for electrochemical promotion study (a) ethylene oxidation and (b) propane oxidation on the metal catalyst electrode deposited on Yttria-stabilized zirconia, modified from [55]

The typical experimental set up is shown in Figure 2.4. A key parameter as mention above is U_{WR}, where the potential between working and reference electrode. It is clear that the variation of current or potential application affects the change of rate of reaction, r, from the unpromoted rate, r_0, under open circuit condition, relating to the operating conditions (temperature and gas mixture compositions).

2.1.5 Reactor configuration for electrochemical promotion experiment

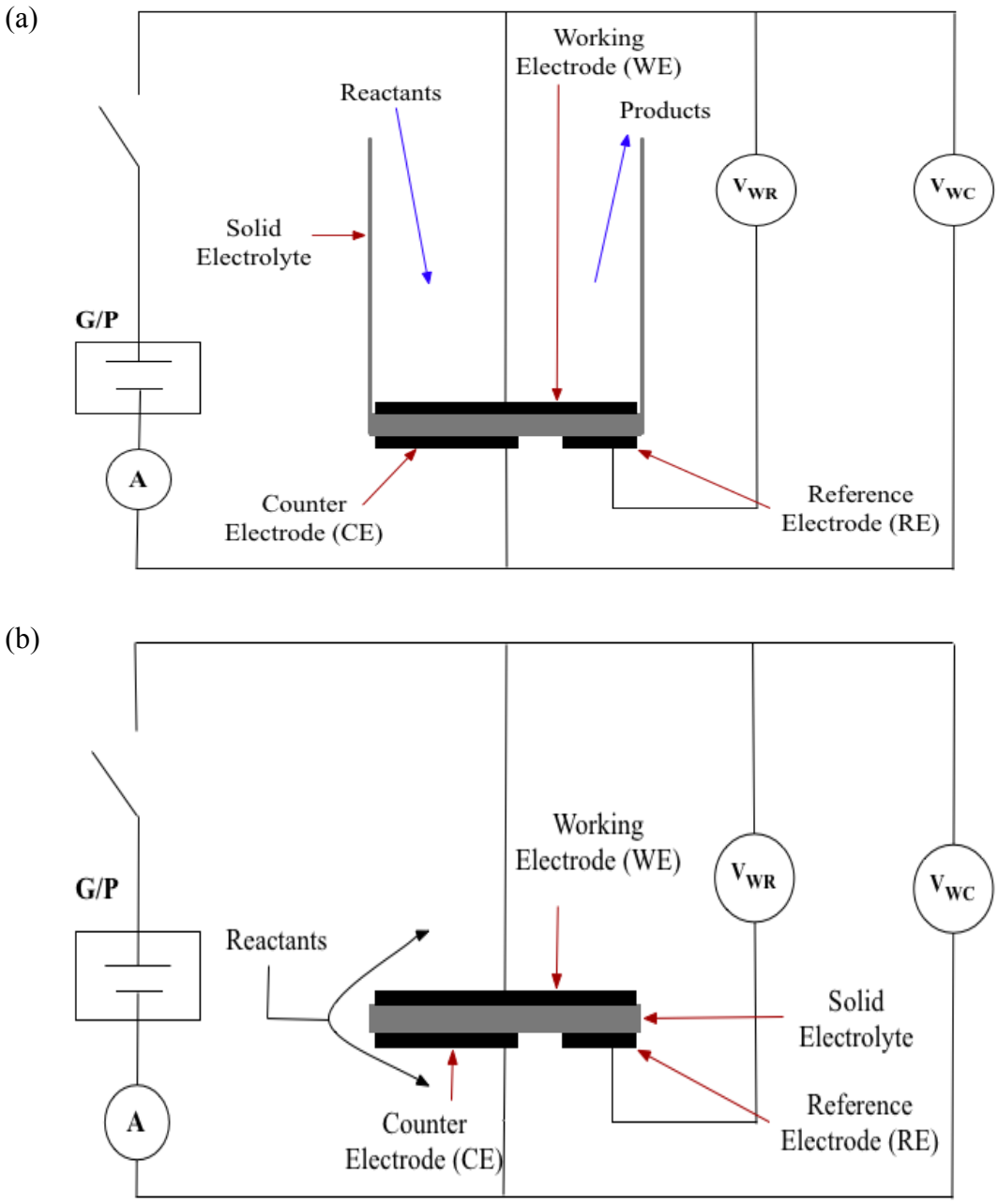

Figure 2.5 Reactor configuration (a) fuel-cell type configuration, (b) single-pellet design configuration [9]

In electrochemical terms the catalyst also acts as the working electrode of the solid electrolyte cell. The second (catalytically inert) electrode is the counter

electrode, while a third metal film, acting as a reference electrode is also useful to deposit on the solid electrolyte for fundamental EPOC studies.

As also shown in Figure 2.5, there are normally two types for electrode configuration including the fuel cell type and the single pellet type for the electrochemical promotion of catalyst. The working electrode (WE) for the both the types served as the catalyst for the catalytic reaction.

1. A fuel cell design configuration, feed reactant and auxiliary gases are separated in the other side of reactor as in Figure 2.5a. The working electrode (WE) is exposed to the reactive and product gas as well as the counter electrode is exposed to auxiliary gas.

2. A single pellet design confabulation is normally co-feed over the catalyst film that both working electrode and counter electrode are exposed to reactant, auxiliary gas and product as shown in Figure 2.5b.

2.1.6 Status of NEMCA in commercial system

This non-Faradaic activation of heterogeneous catalytic activity (NEMCA) is a promising application mixed with many scientific fields, e.g. heterogeneous catalysis, fuel cell, electrolysis and battery as shown in Figure 2.6. It becomes important to be the exhaust gas treatment in industrial part.

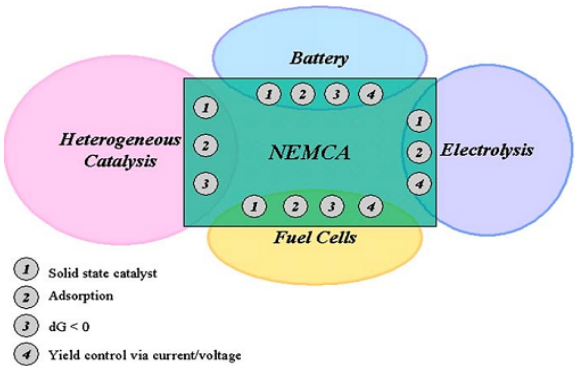

Figure 2.6 NEMCA interface to heterogeneous catalysis, fuel cells, electrolysis, and battery [56]

From previous studies, it was clearly enough that the utilization of NEMCA has been successful and effective with the environmental concerned problem like the treatment of gas exhaust (hydrocarbon or other oxides). The recent study of

monolithic electrochemical promoted reactor (MEPR) can be considered as a hybrid between a conventional monolithic honeycombs, which is significant novel applications.

Unfortunately, NEMCA has been far from existing in the real industrial systems. It may be two main hindered obstacles for the development of the NEMCA [57].

1. NEMCA required the specified technology for the electrical connection compared to the classical reactor.
2. The low dispersion of catalyst with single pellet design: commonly catalyst particle varied from 0.1 to 1 μm compared to the conventional catalyst having metal particle size around 10 nm. Then, NEMCA phenomenon is difficult to occur.

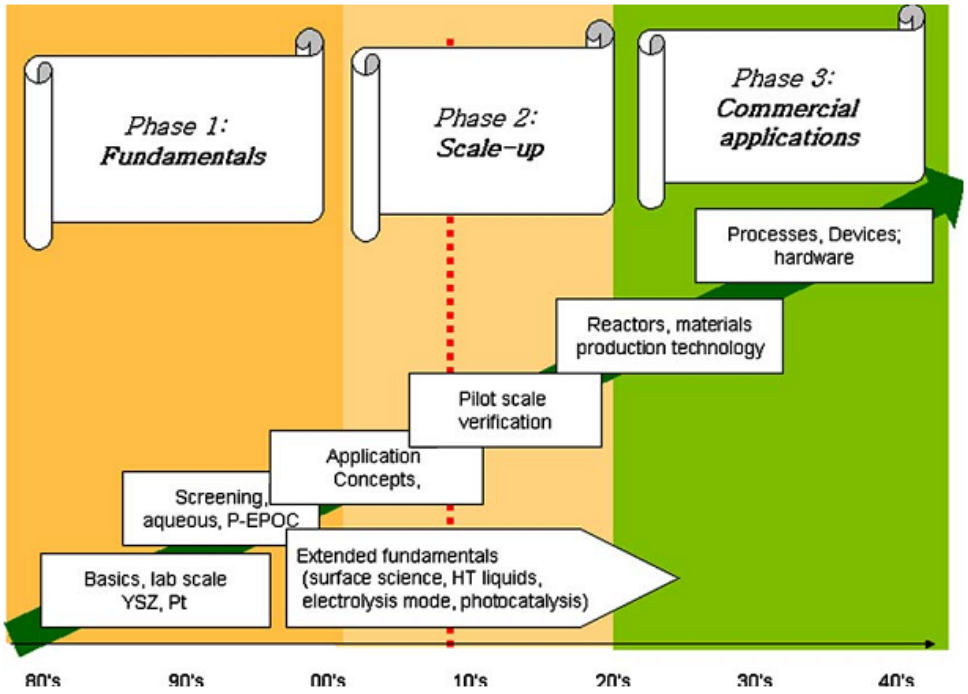

Figure 2.7 NEMCA road map from researcher's point of view [56]

As shown in Figure 2.7, researchers predicted the NEMCA aspect to the economic point of view. Firstly, it starts from the basic experiment with a small scale with fundamental catalyst electrodes like metal or metal oxides deposited on solid electrolyte supports, and then it may be studied in more details namely permanent

electrochemical promotion of catalyst (P-EPOC) because of its irreversibility or the role of interlayer. After that, it will be up to closer industrial system in pilot scale, and finally continue to the commercial application.

2.2 Ethylene and propane oxidation

Light hydrocarbons, i.e. ethylene and propane are important light hydrocarbons present in the exhaustive gas emission.

Ethylene is normally occurred from some chemical production or also released from the vehicle exhausted gas as well as incineration plants. Moreover, it can be from natural release. Above all, it is also recognized as an important chemical reactant that is mainly used for plastic production. However, ethylene can be related to the reactions that produce ground level ozone. Therefore, the crop and many materials can be damaged and it has an effect on human inhalation.

Propane is the derived gas from the natural gas and petroleum that is the type of the liquefied petroleum gas (LPG). Its major use is in industry, heating and transportation, thus propane is the kind of important hydrocarbon. Moreover, the catalytic combustion of hydrocarbon has been widely used for power generation and controlling emission from both stationary and mobile sources. While the precious metals e.g. palladium and platinum are recognized as highly active oxidation catalysts for the lower alkanes even at low and high reaction temperature. However, palladium exhibits the best for only methane, platinum is the most active for higher hydrocarbons in the conventional fixed bed reactor [58, 59].

The overall reaction of ethylene oxidation may be represented by

$$C_2H_4 + 3O_2 \rightarrow 2CO_2 + 2H_2O \qquad (2.8)$$

The overall reaction of propane oxidation may be represented by

$$C_3H_8 + 5O_2 \rightarrow 3CO_2 + 4H_2O \qquad (2.9)$$

This overall equation is, however, a gross simplification with the actual reaction mechanism involving many free radical chain reactions. Gas-phase

combustion can only occur within given flammability limits, and the temperatures produced during combustion can be higher than 1600^{o}C, where the direct combination of nitrogen and oxygen to unwanted nitrogen oxides could occur [60].

The general pattern of catalytic combustion is shown in Figure 2.8. The reaction approaches the complete conversion of one or both reactants and the heat generated from the combustion results in a significant increase in catalyst temperature. Therefore, the stability of catalysts at high temperatures is deeply concerned. An on set oxidation at temperature relates to the hydrocarbon and nature of catalyst, followed by an exponential increase of conversion in zone B resulting from heat generated by combustion which is much greater than heat supplied. In the zone C corresponds to mass controlled until the reactants are completed in zone D.

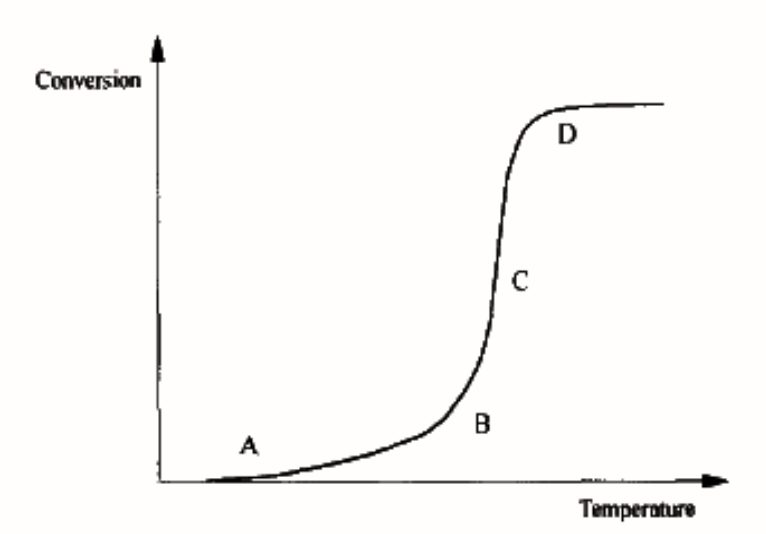

Figure 2.8 General pattern between conversion and temperature of catalytic combustion [61]

In addition, the light-off temperature is an important parameter for catalytic oxidation, which refers to temperature at the mass transfer controlled reaction (Zone C in Figure 2.8). In addition, the geometry of the catalytic combustor together with the porosity of the catalyst support has a significant effect in this region.

CHAPTER III
LITERATURE REVIEWS

This chapter presents previous studies related to light hydrocarbon oxidation with conventional catalysts and non-Faradaic electrochemical modification of catalytic activity (NEMCA) or electrochemical promotion of catalysis (EPOC) for several reaction types. Literatures are summarized in this section.

3.1 Hydrocarbon oxidation by conventional catalysts

Many researchers have paid attention on the catalytic oxidation of hydrocarbons and the enhancement of the catalytic activity and selectivity of precious metals, i.e. the effect of support materials, the effect of particle size, and the effect of additive promoters [59, 62, 63]. It can be concluded that Pt is recognized as the most active and widely used for propane combustion, whereas Pd is more active for methane oxidation [58].

Bara et al. [64] studied the catalytic oxidation of both CH_4 and C_3H_8 over synthesized nanoparticle of Pt, Pd, Ag, and Au on α–Al_2O_3 by using the temperature programmed reaction technique in a packed-bed tubular reactor. It was concluded that both Ag/Al_2O_3 and Au/Al_2O_3 require much higher temperature operation than the others for complete conversion. Pd/Al_2O_3 was observed as a good catalyst for CH_4 oxidation, whereas Pt/Al_2O_3 was observed as the most active for C_3H_8 oxidation. Yazawa et al. [59] studied the support effect over palladium catalyst for propane combustion by using several support materials: MgO, ZrO_2, Al_2O_3, SiO_2, SiO_2–ZrO_2, SiO_2–Al_2O_3, and SO_4^{2-}–ZrO_2. The result exhibited the significantly different catalytic activity upon the different kinds of the support material; the maximum conversion was obtained by a support material with moderate acid strength, here for Pd/SiO_2–Al_2O_3. It corresponded to the sequence acid strength of the support materials measured by Hammett indicators. Moreover, the catalytic activity was varied with both support materials and additives. The catalyst on the more acidic support showed a higher activity, and the catalytic activity on each support material was increased by the increase of electronegativity of additives, while some additives had a negative

effect on the activity, where the catalytic activity was decreased [63]. Pt/MgO, Pt/Al_2O_3, and Pt/SiO_2-Al_2O_3 were investigated. They showed a high activity. Moreover, Yazawa et al. [65] studied the oxidation state of palladium over SiO_2-Al_2O_3. It was found that the state of palladium also had an effect on the catalytic activity. In addition, the enhancement of the intrinsic catalytic activity was obtained by the addition of the additive including tungsten and molybdenum into the support [66]. It was also found that the introduction of vanadium to Pd/Al_2O_3 could improve the catalytic activity for propane combustion.

There are several investigators [67-70] reporting that the sulfated species on the catalytic surface could promote the catalytic combustion of propane over Pt/γ-Al_2O_3. Their works revealed that the sulfation attributed to the reduction and partial sintering of PtO_2 which is inactive for propane oxidation [67]. The presence of SO_2 had a strong effect on catalytic activity of the alumina-supported catalysts, whereas it had no effect on silica-supported catalysts.

Further to a high cost and limitation of noble metals [21], there are many efforts to develop or use low cost materials, i.e. copper and manganese oxide for carbon monoxide and hydrocarbon oxidation [19, 71-73]. Lahousse et al. [74] compared the activity of MnO_2 and Pt/TiO_2 catalyst for VOCs elimination. It could be concluded that manganese oxide was less active than precious catalysts. However, Cu-Mn mixed oxides catalyst was investigated for total oxidation of ethanol and propane by Morales et al. [73]. The better performance was observed in Cu-Mn than the bulk Mn_2O_3 and CuO (prepared by the same method). Recently, propane oxidation had been successful using Cu-Mn oxide mixed catalyst [19]. The Cu-Mn mixed oxides at various Cu/Mn ratios prepared by co-precipitation method was examined. It was found that mixed phase of Cu-Mn oxide exhibited higher activity than CuO and Mn_xO_y single phase catalyst.

Therefore, it can be concluded that propane combustion is the structure sensitive reaction.

3.2 Non-Faradaic electrochemical modification of catalytic activity (NEMCA) or electrochemical promotion of catalysis (EPOC)

Vayenas et al. [22, 75] first demonstrated the non-faradaic electrochemical modification of catalytic activity (NEMCA) or electrochemical promotion of catalysis (EPOC) that can enhance the catalytic performance either activity or selectivity for oxidative reaction. Most of studies have been focused on preparation methods and modification of catalyst-electrodes as well as the numerous on surface science techniques for the investigation of origin on this phenomenon. The electrochemical promotion has an effect on a variety of catalytic reaction systems (oxidation, hydrogenation, dehydrogenation, isomerization, decomposition) without limitation of the class of solid electrolyte supports [11, 76].

3.2.1 Non-Faradaic electrochemical modification of catalytic activity (NEMCA) for hydrocarbon oxidation

There are many effords to investigate the origin of electrochemical promotion by several surface techniques and a small hydrocarbon molecule, e.g. CH_4, C_2H_4, and so on served as the model reactions. Because the catalytic and chemisorptive properties of metal film over solid electrolyte or mixed ionic conductors can affect the electrochemical promotion [43]. The result was shown that C_2H_4 and other light hydrocarbons such as CH_4, C_2H_6, C_3H_8 or even alcohol like CH_3OH and C_2H_5OH exhibited the electrochemical promotion effect under polarization at appropriated operating conditions. In addition, C_2H_4 is one of the mostly used hydrocarbons for electrochemical promotion study with various materials of catalyst-electrodes (both metals (Pt, Rh, Pd, etc.) and metal oxides (IrO_2, RuO_2, etc.)) deposited on solid electrolyte supports. Table 3.1 summaries kinetic studies of ethylene oxidation of Pt catalyst-electrode upon different operating conditions exhibiting the different electrochemical promotion behaviors.

Table 3.1 Kinetic data from isothermal studies of ethylene oxidation on Pt/YSZ

Catalyst	T/^{o}C	Pressure /kPa		Reaction order		E_{ac}/ kJmol^{-1}	EPOC Rule	Ref.
		C_2H_4	O_2	C_2H_4	O_2			
Pt paste	260-450	3-15	5-30	+1 (low p) 0 (high p)	0 +1	25 70	(/) (\)	[77] [78]
Pt paste	300-450			+1 (low p) 0 (high p)	0 +1	46-109 8-25	(/) (\)	[79]
Highly dispersed Pt/YSZ deposited on Au film	425	0.1-2.2	1-17	+1 (low p) 0 (high p)	0 +1	43-63 38	(/) (\)	[80]
Pt paste	280-480	0.19	8.2	n.s.	n.s	n.s.	<T:(/) >T:(⇳)	[81] [82]
Pt PLD[1]	375	0.19	8.2	n.s.	n.s.	n.s.	(/)	[83]

[1] PLD pulsed laser deposition: the Pt film was partially porous.

(/) Electrophopic, (\) Electrophilic, (‿) volcano, (⇳) inverted-volcano behavior

The catalytic and electrocatalytic oxidation of CH_4 on Pd/YSZ was studied at temperatures 550-750^{o}C at the stoichiometric by Athanasiou et al. [84]. The study focused on the oxidative state of palladium during CH_4 reaction via solid electrolyte potentiometry (SEP). It was found that the enhancement in the catalytic rate was up to 30% with increasing catalytic potential. The investigation of the origin of NEMCA on CH_4 oxidation over Pt/YSZ [43] and C_2H_4 oxidation over Rh/YSZ [85] via AC impedance spectroscopy revealed the presence of charged backspillover which reflects the creation of an effective double layer over the entire gas exposed electrode surface [43]. The temperature program desorption (TPD) and the work function measurement are also the methods for monitoring the origin of electrochemical promotion [86]. In the case of temperature program desorption (TPD), it was found that the two-oxygen adsorption state existed on the surface including strongly bonded anionic oxygen and weakly bound atomic oxygen. Scanning tunneling microscope (STM) was also used to confirm the back spillover mechanism of electrochemical promotion and metal support interaction (MSI). The surface of Pt (111) single crystals over YSZ and β"-Al_2O_3 under atmospheric pressure was investigated [87]. In the both cases, the form of (12x12) hexagonal structure on the Pt(111) is related to the

reversible electrochemically controlled dosing (backspillover) of O^{2-} and Na^{+} species on Pt(111) surface.

C_3H_8 oxidation was investigated by using Rh and Pt catalyst-electrode deposited on YSZ both in fuel cell type and single pellet type reactor. Depending on the operating conditions, the different behaviors were found consisting of inverted-volcano and electrophobic behaviors. Vernoux et al. [88] first investigated the electrochemical promotion of propane and propene over Pt/YSZ. The different electrochemical promotion behaviors between propane and propene were found, here for propane oxidation exhibited the electrophobic behavior, whereas propene showed the electrophilic behavior resulting from strong adsorption of alkene and weak adsorption of alkane under 300-600^{o}C. Bultel et al. [89] studied the surface oxidation state of Pt during the catalytic reaction of propane and propene combustion as well as NO reduction by C_3H_6 via solid electrolyte potentiometry and cyclic voltammetry. These techniques evidenced that propane has a relatively small effect on the oxygen exchange between gas phase and Pt surface. The presence of propene weakened the strength of Pt-O, whereas the disappearance of Pt-O on the catalyst surface is due to the addition of NO. Kotsionopoulos et al. [11] reported the electrochemical promotion of propane oxidation on Pt and Rh deposited on YSZ. They found that the electrochemical promotion had strong effect on this reaction in both Pt and Rh as well as the increased oxygen consumption rate could exceed the rate of oxygen pumping taking value up to 1350 times and in the case of Pt, by up to 6 in the case of Rh. The inverted-volcano type behavior was found under the reducing condition. The thermodynamic activity of oxygen adsorbed on the catalyst surface during propane oxidation reaction was studied by Kokkofitis et al. [15]. The use of reaction kinetics and SEP technique provided the inverted-volcano behaviour because the reaction become pronounced for both positive and negative potential applications. The impedance spectroscopy was used to investigate the electrical and electrochemical properties of porous Pt-YSZ composites prepared by impregnation method followed by isostatic pressing [57]. It was concluded that the Pt dispersion acted as the obstacle for transferring ionic substrates and they did not find any electrochemical promotion in their operating conditions with porous Pt-YSZ pellet.

There were some researchers [90, 91] focusing on the effect of electrochemical promotion of propane oxidation over Na^+ conductor, i.e. β"-Al_2O_3. They used the similar method to an O^{2-} conductor including SEM, linear sweep, voltrametry, and cyclic voltrametry. It was shown that the behavior was similar to O^{2-} conductor, here for electrophobic behavior under stoichiometric condition under the temperature range of 220-440^{o}C.

In the recent years, many efforts have paid attention on the study of permanent electrochemical promotion (P-EPOC) of catalysis for light hydrocarbon oxidations including ethylene and propane oxidation over Pt catalyst-electrode deposited on YSZ [16, 92, 93]. It has been observed that P-EPOC could be originated from the oxygen storage at Pt/YSZ interface during anodic polarization [93]. The mechanism of P-EPOC was carried out using double step chronoamperometric and linear sweep voltammetric as the model of P-EPOC relating to location of oxygen storage as shown in Figure 3.1 and Figure 3.2 [48, 92, 93].

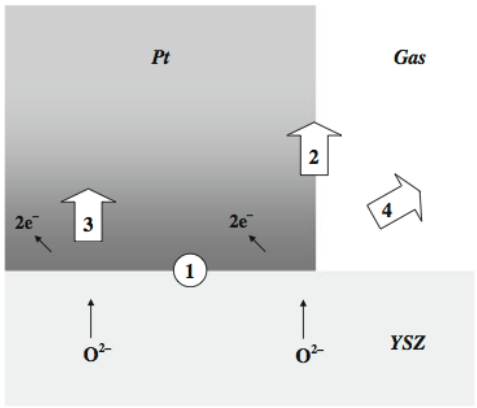

Figure 3.1 Schematic of the oxygen storage (1) at the Pt/YSZ interface (2) the gas expose the gas surface via backspillover (3) in bulk platinum via solid state diffusion (4) leaving to the gas phase [93]

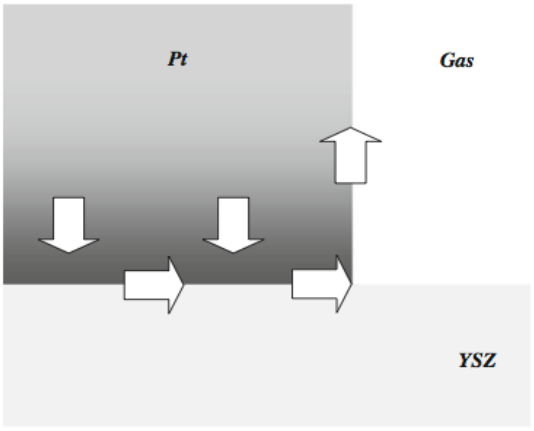

Figure 3.2 Schematic of the pathway of reappearance of the anodic generated hidden Pt-O promoters during open-circuit after current interruption [93]

Moreover, it was evident that the effect of pulse potential application led to the occurrence of P-EPOC because the electrochemical promotion is quite reversible [56]. Lizarraga et al. [16] studied the P-EPOC of nanometric sputtered Pt film comparing to pasted Pt. The sputtered-Pt presented a better result in electrochemical promotion owning to the greater dispersion of sputterd Pt particles and higher polarizability. On the other hand, no evidence of P-EPOC under their operating conditions (stoichiometric condition at T= 390^{o}C and 430^{o}C).

The use of metal oxide catalyst-electrodes, i.e. IrO_2 and RuO_2 had been studied in the ethylene combustion via temperature program and cyclic voltammetry measurements. It was found that the IrO_2 affected the electrochemical promotion relating to charged stored in the oxide catalyst [94]. In the case of RuO_2, higher state of ruthenium oxide could occur at the RuO_2/YSZ interface that influences the catalytic activity of ethylene oxidation and further study found the increase of catalyst work function which attributed to the decrease of the binding strength of adsorbed reactant and oxygen on the surface catalyst, hence an easier ethylene oxidation was observed. In addition, the electrochemical promotion of ethylene oxidation has been investigated by the application of TiO_2 interlayer over catalyst-electrode and electrolyte [95]. It has been found that TiO_2 thin layer led to a significant increase in the magnitude of the electrochemical promotion effect. It could be that the presence of the porous TiO_2 enhances the O^{2-} species transport onto the Pt catalyst surface.

Moreover, the use of TiO_2 as the interlayer between metal catalyst film and solid electrolyte was investigated in the selective oxidation of CH_4 with O_2 in order to produce syngas (CO and H_2) on the $Rh/TiO_2/YSZ$ system [96]. The particular behavior of having two stable states including an inactive (oxidized) and an active (metallic) state was observed. The results showed that the permanent electrochemical promotion provided the rate enhancement ratio up to 11 and CO selectivity of 45%. However, the different electrochemical promotion behavior was observed by the application of positive and negative current. In the case of negative current application was shown the electrochemical reduction of the rhodium oxide, whereas the application of positive current having the weakening of Rh-O binding is due to the broken of surface rhodium oxide. Another oxide served as a thin interlayer between solid electrolytes and metal catalyst film was CeO_2 owing to unique redox properties and a high oxygen storage capacity. The system had focused on C_2H_4 combustion over Pd/YSZ and $Pd/CeO_2/YSZ$ at 470-600^oC [1]. $Pd/CeO_2/YSZ$ illustrated a catalyst activity 14 times higher than Pd/YSZ due to good oxygen storage capacity of ceria and PdO formation.

Bebelis et al. [14] studied the effect of supports which are the ionic and mixed ionic conductor as well as promoting species in the ethylene oxidation reaction. It was found that these factors affected the electrochemical promotion. In addition, all supports were exhibited the electrophobic behavior under high $P_{O_2}/P_{C_2H_4}$, while the electrophilic behaviour was observed under low $P_{O_2}/P_{C_2H_4}$.

A proton conductor, Yittria-doped barium zirconia, $BaZr_{0.9}Y_{0.1}O_{3-\alpha}$ (BSZ) which is a mixed ionic conductor was reported by Poulidi et al. [97]. BSZ was chosen due to good mechanical and chemical stability at low temperature operating conditions [98]. The C_2H_4 oxidation was used as the model reaction and found that the reactive gas mixture ratio was the key parameter in the electrochemical promotion system. This system was shown both the electrophilic and electrophobic behavior in several gas mixture compositions. Balomenou et al. [99] reported that industries were interested in some reactions e.g., selective ethylene dehydrogenation, ammonia decomposition in several catalyst-electrodes and solid electrolyte supports. They set up the experiments using industrial reactions for the practical utilization of the electrochemical promotion to avoid the classical catalyst restrictions by increasing

catalyst electrode surface area and dispersion. In addition, there are many efforts to use an inexpensive metallic catalyst that their performance can be improved by electrochemical promotion of catalysis [30, 100, 101]. The use of silver catalyst for toluene combustion had been studied at relatively low temperature (T=310^{o}C) by Gaillard et al. [100, 101]. The small current application can enhance the faradaic efficiency up to the value of -13,000. In addition, they were successfully by silver direct impregnation over solid electrolyte and also found the electrochemical promotion effect [101].

3.2.2 The electrochemical promotion for other reactions

The electrochemical promotion has no limitation on any hydrocarbon oxidation or combustion. There are also many successful reactions on electrochemical promotion system, i.e. CO oxidation, NO reduction, either methanol or ethanol oxidation, CO_2 and CO hydrogenation, H_2S dehydrogenation, and so on.

CO oxidation is one of the environmental-concerned reactions where the electrochemical promotion was carried out using various noble metals catalyst-electrodes, i.e. Pt, Ag, and Ag-Pd alloy deposited on YSZ. It was found that the typical Faradaic efficiency was the order of 10^2-10^3, while the rate enhancement ratio was up to 5 in the case of Pt under oxidizing conditions at 550^{o}C [102]. In the case of Ag catalyst-electrode, the electophobic and electrophiilic behaviors were found under the different operating condtions [103], where the Ag-Pd alloy exhibited the electrophilic behavior giving the rate enhancement ratio up to 20 [104].

The electrochemical promotion of the reverse water gas shift reaction (RWGS) had been recently studied over Pt/YSZ at 650-800^{o}C [105] and over $Cu/SrZr_{0.9}Y_{0.1}O_{3-\alpha}$ at 550-750 ^{o}C [106]. In the case of Pt/YSZ, the rate enhancement ratio was up to 10. In the case of $Cu/SrZr_{0.9}Y_{0.1}O_{3-\alpha}$ higher reaction rate was observed, hydrogen was electrochemically supplied as H^+ rather than as gaseous hydrogen. Moreover, there was the reverse water gas shift reaction (RWGS) in the either YSZ or β"-Al_2O_3 system at temperature range of 533-605^{o}C [107]. In the case of Pd/YSZ, CO formation was enhanced by up to 6 times by applying either negative or positive potential and the inverted-volcano behavior was observed. In the later case

(Pd/β"-Al_2O_3), the CO formation rate was increased by supplying sodium over catalyst surface. Rate increasing up to 6.7 times was observed.

The ethylene epioxidation was carried out in β"-Al_2O_3, a Na^+ conductor [108] and YSZ, an O^{2-} conductor [109]. In the former case, the maximum selectivity to ethylene oxide was up to 88%, which was the highest value reported in patent. The later case, main product (ethylene oxide) selectivity was up to 55% and 78% for the negative potential and positive potential applications, respectively.

The oxidation of ethanol had reported over Pt/YSZ between temperature range of 300 and 350^{o}C [110]. The magnitude of electrochemical promotion was found up to 10^4. The result showed that the yield of acetaldehyde could be increased up to 700% at 300 ^{o}C and up to 540% at 325^{o}C.

NO_x decomposition which is the reaction involving the reduction of NO_x with various reducing agents like H_2, NH_3, CO, hydrocarbon and so on is one of the major environmental importance in order to reduce the toxic emission. The electrochemical promotion of catalysis had strong effect on the performance of metal catalyst for NO reduction including Rh, Pd, and Pt. This promising method exhibits the better enhancement in the aspect of the reducing these pollutants to N_2, which is environmental friendly gas. The reduction of NO by C_3H_6 was successfully in Rh/YSZ/Au via single pellet design reactor at 380^{o}C by Pliangos et al. [111]. The product selectivity to N_2 was significantly affected by positive potential application. Catalytic rate enhancement was up to 15000% and 600% for C_3H_6 oxidation and NO reduction, respectively. In the case of CO acted as the reducing agent, the rate enhancement of NO dissociation and also promote the rate of N_2 formation together with the light-off temperature down to 260^{o}C [112]. There are great efforts to reduce the use of precious metal, i.e. Rh, thus the bimetallic Rh-Ag/YSZ were used in the NO reduction by C_3H_6 under lean burn conditions by Williams et al. [113]. The selectivity of N_2 was improved from 28 up to 55% in comparing of Rh/YSZ and Rh-Ag/YSZ. Moreover, a Na^+ conduction such as NASICON was also used in selective catalyst reduction of NO by C_3H_6 on Pt catalyst-electrode [114]. The result exhibited the great enhancement of the catalytic activity and selectivity to N_2. The application of -100 mA, the selectivity of N_2 was reached to 61%. Recently, electrostatic spray deposition was used for low Pt loading in order to reduce costs and also get better Pt

dispersion in the selective reduction of NO by C_3H_6 [115]. This kind of catalyst was found to be effective for NO reduction by C_3H_6.

Dorado et al. [116, 117] studied the effect of temperature on the reduction of NO under lean burn conditions with Pt catalyst-electrode in fuel cell type reactor. It was found that the temperature had an effect on the effective of the electrochemical promotion, leading the rate enhance ratio up to 1.4 with electrophilic behavior where the rate increase by the application of negative potential at 220^{o}C. During the increase of temperature, the catalytic activity was decreased resulting from oxygen coverage on the catalyst, which leads C_3H_6 adsorption inhibition. They also studied a Pt impregnated catalyst film deposited over a Na^+ conductor, β"-Al_2O_3 [117]. The result showed that the presence of sodium promoters enhanced the selectivity to N_2 with the increasing N_2 rate by a factor of 1.8. However, There have been no studies on the electrochemical promotion for the reduction of nitrous oxide until Lucas-Consuegra et al. [118]. They discovered better selective catalytic reduction of N_2O by C_3H_6 over a K^+ conductor, β"-Al_2O_3. They had focused on the influence of reaction conditions including temperature, oxygen concentration, water vapor presence, and time on-stream on the catalytic performance. It was found that the increase of oxygen concentration had negative effect on this system resulting from an inhibition of C_3H_6 adsorption. On the other hand, the presence of potassium ion on Pt catalyst surface, the catalytic activity was increased owing to decreasing in effect of water vapor.

CO and CO_2 hydrogenations are reaction of interest nowadays. From previous study, CO_2 hydrogenation was carried out on Rh/YSZ [119], whose main products were CH_4 and CO under atmospheric pressure at temperature range of 300-500^{o}C. Depending on the product occurrance, the electrophobic and electrophilic were observed, where CH_4 formation is electrophobic, while CO formation is electrophilic behavior. The observed increase of CH_4 formation and concomitant decrease of CO formation by increasing catalyst potential is remarkable result. In the case of Pd/YSZ [119] under a total pressure of 12.5 kPa and temperature range of 330-370^{o}C, various products were observed, i.e. hydrocarbon, alcohols, and aldehydes. It was found that the catalytic activity and selectivity could be affected by electrochemical promotion operating conditions. Moreover, similar result was observed, where the different electrochemical promotion behaviors were obtained depending on the products.

The electrochemical promotion can even affect the H_2S dehydrogenation which decomposes H_2S to H_2 and S_2 over Pt catalyst-electrodes under 600-750°C at atmospheric pressure [120]. The electrophobic behavior was found with the rate enhancement ratio up to 11.

From the above mentioned, one can conclude that electrochemical promotion is very beneficial option relating to modify the catalytic activity and selectivity for many environmental concerned problems.

CHAPTER IV

EXPERIMENTAL

This chapter presents the electrochemical promotion of catalysis experiment in different catalyst electrodes. First of all the descriptions of material and catalyst preparation are provided including metal-pasted method, metal sputtering, and metal impregnation. Second, the methods of catalytic activity measurement are explained. Third, the characterization of catalyst electrode including XRD and SEM was performed to identify phase and surface morphology, respectively. The last part descries about the details of equipment, e.g. reactor, mass flow controller, and gas analyzes (CO_2 analyzer).

4.1 Materials and catalyst preparation

Six different catalytic films have been prepared and investigated: Pt/YSZ, Pd/YSZ, Ir/YSZ, Ru/YSZ, Cu/YSZ, Pd with a Mn_xO_y interlayer/YSZ and Mn_xO_y/YSZ.

The solid electrolyte was a pellet of 8 mol% yttria-stabilized zirconia (YSZ) of 18 mm diameter and 1-2 mm thickness provided by Ceraflex and Ortech. Prior to Pt, Pd, Ir, Ru, Cu, Au or Mn_xO_y deposition, no surface treatment was performed. Inert gold counter and reference electrodes were deposited on one side of the support before the working catalyst-electrode was applied. Gold behaves as a good pseudo-reference electrode, since previous NEMCA studies have shown a small variation of its potential (<0.1V) over the range of gaseous compositions used in the present study [9].

4.1.1 Pasted catalyst-electrode preparation

The Pt catalyst-electrode was deposited on an yttria-stabilized zirconia (YSZ) disk by application of a thin coating of Engelhard A-1121 Pt paste followed by calcination in air at 830°C for 1 hr. The metal film used exhibits adequate conductivity for NEMCA experiments, since its in-plane resistance was in the range

of 5-20 Ω [9]. The superficial surface area of the Pt catalyst on YSZ was 1 cm^2. The true surface area, (expressed in surface mol of Pt, N_{Pt}), estimated from the catalytic rate transient time constant, τ, during galvanostatic transients (C_2H_4 oxidation) via the expression $\tau=2FN_{Pt}/I$ [9], was found to be 1.5 to $2.8 \cdot 10^{-8}$ mol Pt.

Gold was served as the reference and counter electrodes, which were deposited on the other side of YSZ disk using Engelhard A-1118 Au paste followed by calcination in air at 750°C for 1 hr [9, 14]. Blank experiments were carried out to confirm that the catalytic activity of the Au electrodes was negligible in comparison to that of the Pt catalyst.

4.1.2 Sputtered catalyst electrodes preparation

All the metal electrodes were deposited by DC megnatron sputtering, which provides thin, well-adhered and homogeneous films.

The Sputtered Pd films, which were served as working electrode, were directly deposited on the YSZ substrate (Pd/YSZ) and on Mn_xO_y interlayer previously deposited over YSZ substrate (Pd/Mn_xO_y/YSZ). A pure Pd (99.95%) target provided by Mateck GmbH was used for sputtering target. The sputtering conditions were the following: direct (dc) mode with discharge of 376 V (P=209W). Substrate temperature was kept at 50°C and the sputtering chamber was filled with the pure argon. Pd loading was measured by weighting the sample and was 0.8 ± 0.1 mg Pd. The geometric surface area of the sputtered Pd working electrode was 1.88 cm^2.

The sputtered Ir film, which was served as working electrode, was deposited on YSZ substrate. A pure Ir (99.95%) target provided by Mateck GmbH was used for sputtering target. The sputtering conditions were the following: direct (dc) mode with discharge of 479 V (P=232W). Substrate temperature was kept at 50°C and the sputtering chamber was filled with the pure argon. Ir loading was measured by weighting the sample and was 0.9 ± 0.1 mg Pd. The geometric surface area of the sputtered Pd working electrode was 1.88 cm^2.

The sputtered Ru, which was served as working electrode, film was deposited on YSZ substrate. A pure Ru (99.95%) target provided by Mateck GmbH was used for sputtering target. The sputtering conditions were the following: direct (dc) mode with discharge of 336 V (P=162W). Substrate temperature was kept at 50°C and the

sputtering chamber was filled with the pure argon. Ru loading was measured by weighting the sample and was 0.8 ± 0.1 mg Pd. The geometric surface area of the sputtered Ru working electrode was 1.88 cm^2.

The sputtered Cu film, which was served as working electrode, was deposited on YSZ substrate. A pure Cu (99.95%) target provided by Mateck GmbH was used for sputtering target. The sputtering conditions were the following: direct (dc) mode with discharge of 433 V (P=238W). Substrate temperature was kept at 50^oC and the sputtering chamber was filled with the pure argon. Cu loading was measured by weighting the sample and was 0.6 ± 0.1 mg Pd. The geometric surface area of the sputtered Cu working electrode was 1.88 cm^2.

Gold sputtered deposition was served as the counter and reference electrode. A pure Au (99.95%) target provided by MatecK GmbH was used for sputtering target. Substrate temperature was kept at 50^oC and the sputtering chamber was filled with the pure argon. The sputtering conditions were the following: direct (dc) mode with discharge of 455 V (P=250W).

The summaries of their estimated thickness, based on their mass and density is shown in Table 4.1.

Table 4.1 Sputtering deposition thickness for the catalyst-electrodes (Pd, Ir, Ru, Cu, and Au)

Metal	**Thickness / nm**
Pd	354
Ir	212
Ru	342
Cu	356
Au	303

4.1.3 Mn_xO_y interlayer preparation

The Mn_xO_y films were prepared by an impregnation technique, which consisted of two main steps including deposition and thermal decomposition of a Mn precursor of Manganese(II)nitrate hydrate, $Mn(NO_3)_2xH_2O$ (metal basis) in the form of crystalline aggregates. Initially, 20 mM of a precusor was prepared and then deposited on YSZ substrate using a plastic circular mask in order to obtain approximately 2 cm^2 surface area of catalytic film. Then the solvent was evaporated by keeping at 100^oC for 1h, followed by calcined at 200^oC for 2h. The final Mn_xO_y loading were measured by weighting the sample and was approximately 4.4 mg Mn_xO_y.

4.2 The catalytic activity measurement

The experiments were carried out in a continuous flow atmospheric pressure quartz reactor in which all three electrodes are expressed to the same gas mixture (single chamber), as illustrated in Figure 4.1, for more details as described elsewhere [9, 121, 122]. Reactant gases certified standard of 3.0% C_2H_4 in He (Air Liquide), 3.0% C_3H_8 in He (Linde), 20% O_2 in He (Linde) and He (L'Air liquid, 99.995% purity). Prior to the catalytic activity measurement, all catalyst electrodes except Pt catalyst electrode were pretreated under the reactive gas mixture of 1.2% C_3H_8 and 10% O_2 diluted in He at 450^oC for 2h and the total gas flow rate at 170 cm^3min^{-1} (STP).

Gas flow rates were maintained using Brook mass flow controllers connected to a 4-channel Brose control box (model 5878). The reaction temperature was monitored via a K-type thermocouple placed inside the quartz tube, and controlled via a JUMO (iTRON 08) temperature controller.

The behavior of the catalyst electrodes were investigated at temperature range of 250-450^oC and the gas composition in the range of 0.5 – 12 % O_2, 0.1-0.6% C_2H_4, and 0.2-1.8% C_3H_8 under the total flow rate of 170 cm^3min^{-1}(STP) for all experiments except Pt , the total gas flow through the reactor was 400 - 800 cm^3min^{-1}(STP).

In the case of Mn_xO_y/YSZ, the light-off experiment was only performed under a gas mixture of 1.2% C_3H_8 and 10% O_2 balanced by He at 450^oC for 2h (same as Pd, Ir, and Ru) under the total gas flow rate of 170 cm^3min^{-1} (STP).

In the case of Pd/Mn_xO_y/YSZ, the pretreatment was carried out before the

catalytic activity experiment under the same gas mixture and the total gas flow rate as Mn_xO_y/YSZ. All the catalytic activity measurement was performed at the range of 320-420^oC under the same gas composition in the range of 0.21-10% O_2 and 0.17-1.8% C_3H_8 under the total flow rate of 170 cm^3min^{-1}(STP).

Gas analysis of reactants and products was conducted via on-line gas chromatography (Shimadzu A14 with thermal conductivity detector, equipped with a Porapak column for separation of C_2H_4, C_3H_8, and CO_2 and a molecular sieve for the O_2 detection). The continuous measurement of CO_2 concentration was performed using the infrared analyzer Rosemount Binos 100.

4.3 Catalyst characterization

The external surface structure and morphology characterization of the Pt catalyst electrode were carried out by using a LEO-SUPRA 35VP field emission scanning electron microscope operated at 5 kV in high vacuum mode.

The external surface structure and morphology characterization of the different sputtered catalyst electrodes, i.e. Pd, Ir, Ru, and Cu were carried out by scanning electron microscopy (SEM) using a JEOL JSM-6300 microscope.

The crystalline phases of the Pd, Ir, Ru, and Cu catalyst electrodes and its YSZ support were examined by X-ray powder diffraction (XRD) performed in a PANalytical diffractometer equipped with a X'Celerator detector with monochromatic Cu Kα1 radiation (λ = 1.54 Å). XRD patterns were recorded in the 2θ range between 20^o and 80^o, with a scan step size of 0.017 and 610.5 s per step.

Constant currents or potentials were applied by means of a Solartron electrochemical interface 1286 (potentiostat/galvanostat). The overpotential, η, of the electrochemical cell can be calculated from

$$\eta = U'_{WR} - U^o_{WR} - IR_{ohmic} \qquad (4.1)$$

Taking into account the applied potential, U'_{WR}, the open circuit potential, U^o_{WR} and the total Ohmic resistance of the electrochemical cell via the IR-drop technique. The ohmic resistance of the sample, R_{ohmic}, was evaluated using AC impedance spectroscopy. The measurements were carried out using a Solartron high frequency response analyzer (module 1255). The frequency was varied under open

circuit conditions from 100 kHz to 1 mHz with an AC amplitude of 20 mV. The obtained Nyquist diagram (imaginary part of the impedance vs its real part) allowed the estimation of the ohmic resistance value by calculating the high frequency intersect of the high frequency semicircle with the x-axis (real part of the impedance) [9].

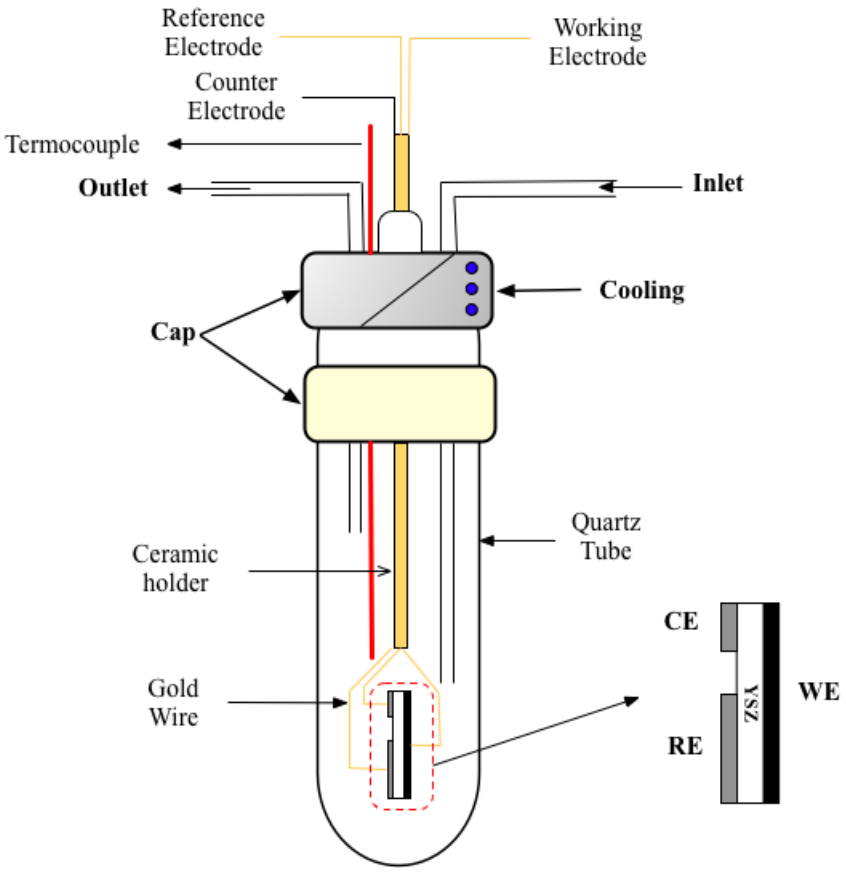

Figure 4.1 Single pellet design reactor configuration

.

CHAPTER V

RESULTS AND DISCUSSIONS

This chapter provides the results and discussion in three main sections consists of reaction kinetic induced changes in behavior of electrochemical promotion of deep ethylene oxidation on Pt/YSZ as shown in Section 5.1 and in the second part, the electrochemical promotion of deep propane oxidation on Pd, Ru, Ir, and Cu catalyst-electrodes deposited on yttria-stabilized zirconia catalyst as present in Section 5.2 and the last part in Section 5.3, the role of Mn_xO_y interlayer of Pd catalyst-electrode on propane oxidation is described.

5.1 The electrochemical promotion of deep ethylene oxidation on Pt/YSZ catalyst deposited on Yttria-stabilized zirconia catalyst

Ethylene oxidation on Pt/YSZ catalyst under the electrochemical promotion conditions has been studied in this present work on the reaction kinetics under the low temperature region to access electrochemical promotion behaviors, i.e. electrophilic, electrophobic, and volcano type behaviors. The details are described in following sections.

5.1.1 Catalyst Characterization

The surface morphology of Pt catalyst working electrode was investigated by SEM technique before it exposured to reactive gas mixture and polarization. The smooth surface with a good adherence was found as shown in Figure 5.1 and its porosity is adequate to facilitate the migration of O^{2-} promoter species from solid electrolyte support to the catalyst-electrode surface during the electrochemical promotion.

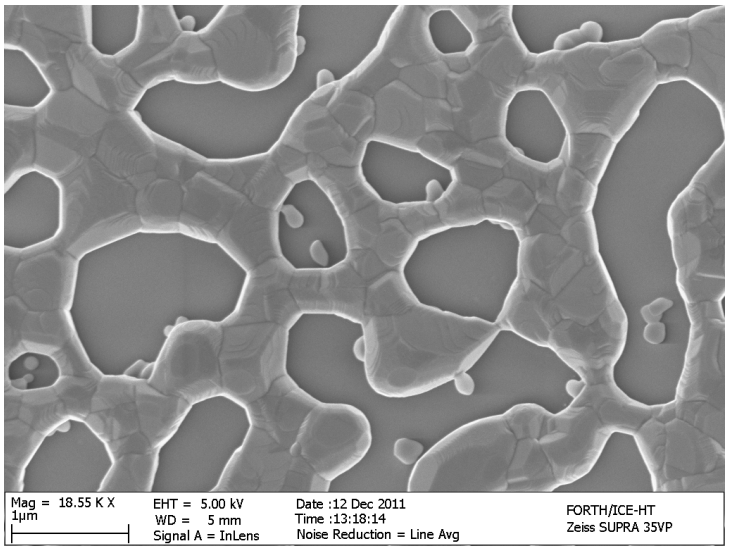

Figure 5.1 Surface image for the on top of the fresh Pt catalyst electrode deposited over YSZ

5.1.2 Steady state measurement

The effect of potential and reactants partial pressure (C_2H_4 and O_2) on the rate of CO_2 formation was investigated at 300-400^oC upon different feed gas compositions.

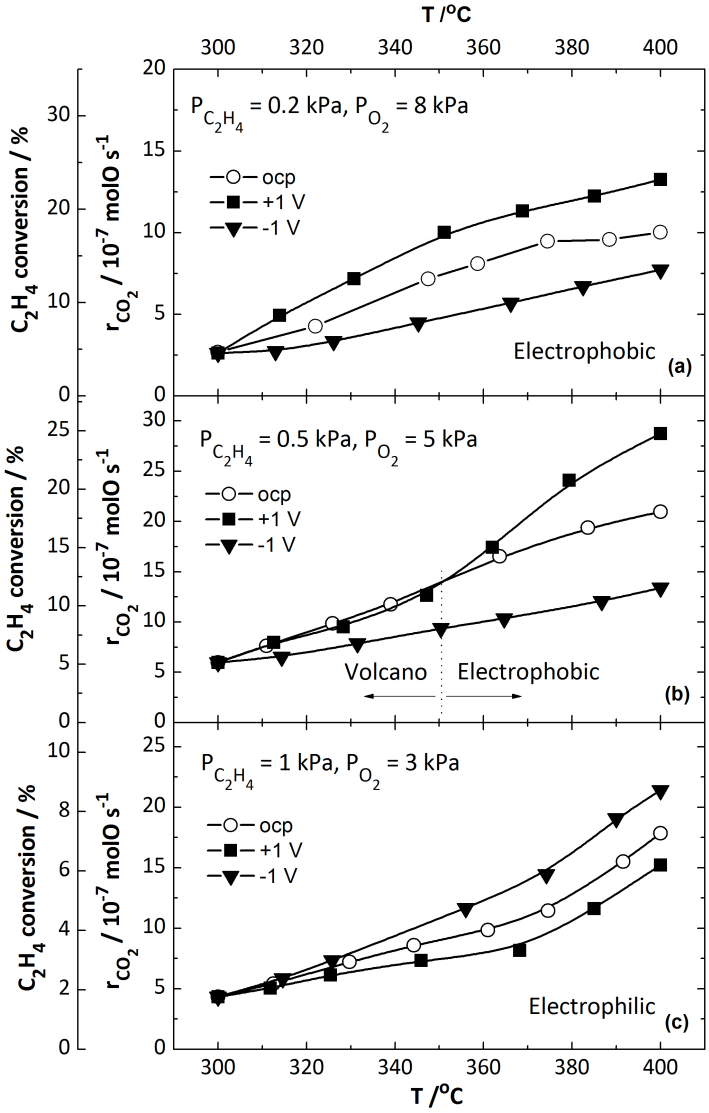

Figure 5.2 Steady-state effect of temperature on the CO_2 formation catalytic rate and on the corresponding ethylene conversion under open-circuit state and positive and negative ($\pm$1V) potential application conditions.

Feed condition: (a) $P_{C_2H_4}$ = 0.2 kPa, P_{O_2} = 8 kPa, (b) $P_{C_2H_4}$ = 0.5 kPa, P_{O_2} = 5 kPa, (c) $P_{C_2H_4}$= 1 kPa, P_{O_2} = 3 kPa, F_v = 400 cm^3min^{-1}(STP)

Figure 5.2 shows the effect of temperature on CO_2 formation rate and corresponding conversion of C_2H_4 under open-circuit state, and positive (+1V) and negative (-1V) potential application conditions at three different feed gas compositions; mildly oxidizing, slightly oxidizing and stoichiometric. As shown in

the figure, under mildly oxidizing conditions (a) a purely electrophobic type behavior is observed, i.e. rate increases with potential, which changes to purely electrophilic-type at stoichiometric feed (c). At the intermediate case (b), an electrophobic type behavior is observed at high temperatures (>350^{o}C), which shifts to volcano type at lower temperatures, where the rate is decreased in both positive and negative polarization.

According to the rules of electrochemical and classical promotion [9, 123], the observed electrophobic-type behavior at mildly oxidizing conditions can be attributed to the weakening in the Pt-O bond strength caused by positive potential application, i.e. O^{2-} supply to the Pt gas-exposed surface, which results in an increase in the work function of Pt. On the other hand, under stoichiometric conditions the rate increase by negative potential application can be attributed to the strengthening in the Pt-O bond strength. The latter indicates that Pt-O bond strength is weaker than that in the case of oxidizing condition and thus, negative potential application, i.e. work function decrease was found to result in a rate increase. The volcano type behavior observed at low temperature under slightly oxidizing condition can be attributed to strongly adsorbed oxygen and ethylene species on Pt surface. The inverted volcano type behavior was not observed in this study perhaps due to the low operating temperature.

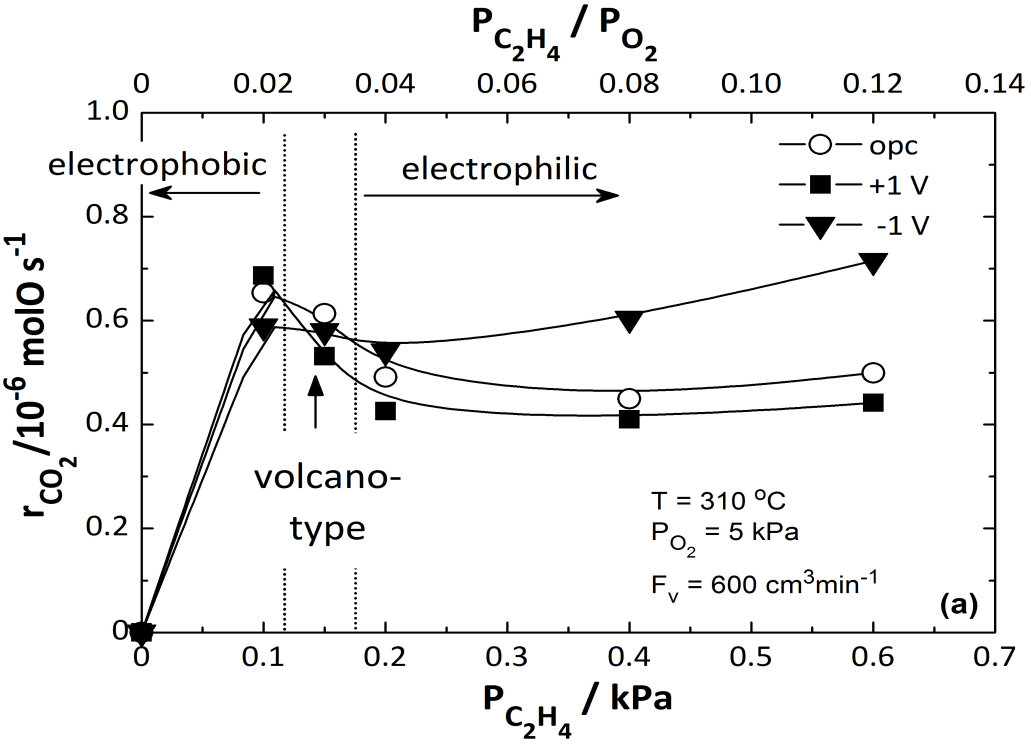
$P_{C_2H_4} / P_{O_2}$
0 0.02 0.04 0.06 0.08 0.10 0.12 0.14
electrophobic
electrophilic
opc
+1 V
-1 V
volcano-type
r_{CO_2} /10^{-6} molO s^{-1}
T = 310 °C
P_{O_2} = 5 kPa
F_v = 600 cm^3min^{-1}
(a)
0 0.1 0.2 0.3 0.4 0.5 0.6 0.7
$P_{C_2H_4}$ / kPa

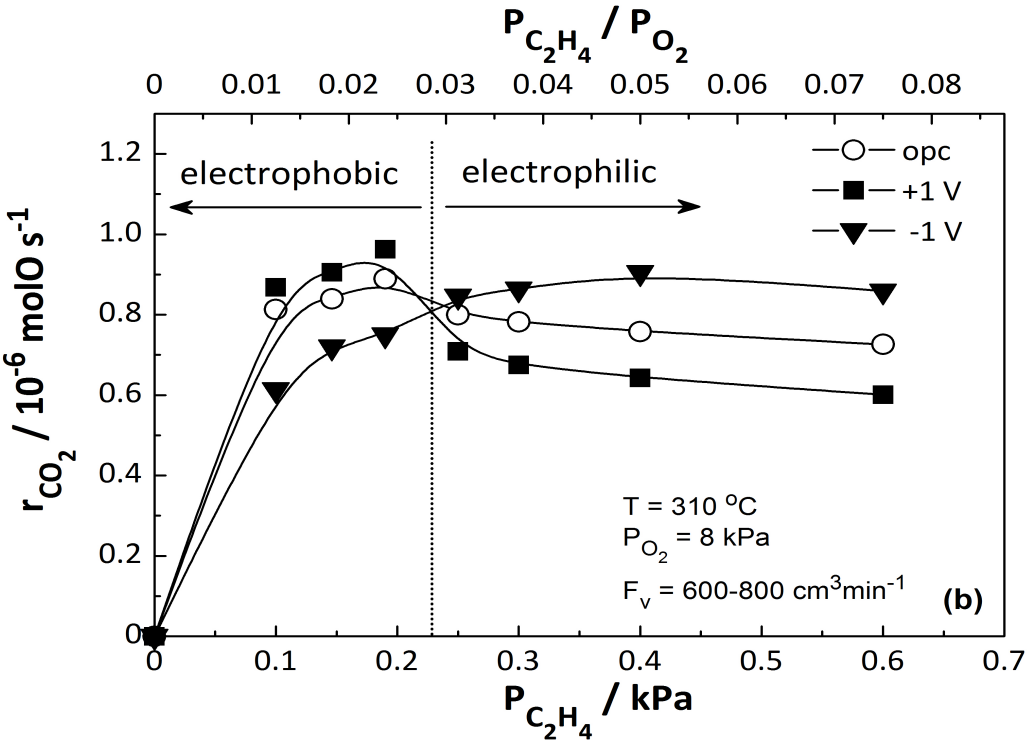
$P_{C_2H_4} / P_{O_2}$
0 0.01 0.02 0.03 0.04 0.05 0.06 0.07 0.08
electrophobic
electrophilic
opc
+1 V
-1 V
r_{CO_2} / 10^{-6} molO s^{-1}
T = 310 °C
P_{O_2} = 8 kPa
F_v = 600-800 cm^3min^{-1}
(b)
0 0.1 0.2 0.3 0.4 0.5 0.6 0.7
$P_{C_2H_4}$ / kPa

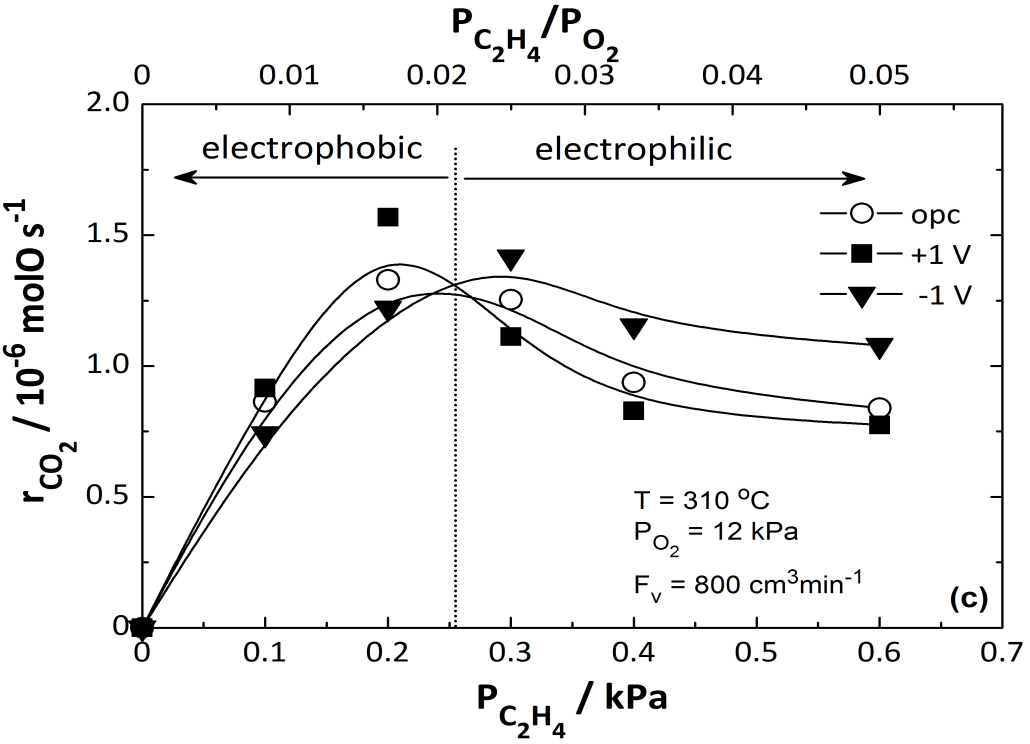

Figure 5.3 Steady-state effect of $P_{C_2H_4}$ on the CO_2 formation catalytic rate under open-circuit state and positive and negative (± 1V) potential application. Feed condition: (a) P_{O_2} = 5 kPa, (b) P_{O_2} = 8 kPa, (c) P_{O_2} = 12 kPa at T= 310°C

The effect of reactants partial pressure (C_2H_4 and O_2) on the rate of the C_2H_4 oxidation reaction was investigated at 310°C. Figure 5.3a shows the effect of $P_{C_2H_4}$ on the steady-state CO_2 formation catalytic rate under open circuit state and positive and negative potential application conditions at fixed P_{O_2} = 5 kPa. As shown in the figure, the catalytic rate exhibited a maximum at low ethylene partial pressures (~0.1 kPa) under open circuit state and positive potential application conditions, while it appeared slightly positive order dependence under negative potential application. Similar behavior was observed under higher P_{O_2} (8 kPa) as shown in Figure 5.3b. In this case only the electrophobic and electrophilic type behaviors were observed at low and high $P_{C_2H_4}$, respectively. Further increase of P_{O_2} to 12 kPa resulted in similar kinetic dependence in C_2H_4.

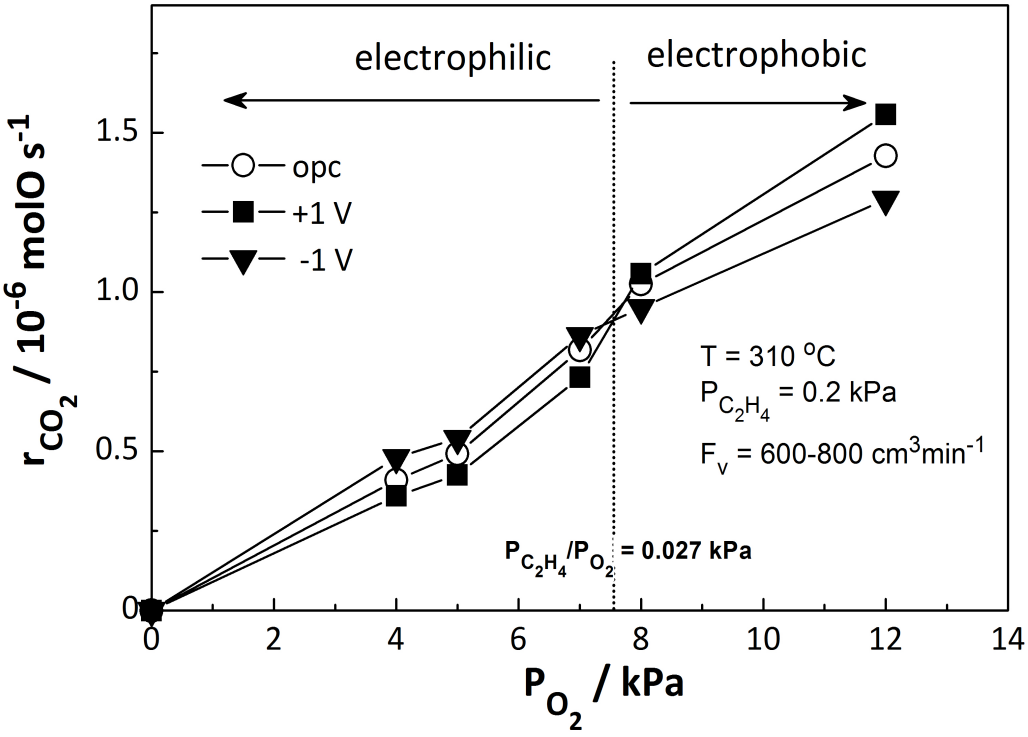

Figure 5.4 Steady-state effect of P_{O_2} on the CO_2 formation catalytic rate under open-circuit state and positive and negative (±1V) potential application. Feed condition: $P_{C_2H_4}$ = 0.2 kPa at T= 310°C

Figure 5.4 shows the effect of P_{O_2} on the steady-state CO_2 formation catalytic rate under open circuit state and positive and negative potential application conditions at fixed $P_{C_2H_4}$ = 0.2 kPa. As shown in the figure, the catalytic rate exhibited a positive order dependence under both open-circuit state and positive and negative potential application conditions. Worth noting is that electrophobic type behavior was observed under high P_{O_2} values, which shifted to electrophilic type under low P_{O_2}. This is in agreement with Figure 5.3, where a critical $P_{C_2H_4}/P_{O_2}$ at ~0.025 was observed at which EPOC behavior changes between electrophilic and electrophobic types behavior.

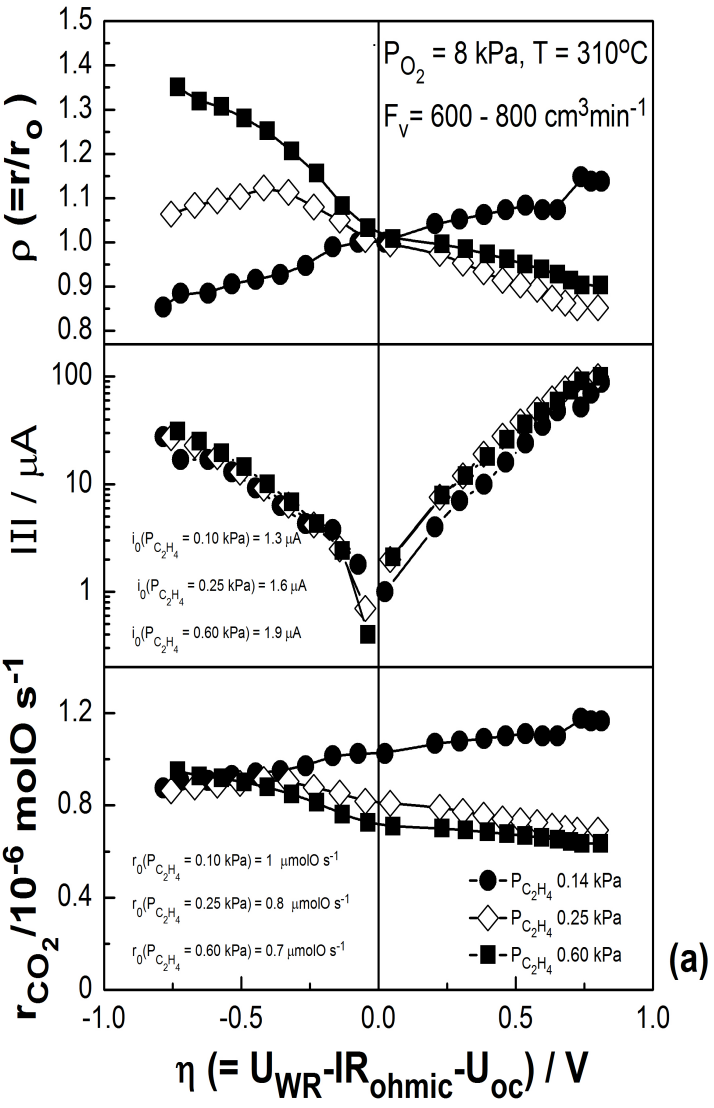
P$_{O_2}$ = 8 kPa, T = 310°C
F$_V$= 600 - 800 cm^{3}min^{-1}
ρ (=r/r$_o$)
|I| / μA
r$_{CO_2}$/10^{-6} molO s^{-1}
i$_0$(P$_{C_2H_4}$ = 0.10 kPa) = 1.3 μA
i$_0$(P$_{C_2H_4}$ = 0.25 kPa) = 1.6 μA
i$_0$(P$_{C_2H_4}$ = 0.60 kPa) = 1.9 μA
r$_0$(P$_{C_2H_4}$ = 0.10 kPa) = 1 μmolO s^{-1}
r$_0$(P$_{C_2H_4}$ = 0.25 kPa) = 0.8 μmolO s^{-1}
r$_0$(P$_{C_2H_4}$ = 0.60 kPa) = 0.7 μmolO s^{-1}
P$_{C_2H_4}$ 0.14 kPa
P$_{C_2H_4}$ 0.25 kPa
P$_{C_2H_4}$ 0.60 kPa
(a)
η (= U$_{WR}$-IR$_{ohmic}$-U$_{oc}$) / V

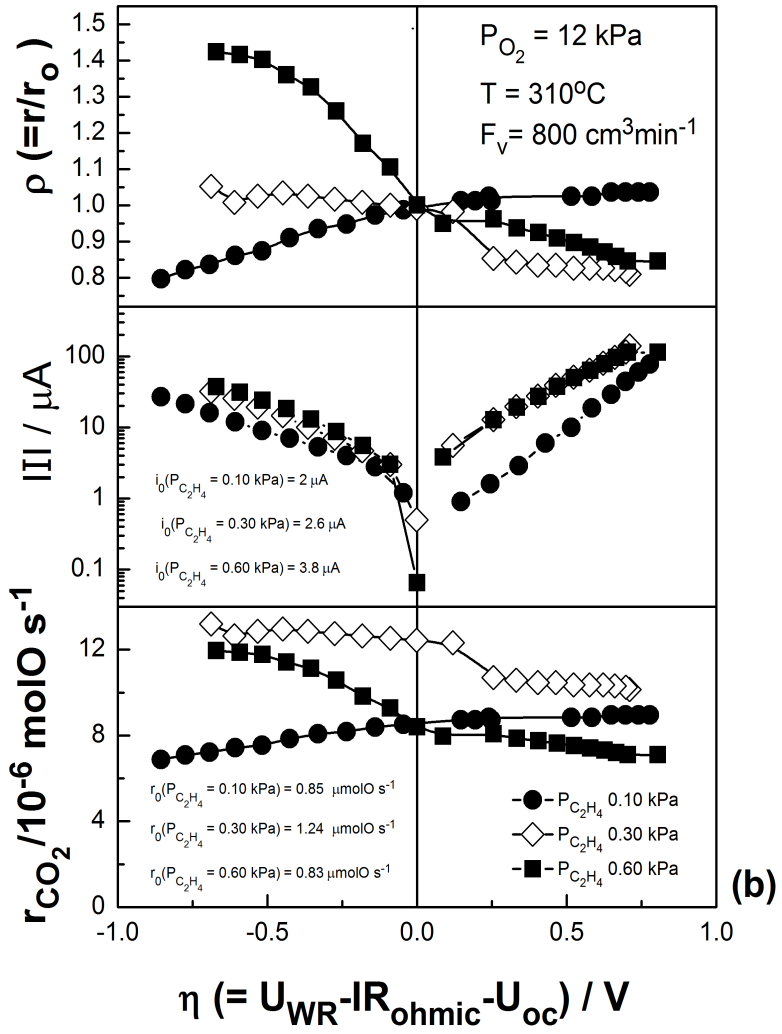

Figure 5.5 Steady-state effect of applied overpotential (bottom) on the CO_2 formation rate, (middle) on the current and (top) on the rate enhancement ratio, ρ, under different $P_{C_2H_4}$ feed. Feed condition: (a) P_{O_2} = 8 kPa and (b) P_{O_2} = 12 kPa, F_v = 600-800 cm^3min^{-1}(STP)

The effect of applied overpotential on the steady-state CO_2 formation catalytic rate (bottom), on the current (middle) and on the rate enhancement ratio, ρ, (top) is shown in Figure 5.5a (P_{O_2}=8 kPa), under three different $P_{C_2H_4}$ at 310°C. A positive effect of the overpotential on the CO_2 formation catalytic rate was found in the case of low $P_{C_2H_4}$, while a negative effect was observed at an intermediate and a higher $P_{C_2H_4}$,

in agreement with Figures 5.2 and 5.3. The rate enhancement ratio was as high as 1.2, i.e. 20% rate increase, in the case of low $P_{C_2H_4}$ where the electrophobic type behavior was observed. On the other hand, rate enhancement ratio, ρ, values up to 1.35 were recorded for the case of high $P_{C_2H_4}$, where an electrophilic type behavior was observed. Furthermore, it was found that there is no significant effect of $P_{C_2H_4}$ on the exchange current, i_0.

Similar effect of the overpotential on the CO_2 formation catalytic rate and EPOC behavior was observed at higher P_{O_2}, i.e. 12 kPa, as shown in Figure 5.5b. In this case the effect of positive potential application in each case was found to be smaller, while that of negative higher.

The effect of ionic current, I/2F, under potential application on the potential induced rate change of CO_2 formation is shown in Figure 6. For the case of P_{O_2} = 12 kPa (bottom) apparent Faradaic efficiency values for the formation of CO_2, Λ_{CO_2}, up to 2000 under positive potential application and up to -4500 under negative potential application were obtained. Furthermore, in the case of P_{O_2} = 8 kPa (top) apparent Faradaic efficiency values of CO_2 formation, Λ_{CO_2}, up to 3000 was obtained under positive potential application, while up to -3000 under negative potential application.

From Figure 5.6, the values of Λ are close to those estimated by the approximate equation (5.1) [9] :

$$\Lambda_{est} \approx \frac{2Fr_o}{i_0} \qquad (5.1)$$

Where i_0 is the exchange current and r_0 is the unpromoted rate of reaction.

The open-circuit, i.e. unpromoted catalytic rate as a function of the exchange current, i_0, is presented in Figures 5.7a (P_{O_2}=8 kPa) and 5.7b (P_{O_2}=12 kPa) under three different feed compositions at 310°C. As shown, in general, the higher the i_0 was, the lower the r_0. Worth noting is the good agreement between the Λ values measured by experiments and those estimated by Eq. (5.1).

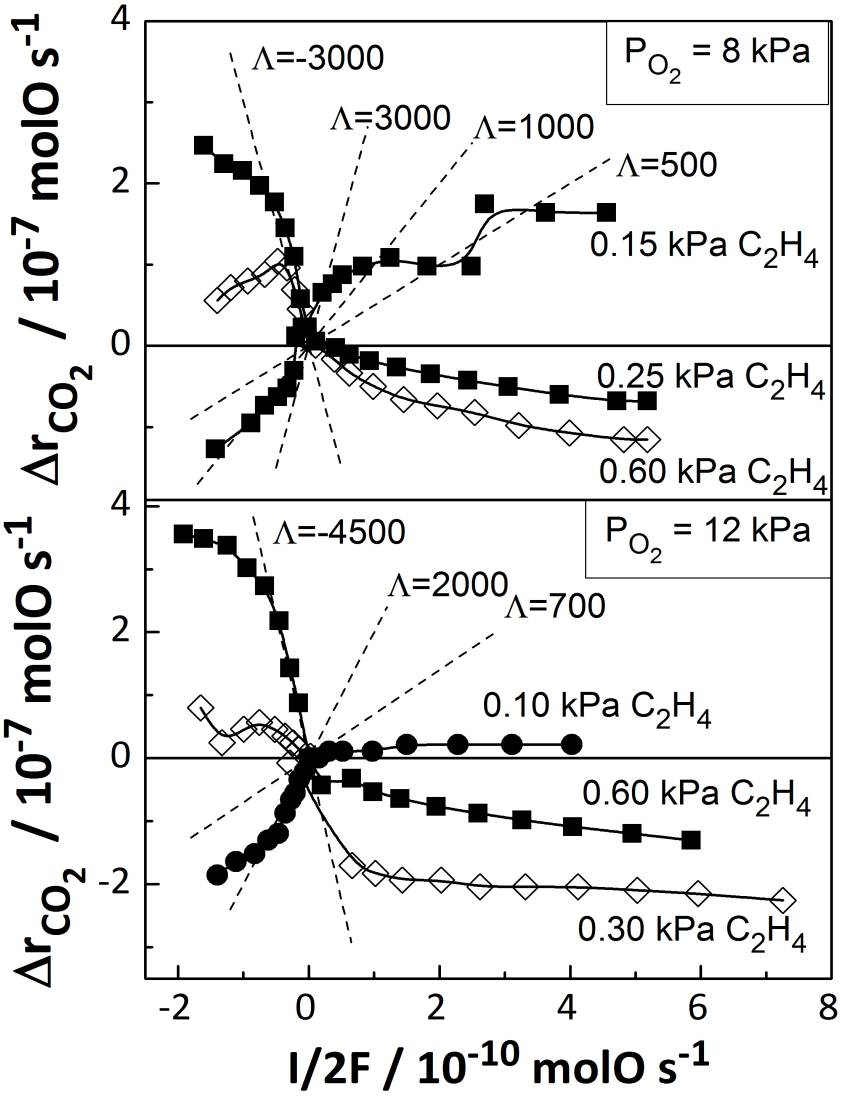

Figure 5.6 Effect of O^{2-} supply (I>0) or remove rate (I<0) to/form the Pt catalyst-electrode, on the rate change of CO_2, Δr_{CO_2}, under (a) P_{O_2} = 8 kPa and (b) P_{O_2} = 12 kPa. T = 310°C

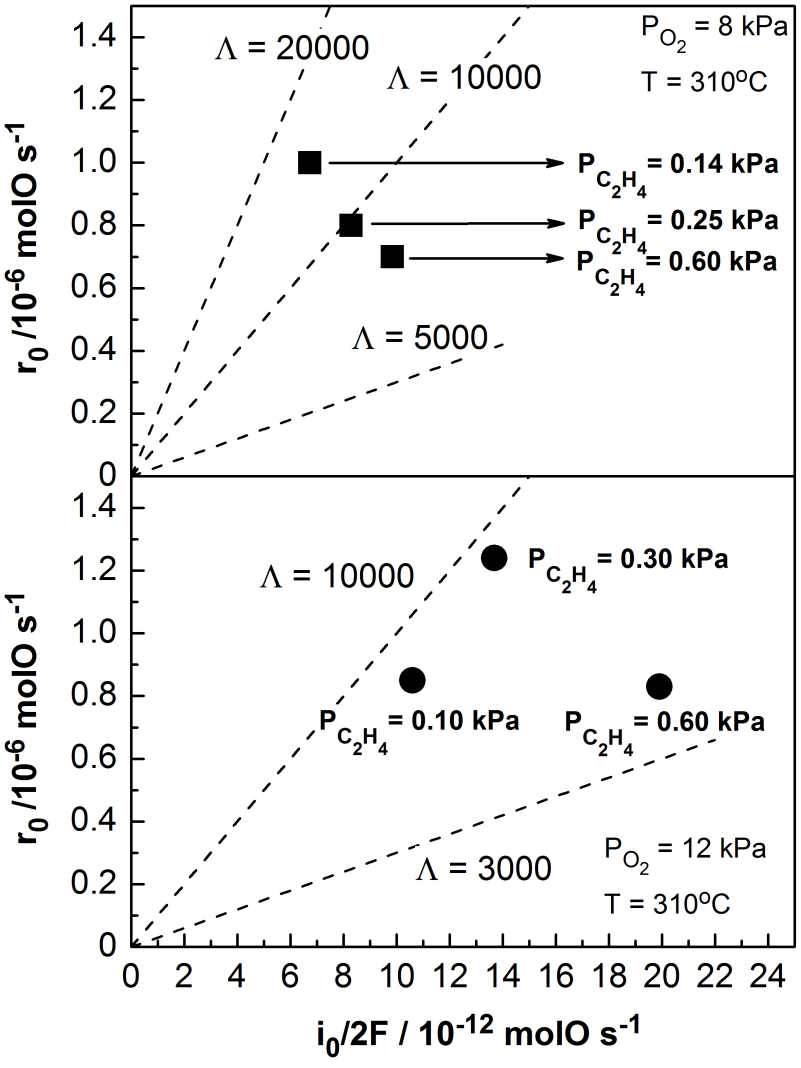

Figure 5.7 Open circuit catalytic CO_2 formation rate as a function of exchange current rate i_0/2F under P_{O_2}=8 (top) and 12 kPa (bottom). T = 310°C

Figure 5.8 shows the dependence of the apparent activation energy, E_{act}, of the C_2H_4 oxidation reaction on the applied overpotential at three different feed gas compositions: mildly oxidizing, slightly oxidizing and stoichiometric. The apparent activation energy of the reaction decreases with overpotential in the case of mildly oxidizing conditions where the electrophobic type behavior was observed, while it

increases in the other two cases where the electrophilic type (or combined electrophilic/volcano type behavior) was observed with the estimation of the apparent activation energies, E_{ac} in the range of 20 to 70 kJ/mol, which are in good agreement with previous isothermal studies and theory of EPOC [9, 78, 79, 81]. Table 5.1 summarizes the activation energy values for open circuit, positive and negative overpotentials.

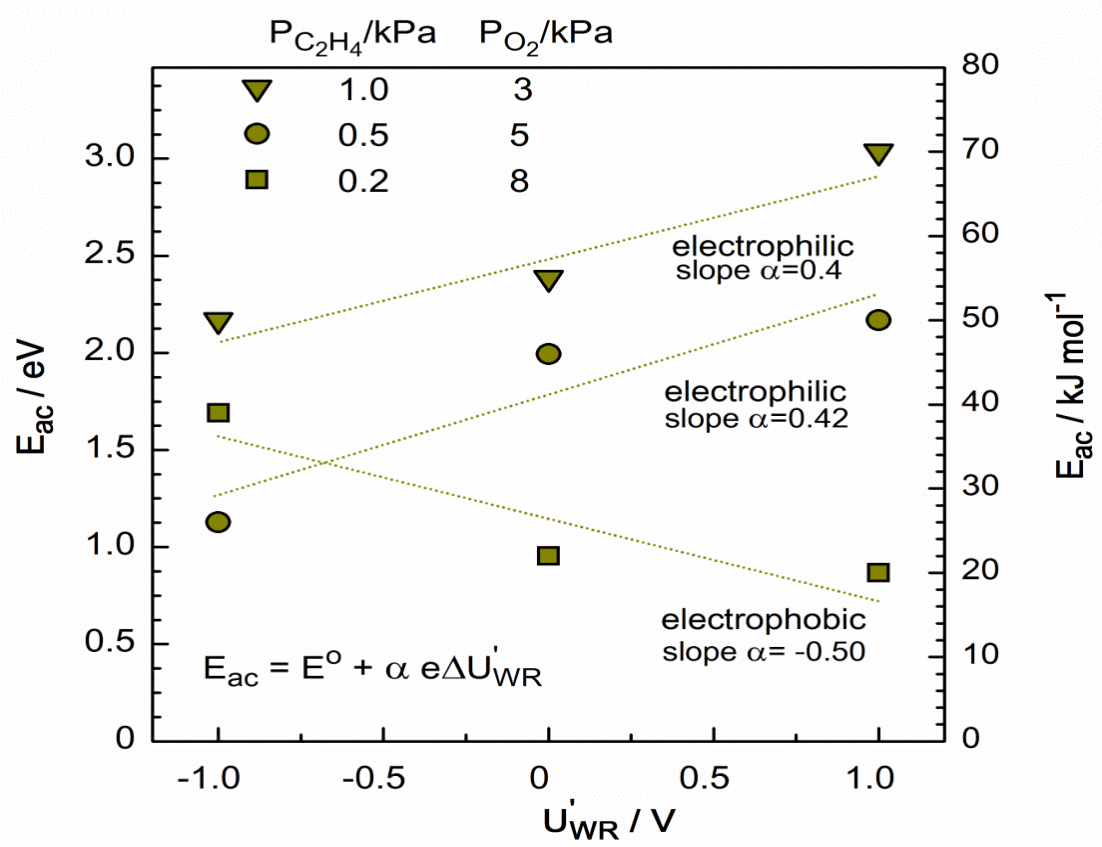

Figure 5.8 Steady-state effect of the applied overpotential on the apparent activation energy, E_{act}, of the C_2H_4 oxidation reaction, at different feed compositions

Table 5.1 Apparent activation energy of the C_2H_4 oxidation reaction on Pt/YSZ under open circuit state and positive and negative potential application at three different feed compositions (i) $P_{O_2}/P_{C_2H_4} = 40$, (ii) $P_{O_2}/P_{C_2H_4} = 10$, (iii) $P_{O_2}/P_{C_2H_4} = 3$

Feed composition	**E_{act} / kJ/mol**		
	Opc	**η = 0.81 V**	**η = -0.78 V**
$P_{O_2}/P_{C_2H_4} = 40$	22	20	39
$P_{O_2}/P_{C_2H_4} = 10$	46	50	26
$P_{O_2}/P_{C_2H_4} = 3$	55	70	50

From Figure 5.8, the apparent activation energy of the reaction decreases with positive applied potential with a slope of -0.5, i.e. under oxidizing conditions where electrophobic behavior is observed. The opposite is found for the potential dependence of E_{ac} for the cases where electrophilic behaviour (or combined electrophilic/volcano type behavior) is observed, i.e. the apparent activation energy decreases linearly with negative applied potential, with a slope of 0.4-0.42. In previous studies a slope of -1.1 [80] and -0.5 [81] has been found for fuel-lean conditions at which electrophobic behaviour dominates, and which is in good agreement with the value of -0.5 found in this study.

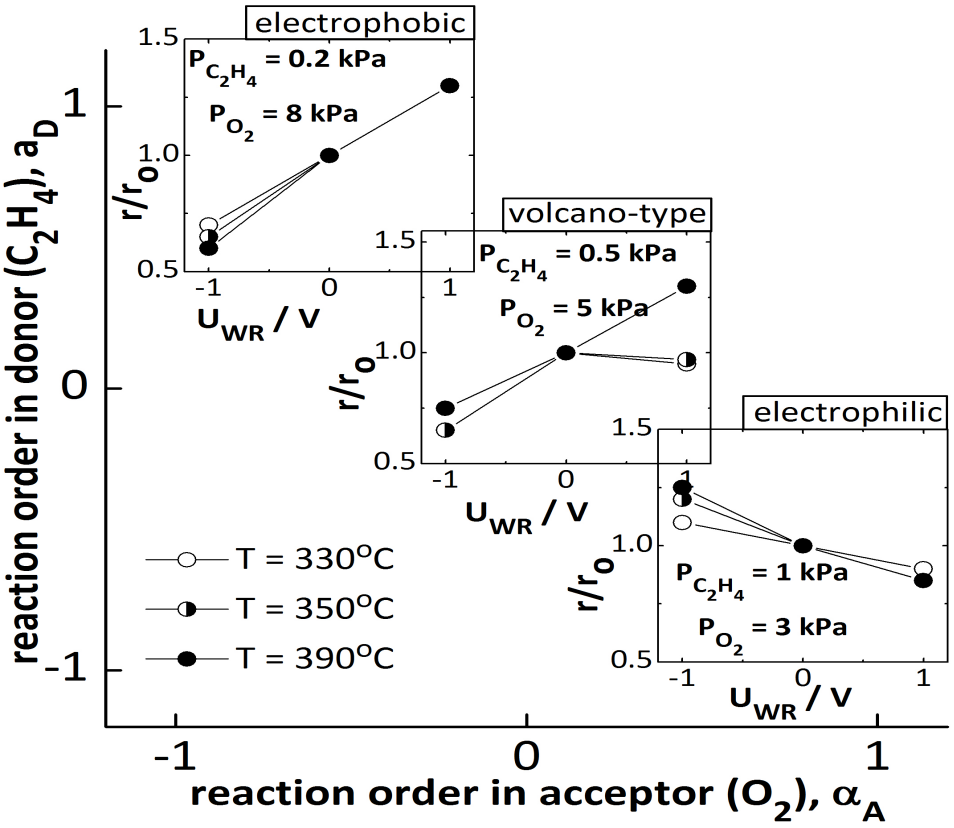

Figure 5.9 Comparison of the observed EPOC-type behavior with the observed kinetic order in electron donor (D, C_2H_4) and in electron acceptor (A, O_2) at 330°C, 350°C and 390°C, under three different feed compositions: mildly oxidizing ($P_{O_2}/P_{C_2H_4}$ = 40), slightly oxidizing ($P_{O_2}/P_{C_2H_4}$ = 10) and stoichiometric ($P_{O_2}/P_{C_2H_4}$ = 3) conditions

Figure 5.9 combines the kinetic behavior of the reaction in the donor and in the acceptor with the EPOC behavior under the same feed conditions at three different temperatures of 330°C, 350°C and 390°C. Three types of electrochemical promotion behavior were observed, i.e. electrophobic, electrophilic and volcano type behaviors. As shown, when the reaction kinetic order is positive in electron donor (C_2H_4) and negative in electron acceptor (O_2) an electrophobic type behavior is obtained. On the other hand, when the reaction kinetic order is positive in electron acceptor (O_2) and

negative in electron donor (C_2H_4) an electrophilic type behavior is observed. Furthermore, when the reaction kinetic order is negative in both electron donor (C_2H_4) and electron acceptor (O_2) a volcano type behavior is obtained. The observed dependence of the EPOC behavior on the reaction kinetic order is in total agreement with the rules of electrochemical promotion of catalysis [52].

5.2 The electrochemical promotion of deep propane oxidation on Pd, Ir, Ru, and Cu catalyst deposited on Yttria-stabilized zirconia catalyst

Propane oxidation upon four different catalyst-electrodes consisting of Pd, Ir, Ru, and Ir deposited on YSZ has been investigated under various characterization and experimental techniques, here for XRD, SEM, electrochemical part, and so on in order to get more understanding in deep details.

5.2.1 Catalyst Characterization

(a) **(b)**

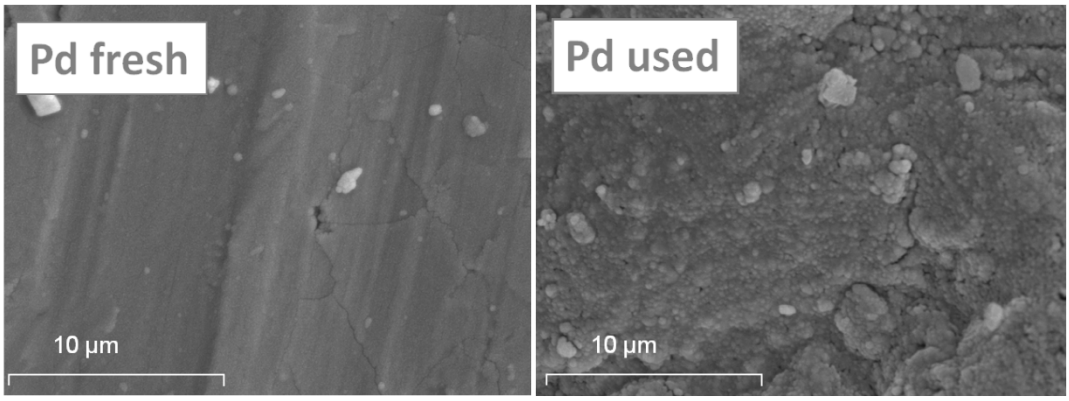

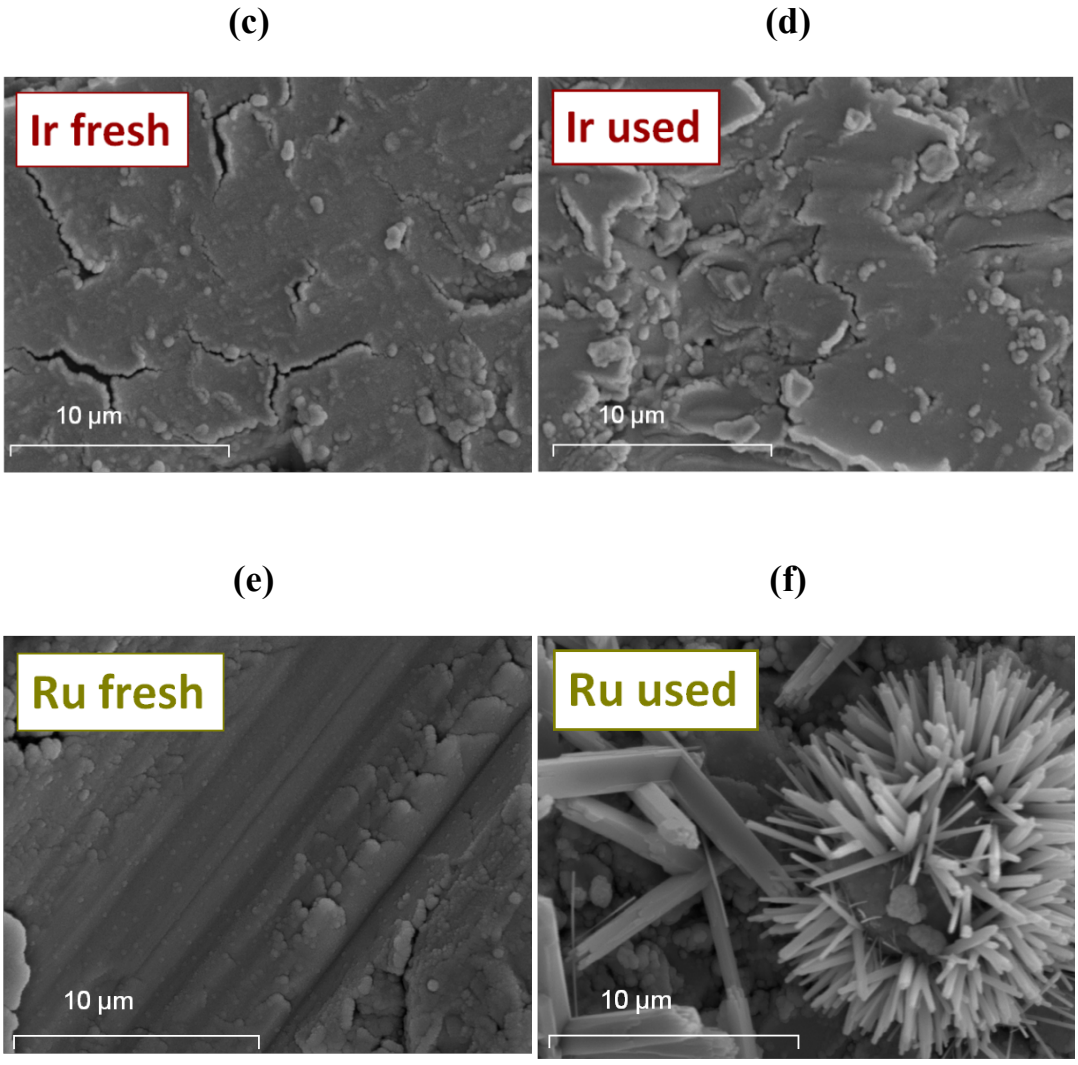

Figure 5.10 SEM micrographs of fresh and used catalyst-electrodes; (a) and (b) for Pd, (b) and (c) Ir, (c) and (d) Ru catalyst-electrodes

Figure 5.10 presents the surface morphology of metal catalyst electrode consisting of Pd, Ir, and Ru deposited on YSZ before (a, c, and e) and after (b, d, and f) exposure to the gas mixture via SEM technique. As shown in the figure for all of the fresh catalyst-electrode films including Pd, Ru, and Ir over YSZ show a smooth thin and uniform metallic film on the surface on the YSZ support. On the other hand, after propane oxidation (used catalyst-electrodes), Pd film does not show any significant difference in the surface structure. However, Ir catalyst film exhibit with different surface morphology with enhance roughness, which can attribute to oxide

formation under O^{2-} supply to surface. In case of Ru catalyst film, the significant different surface was observed; where a remarkable Ru oxide crystallizes structure is obtained to be form after expose in the reaction conditions. The formation of such beautiful Ru oxide crystallizes is reported for the first time. These oxides are of hexagonal crystal structure and cover the entire film after experiment.

(a)

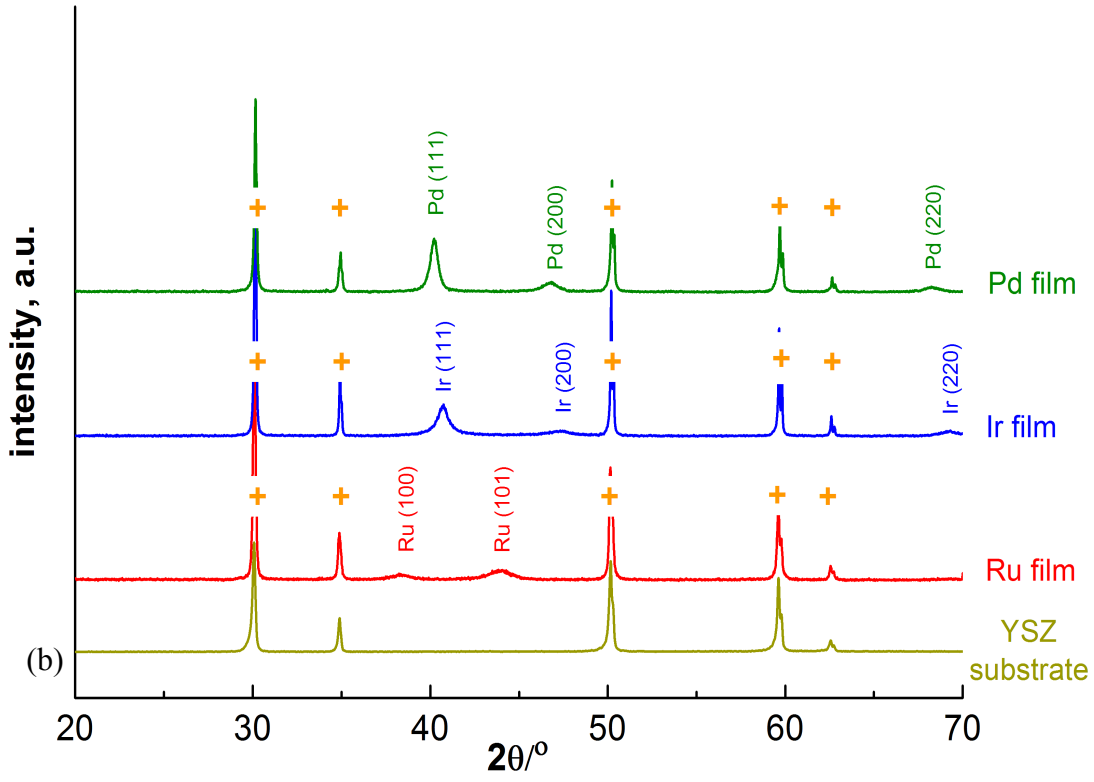

(b)

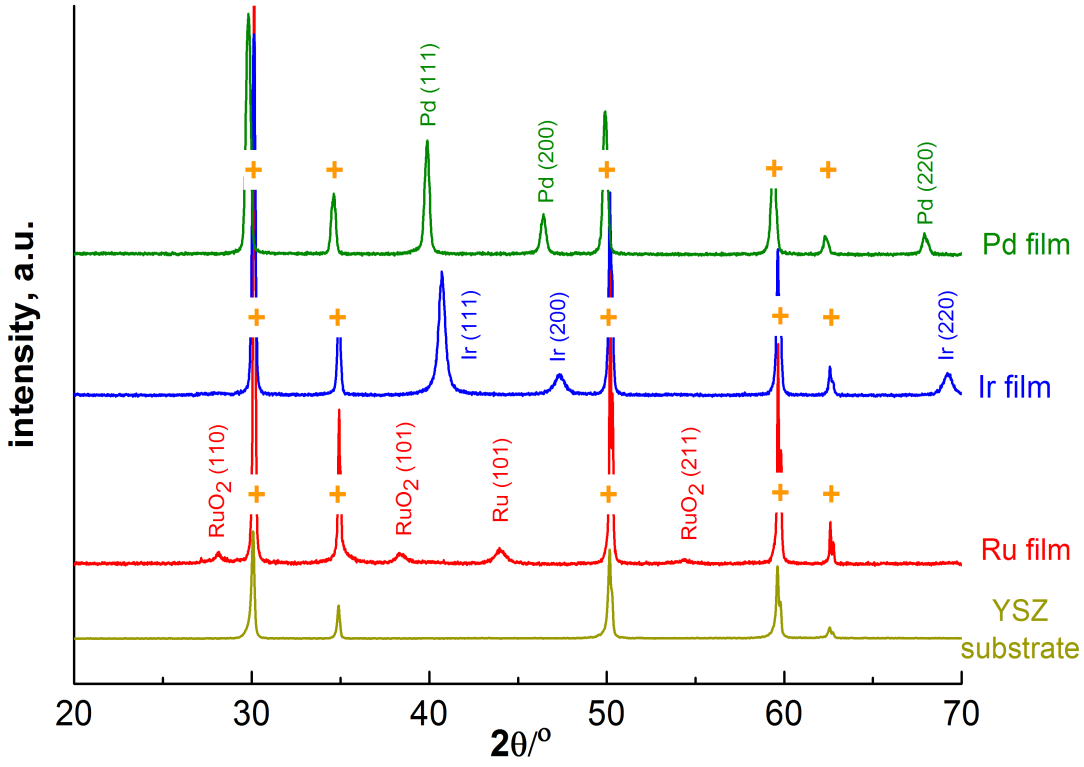

Figure 5.11 XRD spectra for sputtered Pd/YSZ, Ir/YSZ, and Ru/YSZ catalyst electrode; (a) as prepared sputtered metal catalyst electrodes and (b) spent sputtered metal catalyst electrodes

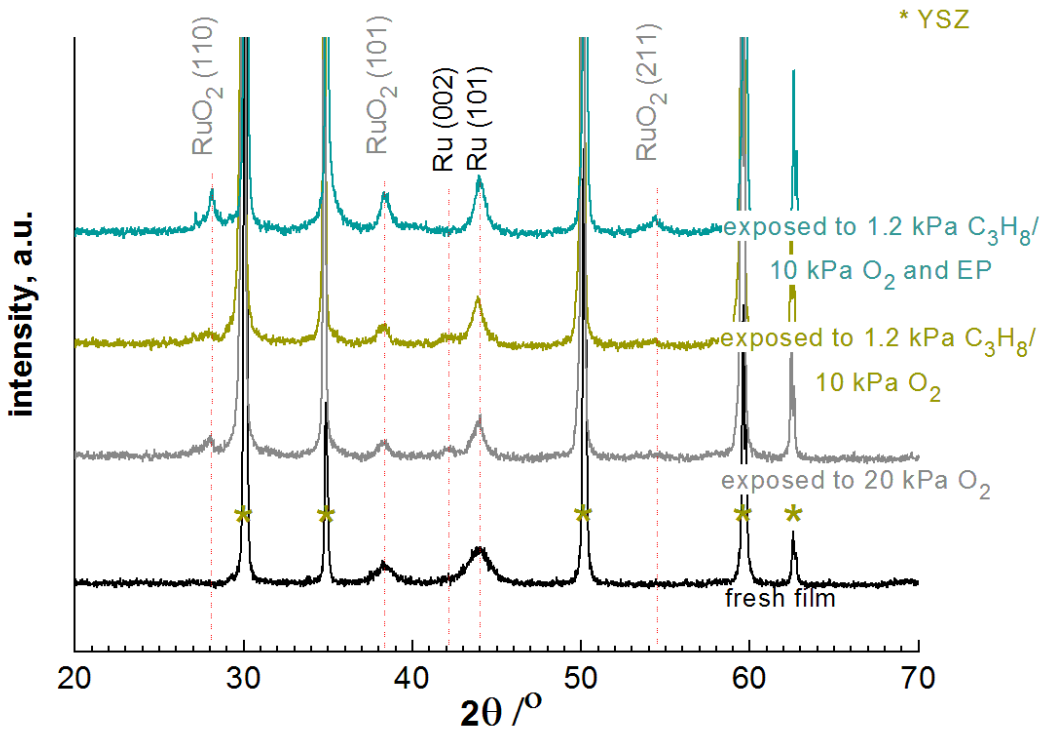

Figure 5.12 XRD spectra for sputtered Ru/YSZ catalyst-electrode electrodes for fresh and after exposed to various operating conditions

To identify phase composition of sputtered metal catalyst electrodes, XRD measurement was performed as shown in Figure 5.11 As expected from SEM micrographs, the XRD pattern exhibits the different phase between fresh and used metal catalyst electrodes. The crystal planes of catalyst electrode were confirmed according to the JCPDS crystallographic database. The reflection peak of YSZ was observed for all metal sputtered film corresponding to the (111), (200), (220), and (311) planes (JCPDS-ICDD Card No. 01-082-1246). The fresh sputtered electrodes presents of the metallic Pd, Ir, and Ru phase was found for the fresh corresponding to the (111), (200), and (220) planes of Pd^0 as well as the (111), (200), and (220) planes of Ir^0, together with the (100) and (101) planes of Ru^0. As expected, the fresh metal electrode presents only metallic Pd, Ir, and Ru resulting from conducting under a high purity metal sputtering target under Ar environment without any pretreatment. After

propane oxidation experiment (Figure 5.11b) only the metallic Pd was observed fresh and used catalyst reflections of metallic Pd, which shows sharper reflections after exposure due to improved crystallinity confirming by SEM picture as in Figure 5.11b, whereas the ruthenium oxide was found, which consists of RuO_2 (110), RuO_2 (101), and RuO_2 (211) planes. From Figure 5.12 it is very clear, that Ru fresh is mostly metal, there is only one reflection of RuO_2 (101). All samples which have been treated show Ru metal (101) and (002) and Ruthenium oxide. Therefore, Ru forms stable oxides at the reaction conditions explored in this study.

5.2.2 Catalytic activity measurement

The effect of potential, gas composition and temperature on catalytic activity of propane oxidation had been investigated for the different catalyst-electrodes, i.e. Pd, Ir, Ru, and Cu.

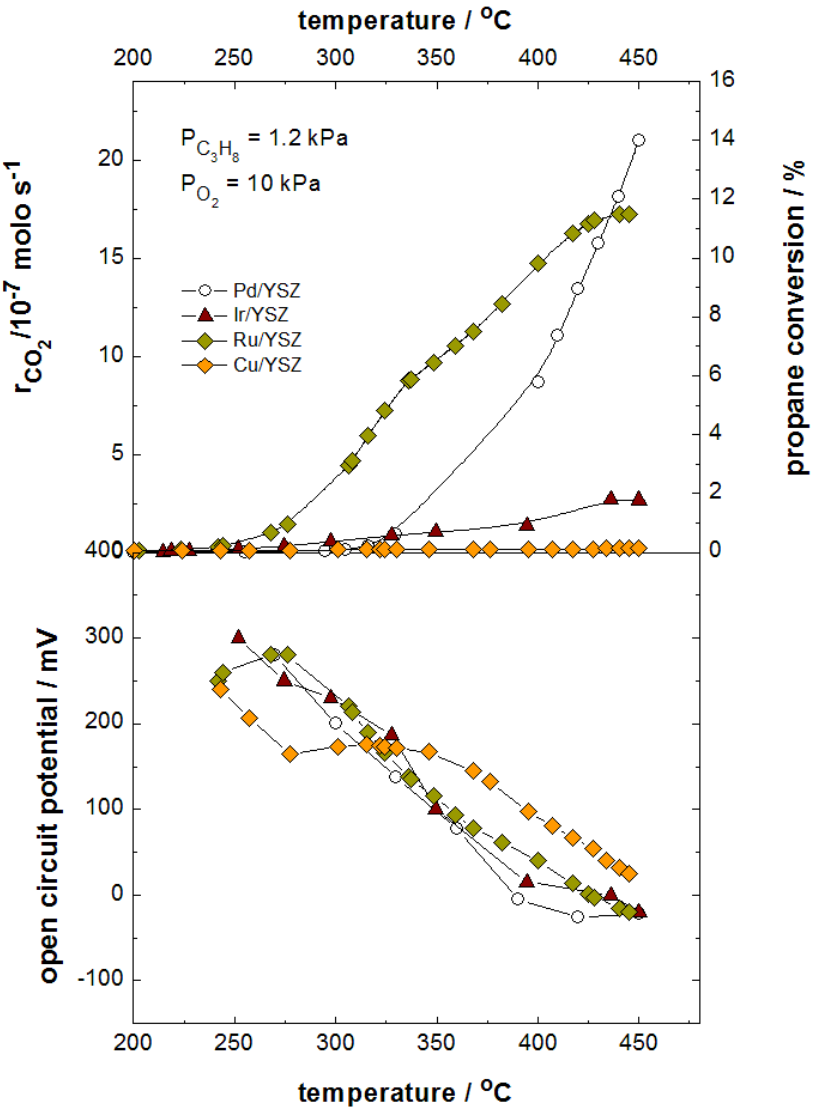

Figure 5.13 The first light-off propane oxidation upon different catalyst electrodes: sputtered-Pd, Ir, Ru, and Cu deposited on YSZ; (top) CO_2 formation rate and propane conversion (bottom) open circuit potential as a function of temperature

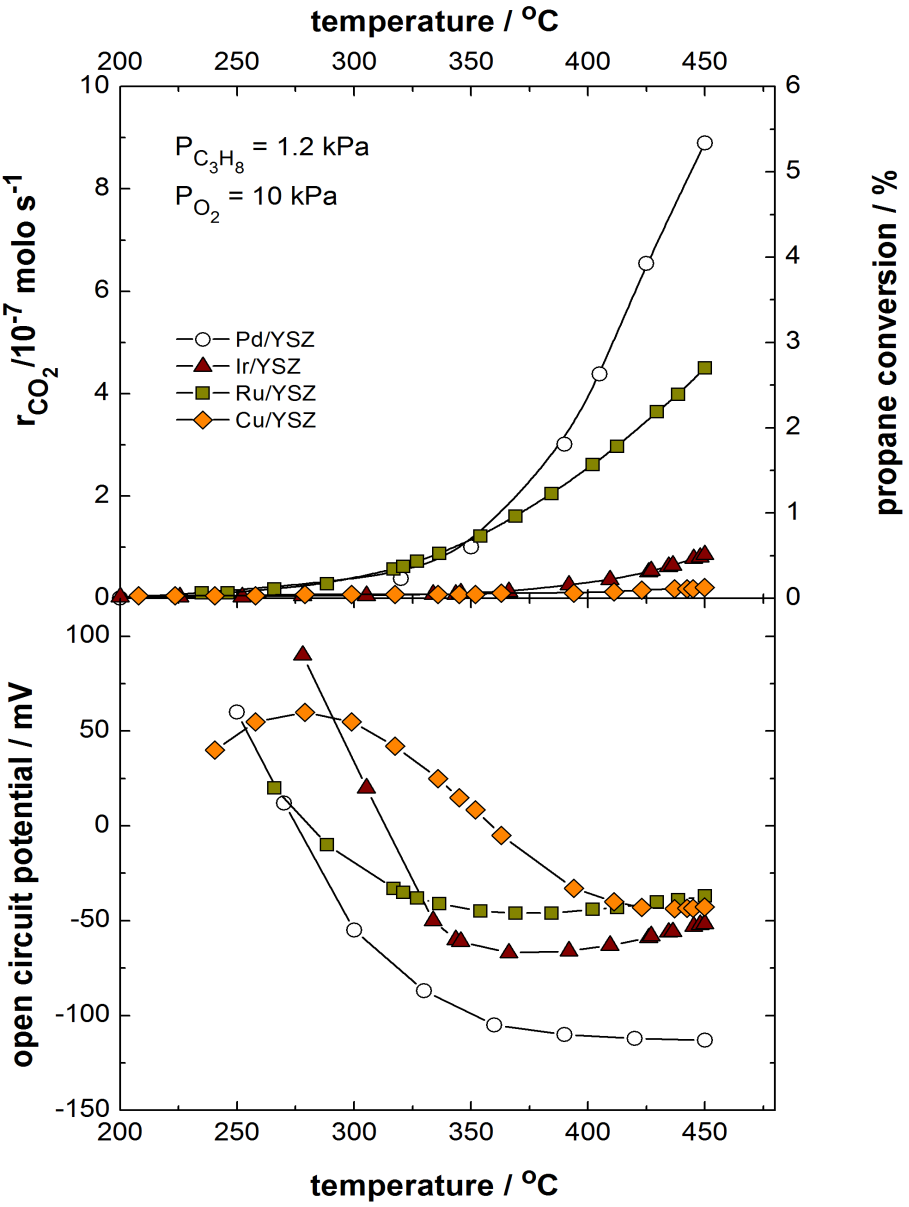

Figure 5.14 The second light-off propane oxidation upon different catalyst-electrodes: sputtered-Pd, Ir, Ru, and Cu deposited on YSZ; (top) CO_2 formation rate and propane conversion (bottom) open circuit potential as a function of temperature

Figures 5.13 and 5.14 present the steady state effect of temperature on rate of CO_2 formation, CO_2 conversion, and open circuit potential under open circuit conditions by fresh and used Pd, Ir, and Ru catalyst-electrodes, respectively. As shown in Figure 5.13, in the case of fresh catalyst electrodes Ru exhibits higher

catalytic activity than Pd, and Ir while Cu is the less active (conversion < 1%). In addition, the onset of propane oxidation for fresh catalysts is found Cu (almost inactive) <Ru (270^{o}C) < Pd = Ir (320^{o}C). Worth noting is that at high temperatures catalytic activity of Pd becomes higher than that of Ru. The Pd first light off leads to a propane conversion up to 14% at 450^{0}C, whereas the propane conversion decrease to 11% and 2% in the case of Ru and Ir catalyst-electrodes, respectively. On the other hand, OCP is reduced from ~300mV at 250^{o}C to ~-50mV at 450^{o}C, indicating a lower oxygen coverage of the catalytic surface and thus perhaps a weaker metal-oxygen bond strength by temperature increase [9, 124].

As shown, fast catalyst deactivation is observed mainly for Ru and Ir catalyst-electrodes due to increased particle size as obtained and the different oxidation state, as obtained by SEM (Figure 5.10) and XRD (Figure 5.11). As discussed in Figure 5.11, only Pd sustains its oxidation state, while Ir and Ru form stable oxide species under the reaction conditions investigated in this study.

In addition, the OCP at low temperatures (250^{o}C) is lower in the case of used catalyst electrodes, indicating lower oxygen coverage of the catalytic surface and thus perhaps a weaker metal-oxygen bond strength [9].

(a)

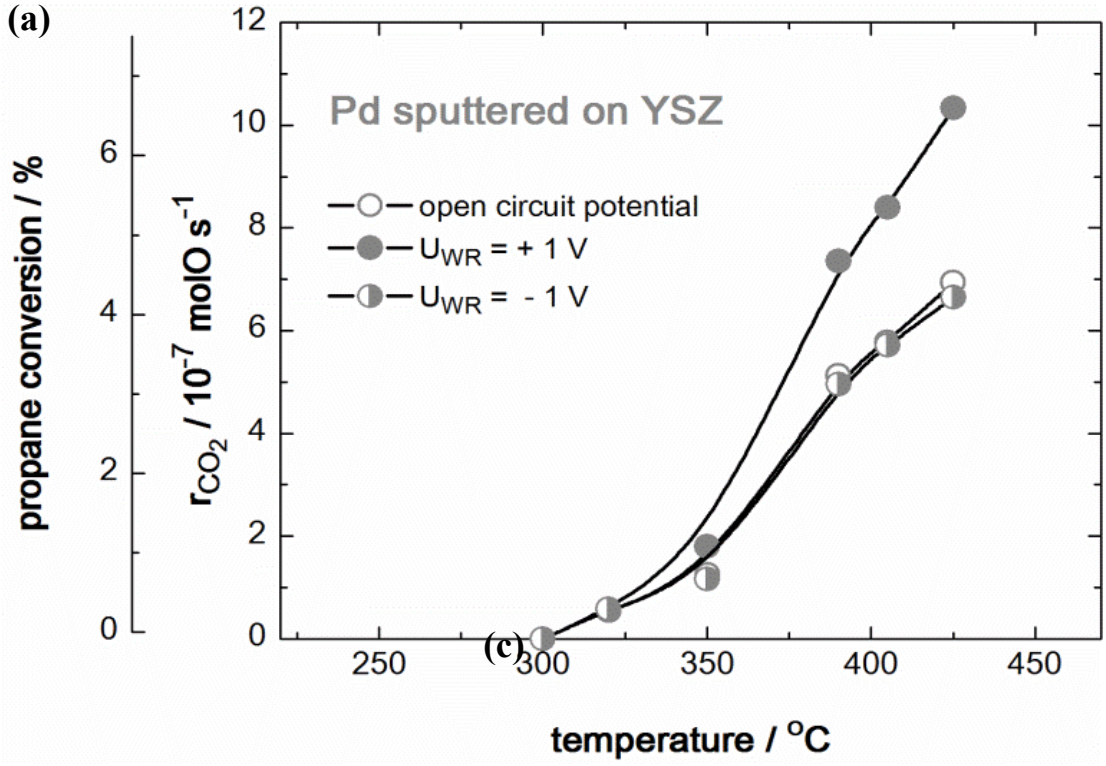
Pd sputtered on YSZ
open circuit potential
U_{WR} = + 1 V
U_{WR} = - 1 V
propane conversion / %
r_{CO_2} / 10^{-7} molO s^{-1}
temperature / °C

(c)

(b)

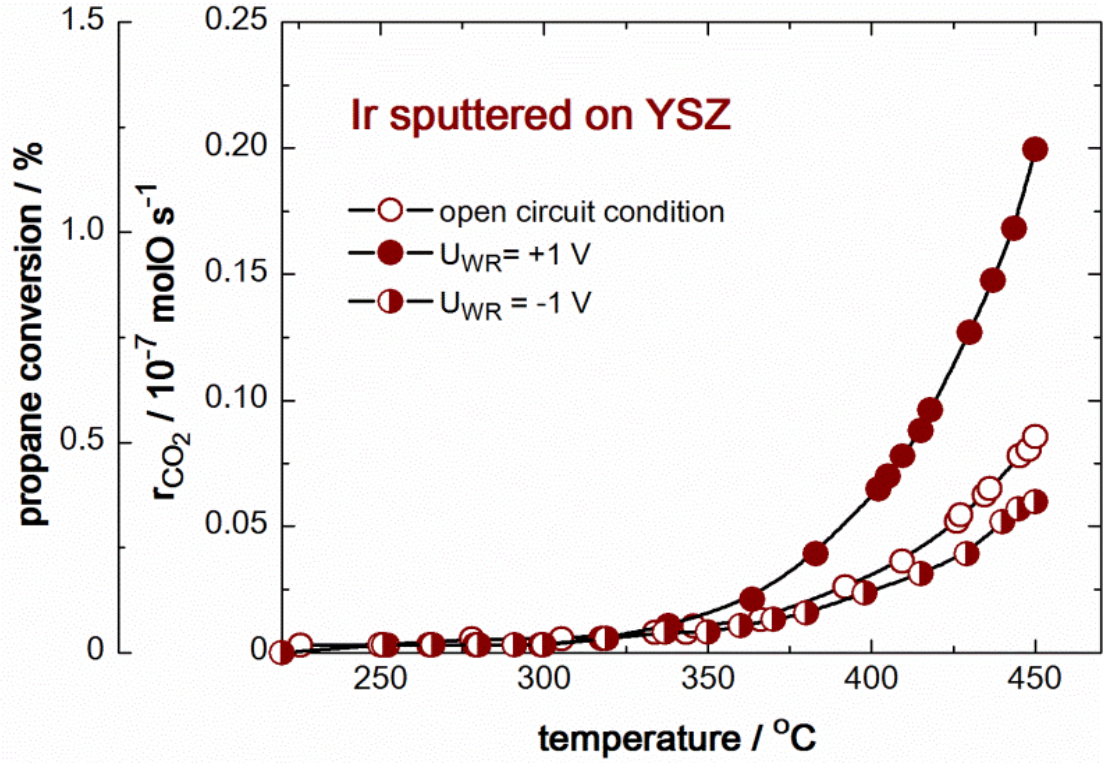
Ir sputtered on YSZ
open circuit condition
U_{WR}= +1 V
U_{WR} = -1 V
propane conversion / %
r_{CO_2} / 10^{-7} molO s^{-1}
temperature / °C

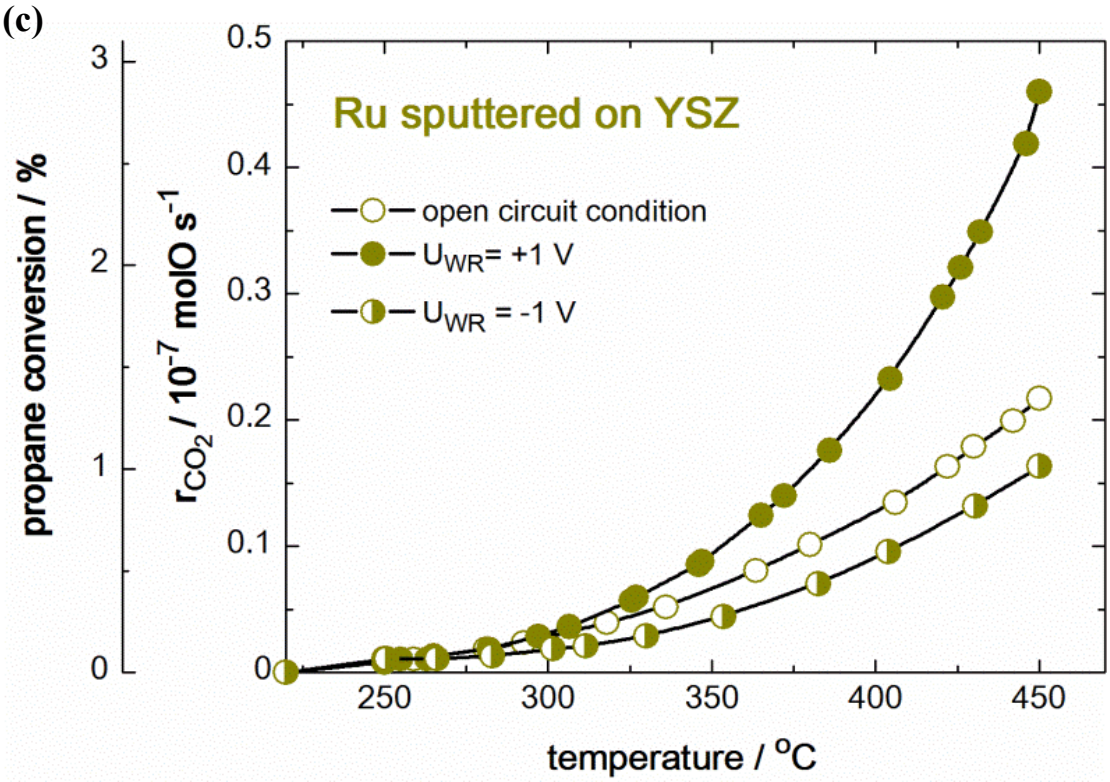

Figure 5.15 Effect of temperature on propane conversion and rate of CO_2 formation (TPR experiments) under (open symbol) open circuit and upon different catalyst potential (filled symbol) U_{WR} = 1 V and (half-filled symbol) U_{WR} = -1 V. Catalyst electrode: (a) sputtered-Pd/YSZ, (b) sputtered-Ir/YSZ, and (c) sputtered-Ru/YSZ. Feed condition: $P_{C_3H_8}$ = 1.2 kPa, P_{O_2} = 10 kPa, F_v = 170 cm^3min^{-1} (STP)

The continuous measurement of the rate of reaction, r, by the effluent CO_2 formation was performed. Figure 5.15 shows the effect of temperature on CO_2 formation rate and C_3H_8 conversion under open circuit and positive and negative potential application conditions for Pd (a), Ir (b) and Ru (c) catalyst electrodes. A constant heating ramp of 2 K min^{-1} has been used in this experiment in the temperature range between 250 and 450°C. First, the samples were investigated under open circuit conditions. After that these samples were cooled down to 250°C, a positive potential of U_{WR} was applied and concomitant heated again under closed circuit to 450°C. Finally, the same procedure was performed for a negative potential

application. The application of positive potential (anodic polarization) leads to an increase in propane conversion for all catalyst electrodes, i.e. Pd, Ir, and Ru. As shown in figure, the negative potential application (cathodic polarization) had no effect on propane conversion in the case of Pd, whereas a slightly decrease in propane conversion for Ir and Ru catalyst-electrodes. Therefore, all of catalyst-electrodes are termed electrophobic type behavior, where the rate of reaction increases upon the anodic polarization as in agreement with the global electrochemical promotion rule [52]. This EPOC behavior type is observed when electron acceptor species, i.e. oxygen, are strongly adsorbed on the catalyst surface according to EPOC rules. However, the effect of negative potential application on the catalytic rates was less pronounced than the effect of positive potential application. This is possibly due to the high oxygen excess in the gas mixture, which results in already high oxygen coverage of the catalysts surface and in the observed low catalytic activity.

(a)

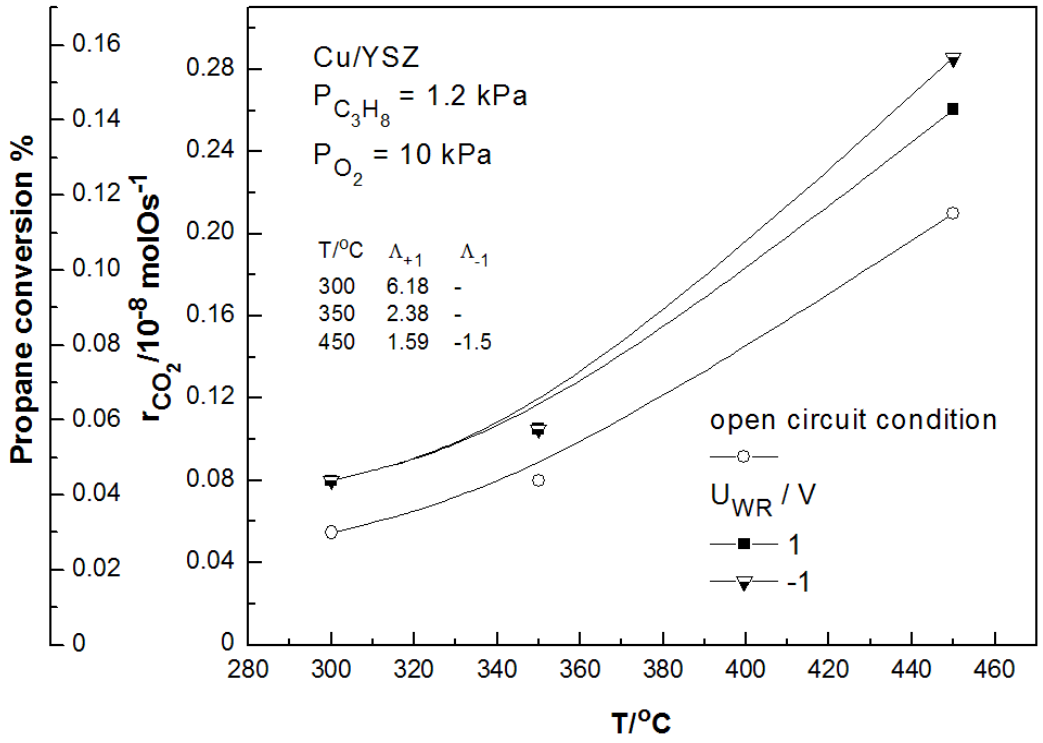
Cu/YSZ
$P_{C_3H_8}$ = 1.2 kPa
P_{O_2} = 10 kPa
T/°C Λ_{+1} Λ_{-1}
300 6.18 -
350 2.38 -
450 1.59 -1.5
open circuit condition
U_{WR} / V
1
-1
Propane conversion %
$r_{CO_2}/10^{-8}$ molOs^{-1}
T/°C

(b)

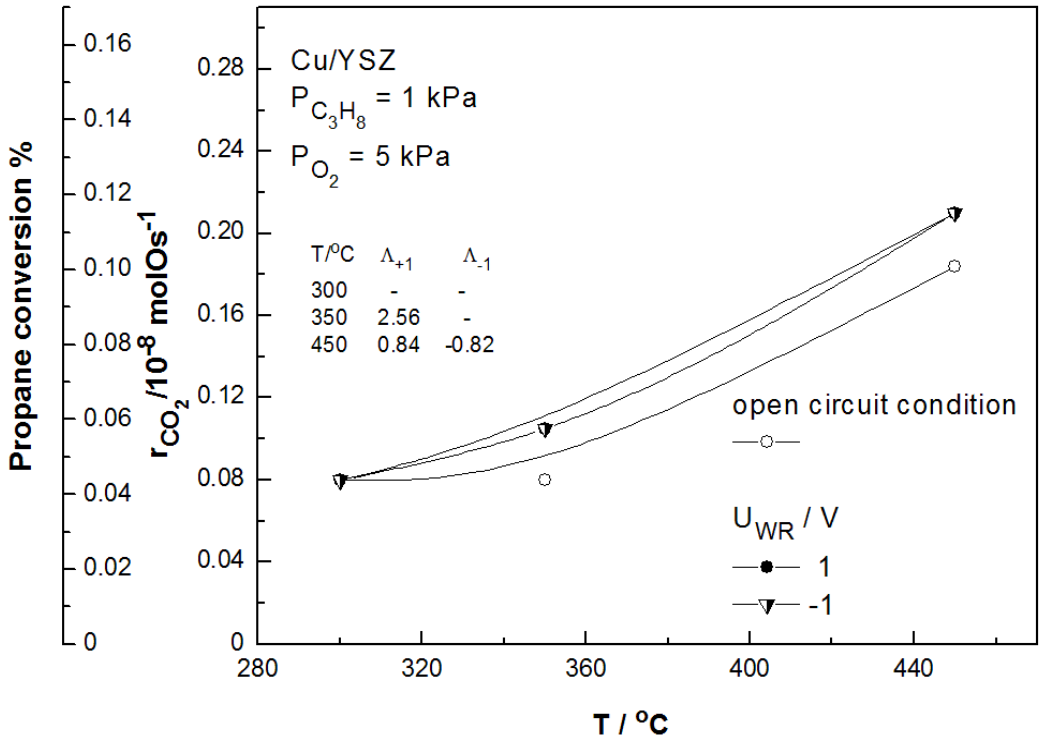
Cu/YSZ
$P_{C_3H_8}$ = 1 kPa
P_{O_2} = 5 kPa
T/°C Λ_{+1} Λ_{-1}
300 - -
350 2.56 -
450 0.84 -0.82
open circuit condition
U_{WR} / V
1
-1
Propane conversion %
$r_{CO_2}/10^{-8}$ molOs^{-1}
T / °C

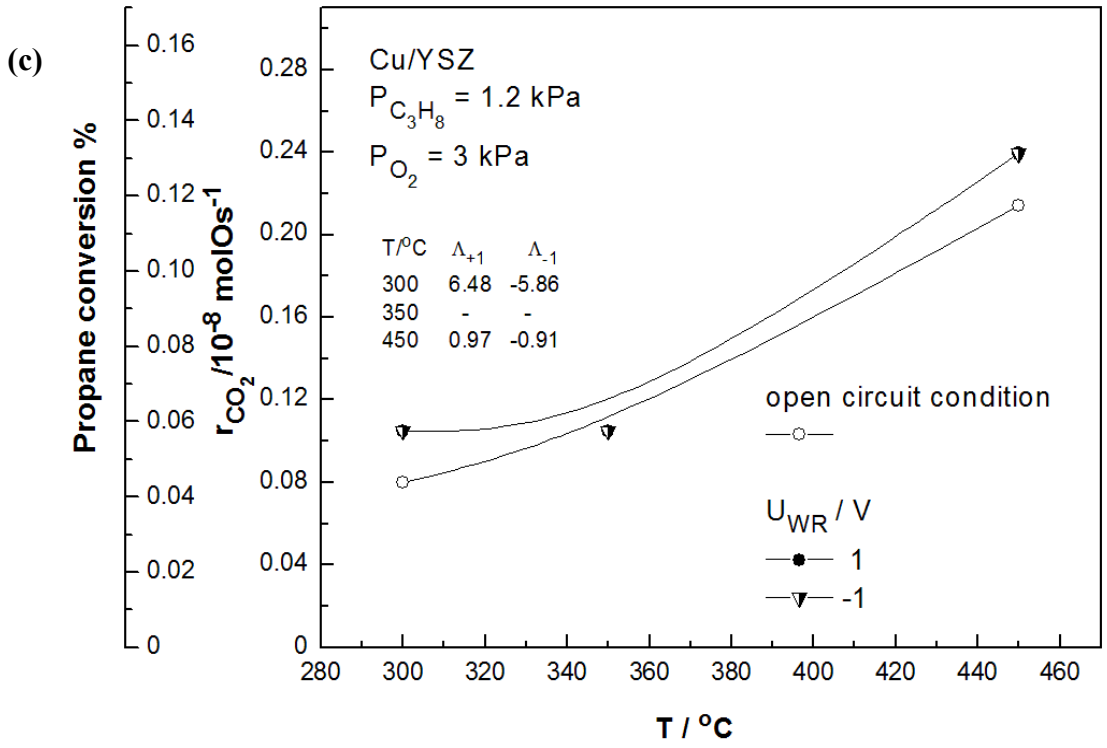

Figure 5.16 Effect of temperature and feed conditions on propane conversion and rate of CO_2 formation for Cu/YSZ (transient experiments) under (open symbol) open circuit and upon different catalyst potential (filled symbol) U_{WR} = 1 V and (half-filled symbol) U_{WR} = -1 V. Feed condition: (a) $P_{C_3H_8}$ = 1.2 kPa, P_{O_2} = 10 kPa, (b) $P_{C_3H_8}$ = 1.0 kPa, P_{O_2} = 5 kPa, (c) $P_{C_3H_8}$ = 1.2 kPa, P_{O_2} = 3 kPa, F_v = 170 cm^{3}min^{-1} (STP)

Figure 5.16 shows the steady-state effect of temperature on the rate of CO_2 formation and propane conversion upon different feed compositions, i.e. oxidizing, stoichiometric, and reducing conditions for Cu/YSZ. The rate of CO_2 formation and propane conversion were found to be relatively small all entire temperature range and feed conditions. Furthermore, the Faradaic efficiency, Λ, taking value less than 10 Therefore, sputtered-deposited Cu film deposited on YSZ cannot be acceptable for electrochemically promoted for propane oxidation. In addition, it could be due to the low conductive value of Cu film deposited on YSZ as in agreement with a small value of CO_2 formation in the light-off experiment as discussed in previous paragraph.

According to relative small value of Faradaic efficiency, it is not worth performing characterization and catalytic activity experiments.

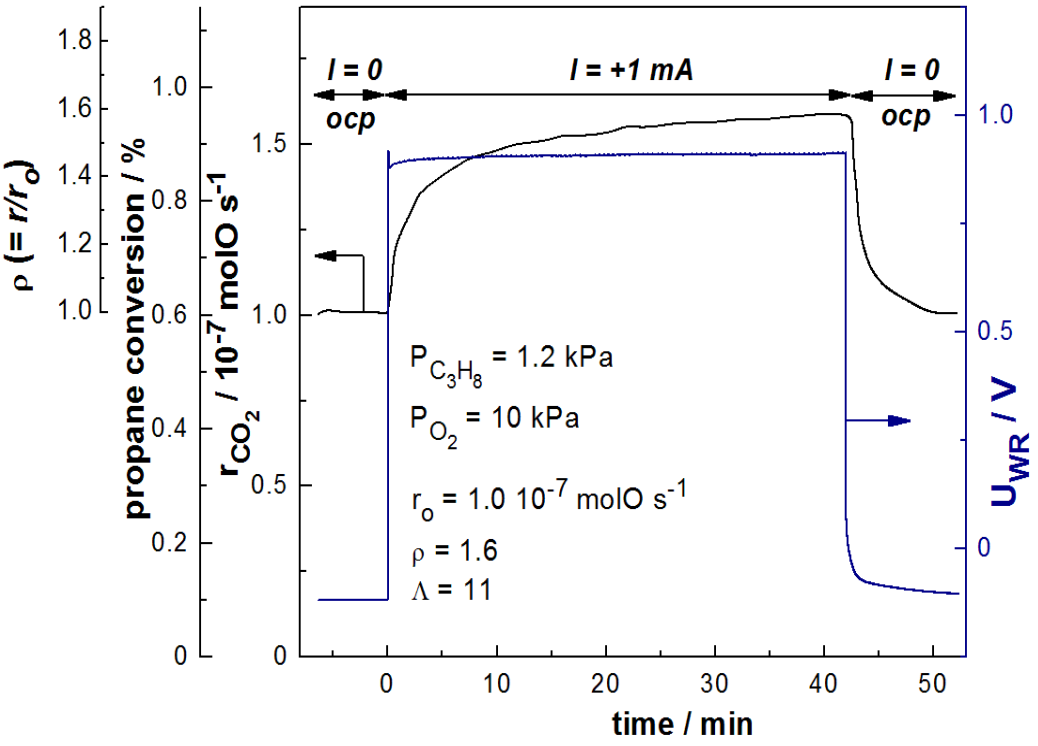

Figure 5.17 Rate of CO_2 formation, r_{CO_2}, and catalyst potential, U_{WR}, corresponds to a step change in an applied positive current of 1 mA at T = 350°C, (a) $P_{C_3H_8}$ = 1.2 kPa, P_{O_2} = 10 kPa, F_v = 170 cm^3min^{-1} (STP). Catalyst: Sputtered Pd catalyst-electrode deposited on YSZ

Electrochemical promotion experiments have been studied after propane conversion stabilized, i.e. after the second light-off experiment. Figure 5.17 presents the transient effect of a constant positive current application (I=1mA) on the catalytic CO_2 formation rate versus potential different at 350°C. A reversible rate enhancement is observed, here for the increase in the catalytic rate, Δr, is relatively small with ρ value of 1.6, however, the significant higher rate of ion transport, I/2F, was observed. At the beginning of the experiment in Figure 5.17, at t<0, an open circuit rate of $1x10^{-7}$ molO s^{-1} is observed whereas the catalytic potential is equal to -50 mV. At t = 0, a constant current of 1 mA is applied galvanostatically and O^{2-} ions are transferred

to the Pd film at a rate I/2F = $5.2\text{x}10^{-9}$ molO s^{-1}. This induces an increase in the catalytic rate to new value of $1.6\text{x}10^{-7}$ molO s^{-1}, i.e. the rate enhancement ρ ($=r/r_0$) equals 1.6. The corresponding steady state value of the catalyst potential, U_{WR}, equals 900 mV. The rate increase Δr ($= r\text{-}r_0$) = $0.6\text{x}10^{-7}$ molO s^{-1} is 11 times larger than the rate of O^{2-} supply I/2F, i.e. the Faradaic efficiency, Λ, equals 11.

(a)

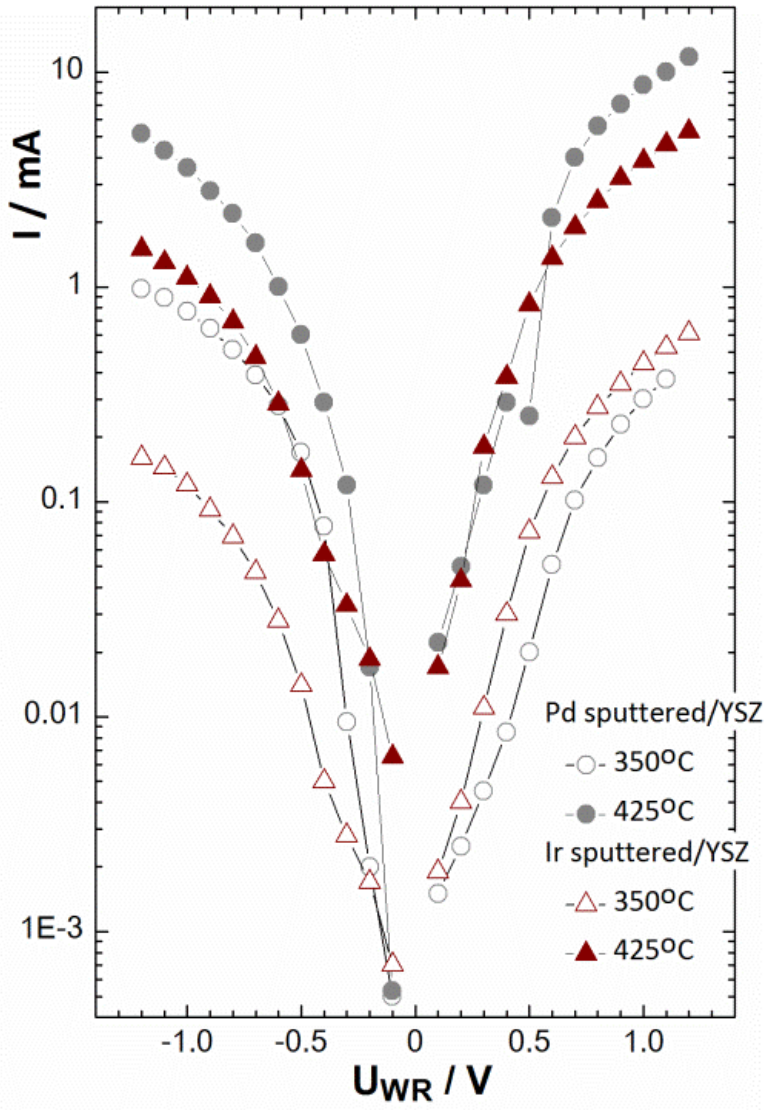

(b)

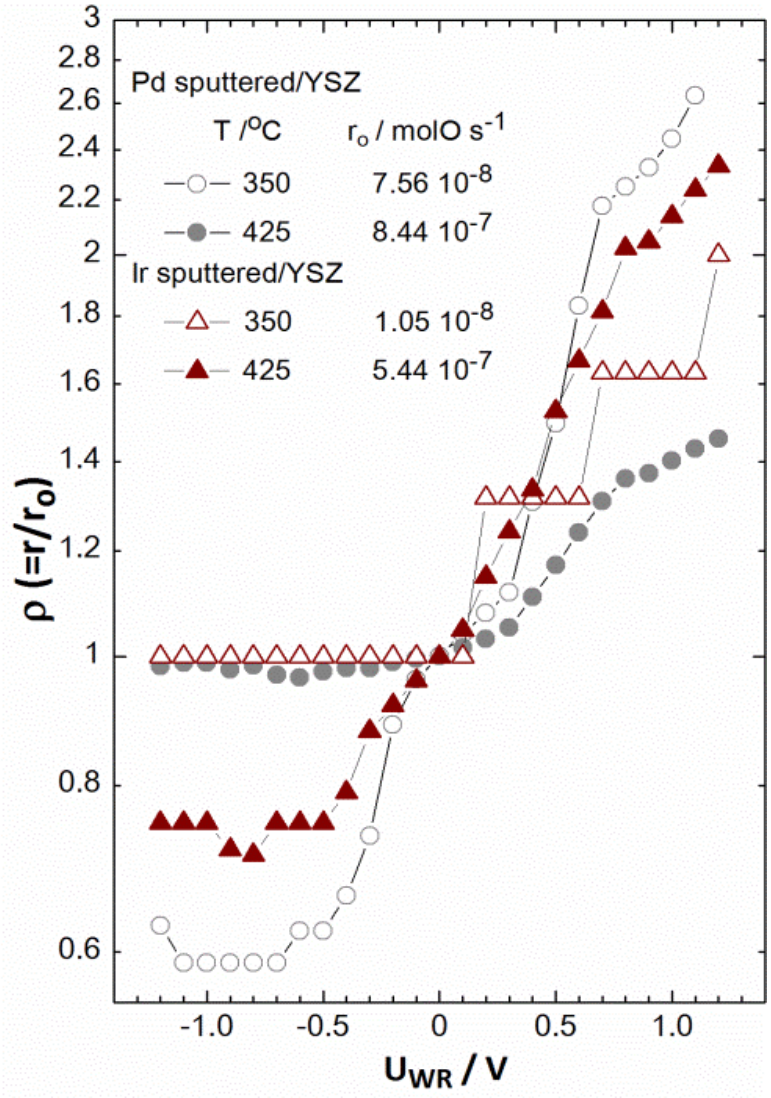
Pd sputtered/YSZ
T /°C
r_o / molO s^-1
350
7.56 10^-8
425
8.44 10^-7
Ir sputtered/YSZ
350
1.05 10^-8
425
5.44 10^-7
ρ (=r/r_o)
U_WR / V
3
2.8
2.6
2.4
2.2
2
1.8
1.6
1.4
1.2
1
0.8
0.6
-1.0
-0.5
0
0.5
1.0

(c)

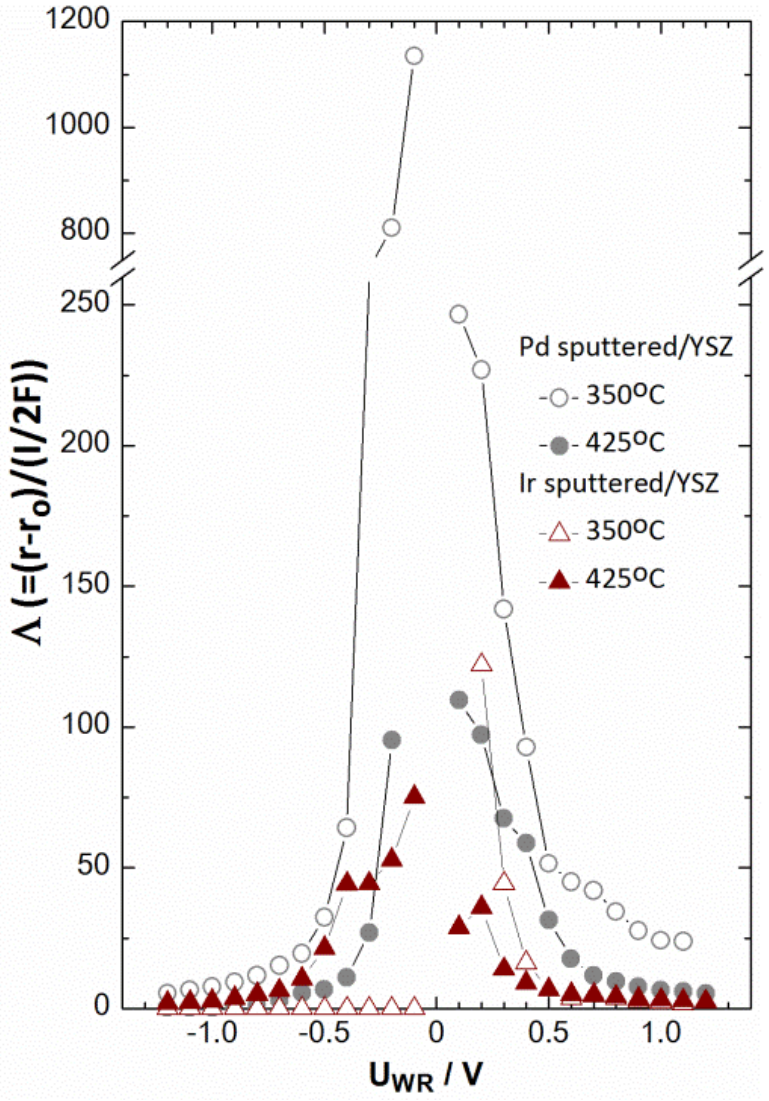

Figure 5.18 Steady-state effect of applied potential, U_{WR}, on (a) current, (b) rate enhancement ratio, ρ, and (C) the apparent Faradaic efficiency, Λ on Pd and Ir catalyst-electrodes at 350°C and 450°C.

Condition: $P_{C_3H_8}$ = 1.2 kPa, P_{O_2} = 10 kPa, F_v = 170 cm^3min^{-1} (STP).

Catalyst: Sputtered Pd catalyst-electrode deposited on YSZ

Figure 5.18 shows the steady-state effect of the applied potential (U_{WR}) on the current (Figure 5.18a), the rate enhancement ratio, ρ, (Figure 5.18b) and the apparent Faradaic efficiency, Λ, (Figure 5.18c) under $P_{C_3H_8}$ = 1.2 kPa and P_{O_2} = 10 kPa at two different temperature 350 and 425°C for Pd and Ir catalyst-electrodes. Figure 5.18a

shows in the form of a Tafel plot, for the current versus applied potential, U_{WR} in comparing between Pd and Ir. In the case of 425^{o}C, the exchange current i_o exhibits higher than 350^{o}C for both Pd and Ir.

As shown in Figure 5.18b there is a linear dependence of the logarithm of rate enhancement ratio, ρ, on the applied potential, which agrees with EPOC theory. As one can seen, a maximum ρ value was relatively small taking value of 2.6, i.e. 160% rate increase, where obtained for Pd and up to 2.3 for Ir at 425^{o}C. Furthermore, Figure 5.18c presents the effect of applied potential on the apparent Faradaic efficiency, Λ, for Pd and Ir catalyst-electrodes. The maximum Faradaic efficiency, Λ, value was reached to 250 for Pd catalyst electrode and 125 for Ir catalyst-electrode at 350^{o}C under anodic polarization, while apparent Faradaic efficiency, Λ, values up to 110 where recorded for the case of Pd and up to 75 in the case of Ir at 450^{o}C. Larger Λ values were recorded at lower temperatures because of longer lifetime of $O^{\delta-}$ species on catalyst surface. This number expresses the number of catalytic turnovers promoted by each electrochemically supplied O^{2-} before its ultimate consumption by the fuel, here for propane. In agreement with previous studies on the electrochemical promotion [9], the order of magnitude of the estimated enhancement factors, Λ, using the open circuit (unpromoted) catalytic rate and exchange current, I_o, calculates from $2Fr_0/I_0$. At 425^{o}C, Λ is estimated to be 160 and 210 for Pd and Ir respectively, which are very near to those calculated by the experiment.

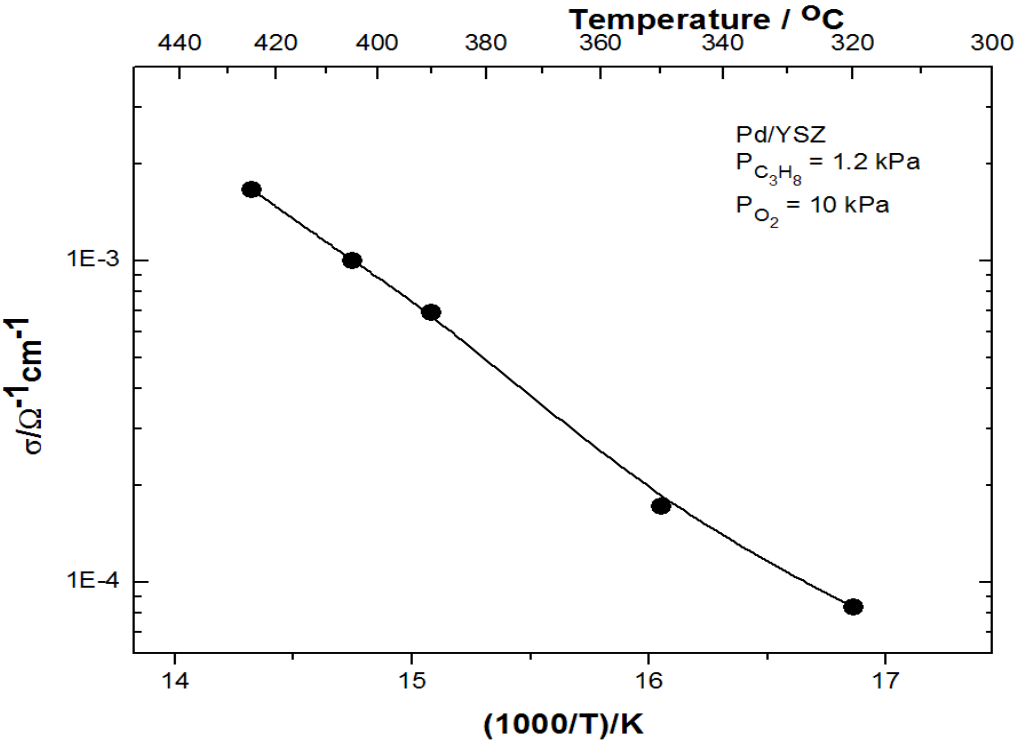

Figure 5.19 Temperature dependence of the ionic conductivity for YSZ solid electrode under $P_{C_3H_8}$= 1.2 kPa, P_{O_2} = 10 kPa, F_v = 170 cm^3min^{-1}

The conductivity of YSZ solid electrolyte information on this study is provided in Figure 5.19. The ionic conductivity was found in the range of value of 10^{-4}-10^{-3} $\Omega^{-1}cm^{-1}$ in agreement with previous studies [9]. For the catalytic and sensor application, a relative small conductivity material (~10^{-4} $\Omega^{-1}\cdot cm^{-1}$) are normally adequate in agreement with this present work all the entire range of operating temperature (320-435^{o}C) as shown in this figure.

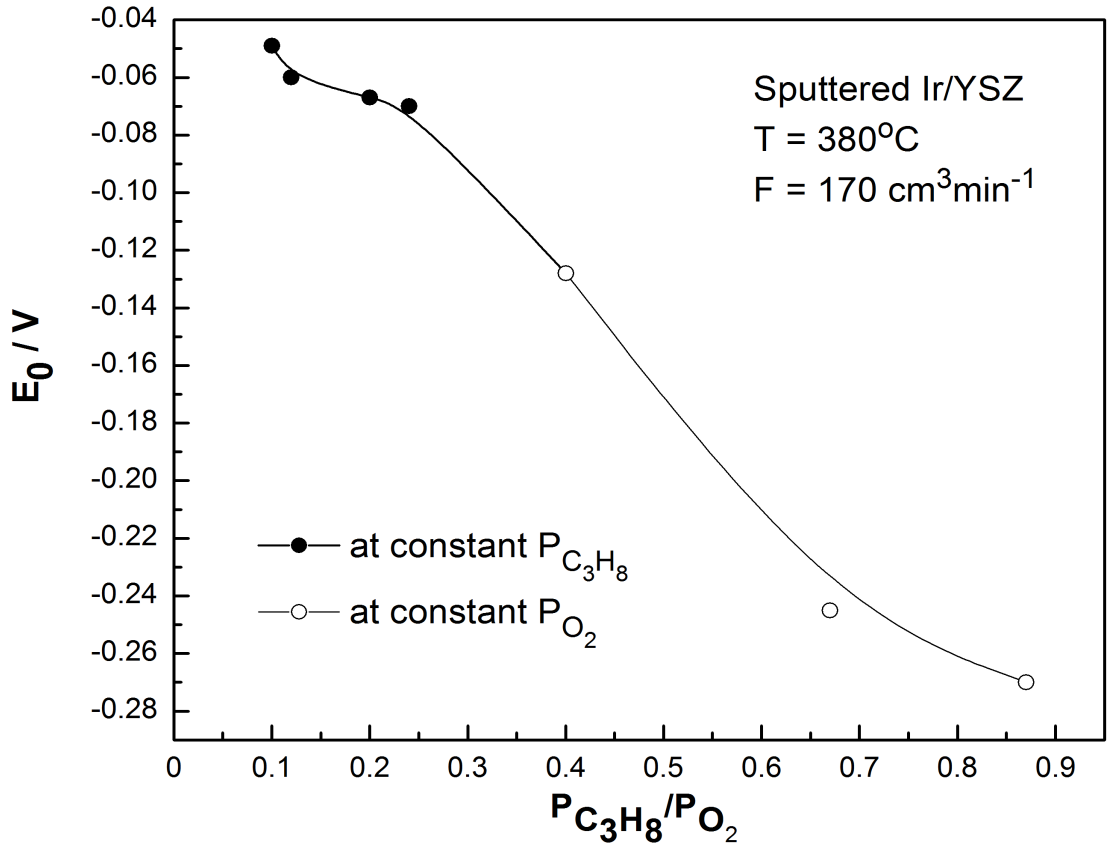

Figure 5.20 Steady-state effect of propane and oxygen partial pressure ratio on the open circuit potential, E_0 at a constant volumetric gas flow rate and temperature, T= 380°C

Figure 5.20 shows the effect of reactants partial pressure ratio, $P_{C_3H_8}/P_{O_2}$, on the open-circuit potential, E_0 at 380°C. It was found that in the range $P_{C_3H_8}/P_{O_2}$=0.1 to 0.9, an increase in $P_{C_3H_8}$ leads to a shift of open circuit potential to more negative values (or equally an increase in P_{O_2} leads to a shift of open circuit potential to less negative values). Filled symbols stand for results where $P_{C_3H_8}$ was kept constant, while open symbols for results where P_{O_2} was kept constant.

As shown, there is a strong effect of $P_{C_3H_8}/P_{O_2}$ at high $P_{C_3H_8}$, while the effect is less pronounced at high P_{O_2}. Accounting for the fact that open circuit potential (ocp) is affected only by adsorption at constant temperature, the latter observation possibly indicates strong adsorption of oxygen species (electron acceptor) and weak adsorption of C_3H_8 species on the catalyst-electrode surface.

(a)

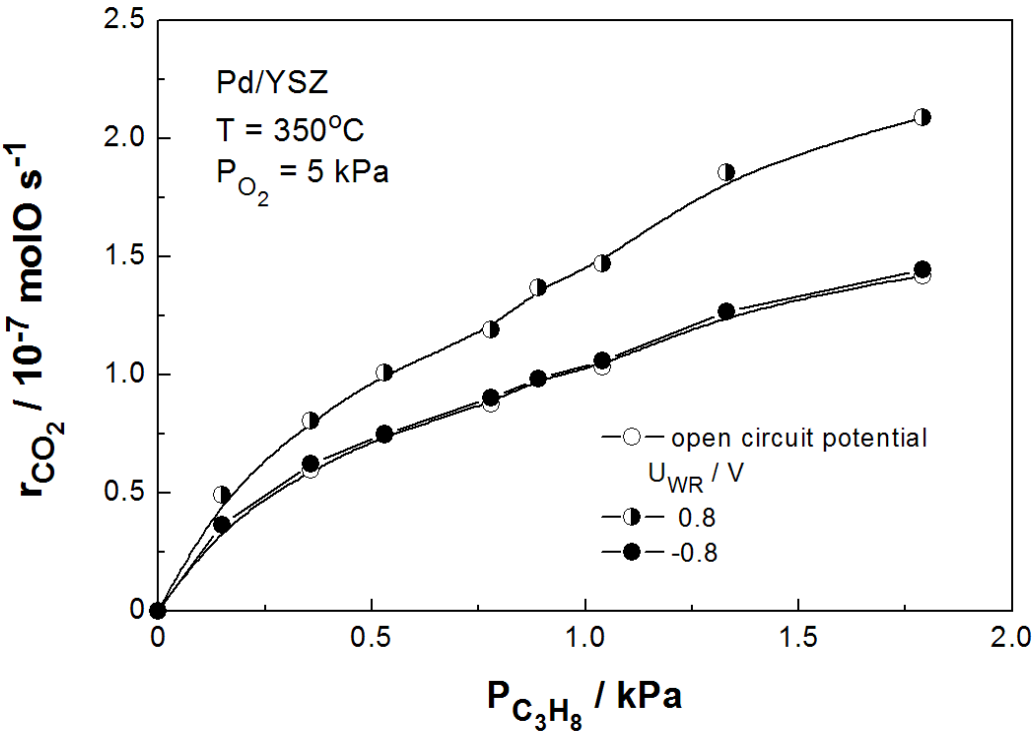
Pd/YSZ
T = 350°C
P$_{O_2}$ = 5 kPa
open circuit potential
U$_{WR}$ / V
0.8
-0.8
r$_{CO_2}$ / 10^{-7} molO s^{-1}
P$_{C_3H_8}$ / kPa
0
0.5
1.0
1.5
2.0
2.5

(b)

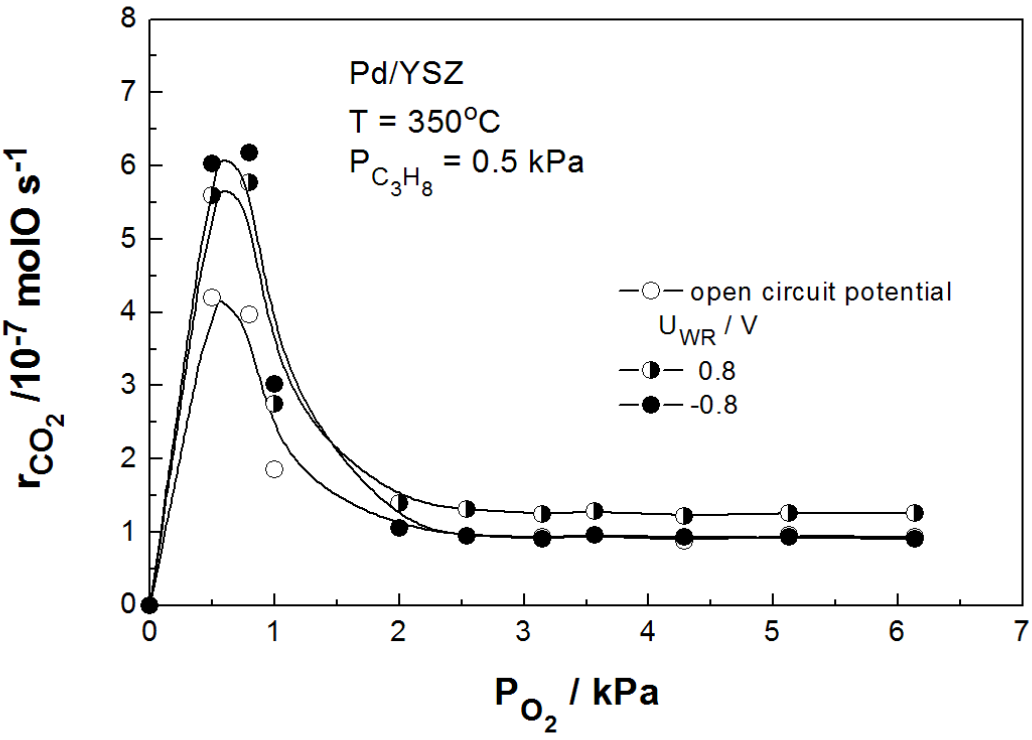

Figure 5.21 Dependence of open circuit and positive and negative potential application of sputtered Pd catalyst-electrode deposited on YSZ for propane oxidation of (a) at constant P_{O_2} (P_{O_2}= 5 kPa) and (b) at constant $P_{C_3H_8}$ ($P_{C_3H_8}$= 0.5 kPa) under T = 350°C

The effect of reactant partial pressure (P_{O_2} and $P_{C_3H_8}$) on the kinetic study of sputtered Pd and Ir deposited on YSZ for propane oxidation was investigated under differential condition (i.e., with less then 20% conversion) at 350°C and 380°C, respectively.

According to the rule of electrochemical promotion and classical promotion [9]. The observed behavior, here for electrophobic behavior suggests that the catalytic rate must be positive order in an electron donor (propane) and zero or negative order in an electron acceptor (oxygen). This is indeed the case for sputtered-Pd and Ir film deposited on YSZ for propane oxidation, as shown in Figures 5.21 and 5.22, respectively. At high oxygen partial pressure, as in the case of this present study, the oxygen coverage is high and the Pd active sites are occupied almost entirely by oxygen. Surface PdO is formed at the expense of surface Pd°. This is apparently why

in excess of oxygen the electrochemical promotion effect is smaller than in the case of reducing conditions for the same reaction [43], since anodic polarization of the Pd film is apparently not sufficient to decompose, at least partially the surface PdO layer, as in the case of Rh films [26]. In the case of fixed $P_{C_3H_8}$, these results showed that catalyst activity initially increased with the degree of reduction, reaching a maximum and then decreasing continuously as the oxygen is depleted as in agreement with the electrochemical rules.

(a)

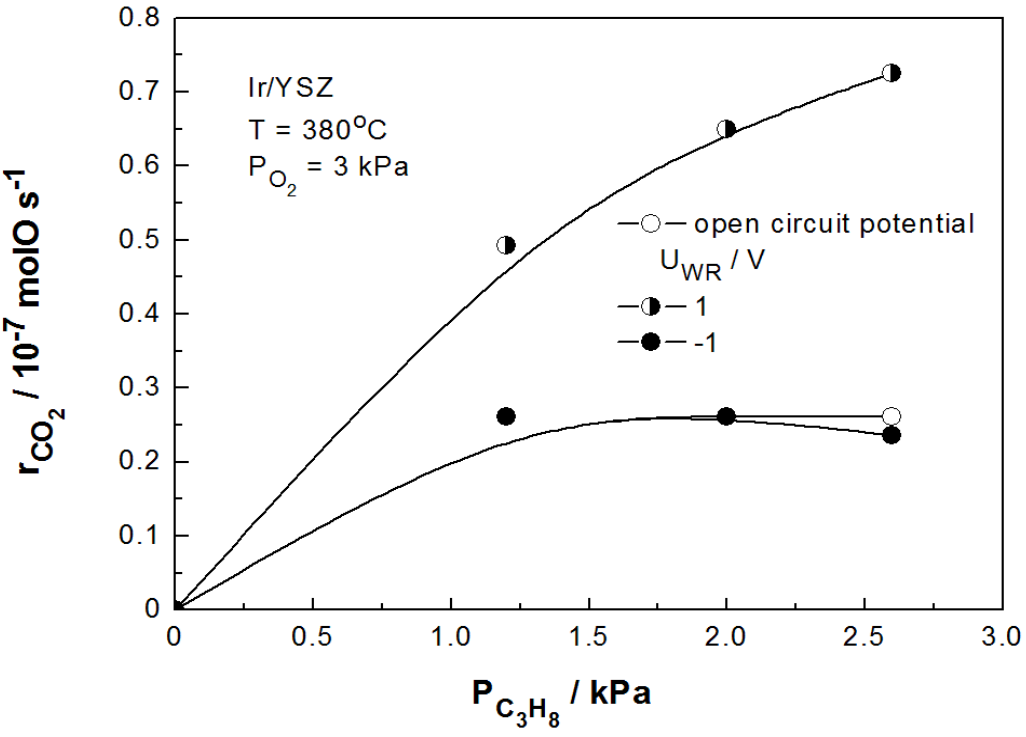

(b)

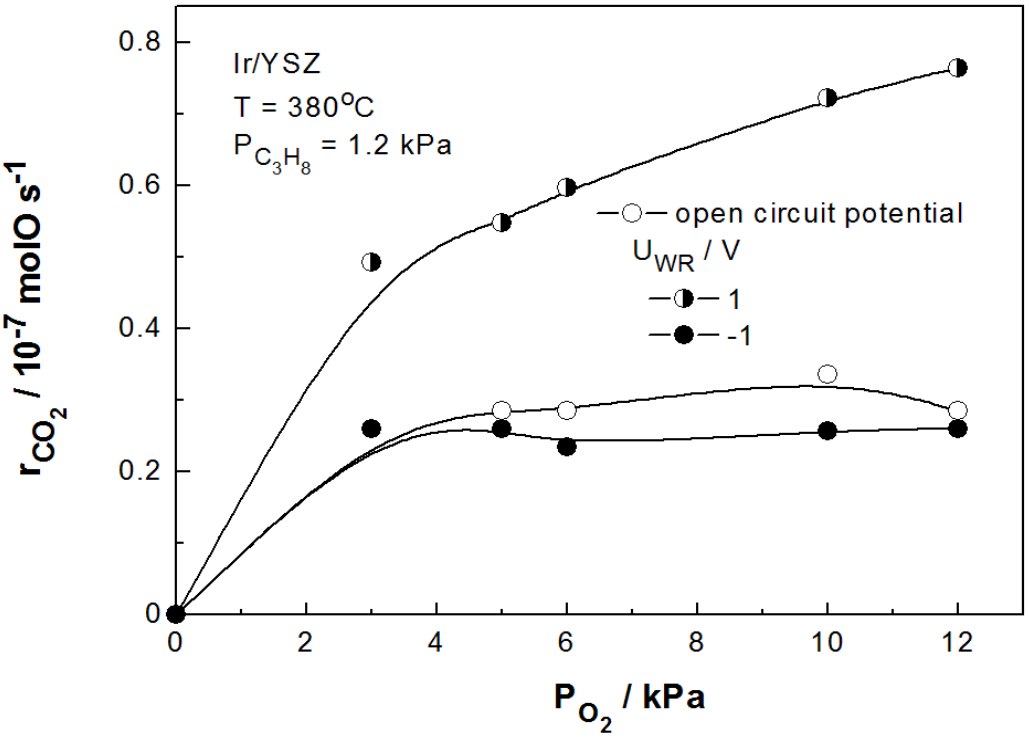

Figure 5.22 Dependence of open circuit and positive and negative potential application of sputtered Ir catalyst-electrode deposited on propane oxidation of (a) at constant P_{O_2} (P_{O_2}= 3 kPa) and (b) at constant $P_{C_3H_8}$ ($P_{C_3H_8}$= 1.2 kPa) under T = 380°C

Figure 5.22 shows the effect of O_2 and C_3H_8 partial pressures on propane oxidation of sputtered-Ir film deposited on YSZ. The electrophobic behavior was observed for this catalyst-electrode. These results show clearly that catalytic rate is positive order in electron donor (propane), as shown in Figure 5.22a, while zero order in an electron acceptor (oxygen) under open circuit conditions, as shown in Figure 5.22b. This is indeed case for sputtered-Ir catalyst electrode, there is a limitation of mass flow controller, thus we cannot go to higher partial pressure of reactant in order to obtain more clear trend of kinetic experiments. The effect of P_{O_2} for sputtered-Ir over YSZ is similar to in the case of sputtered-Pd over YSZ, where rate of CO_2 formation is zero order in oxygen for electrophobic behavior.

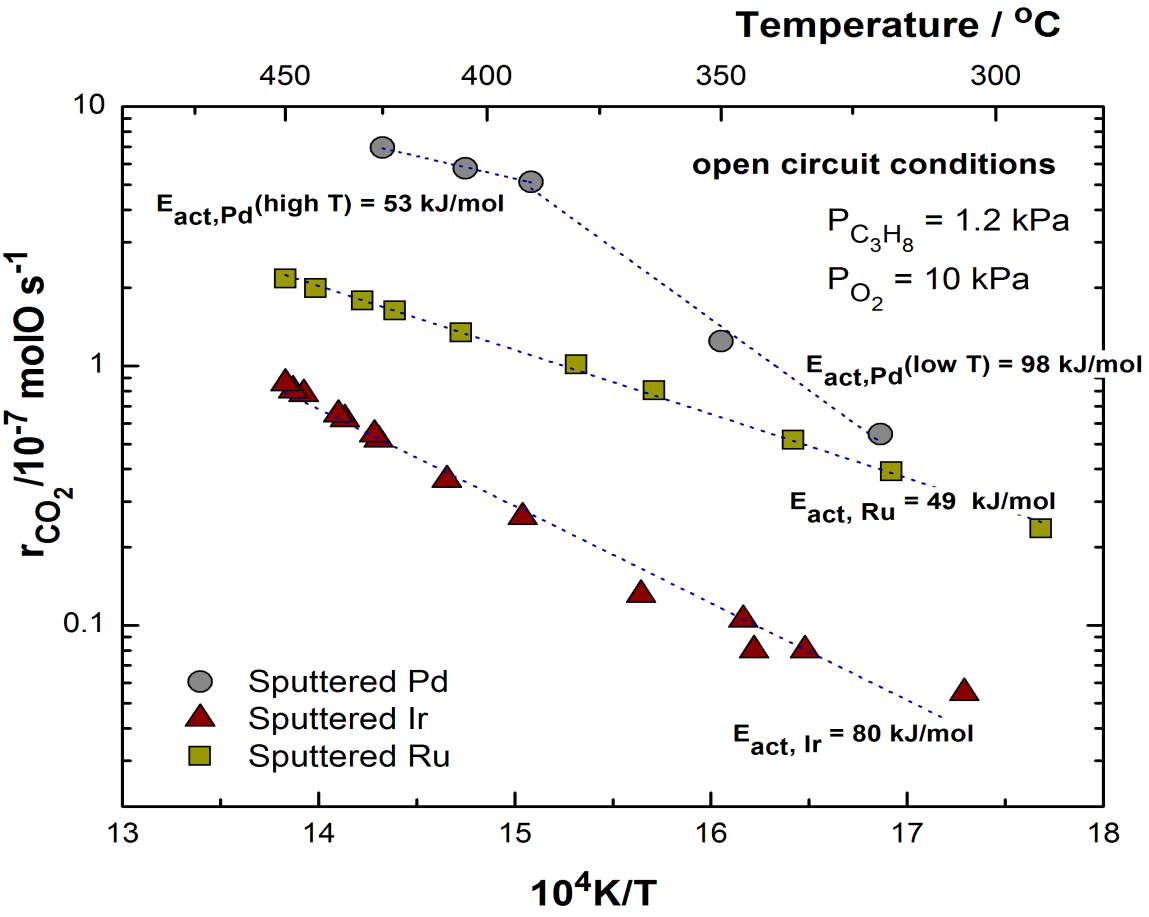

Figure 5.23 Arrhenius plots for CO_2 formation rate over Pd/YSZ, Ir/YSZ and Ru/YSZ catalysts electrodes under open circuit conditions.
$P_{C_3H_8}$ = 1.2 kPa, P_{O_2} = 10 kPa. F_v = 170 cm^{3}min^{-1} (STP)

Figure 5.23 shows the Arrhenius plot of the CO_2 formation rate under open circuit conditions using Pd, Ir and Ru catalyst electrodes. As shown in the figure, apparent activation energies, E_{act}, in the range of 50-100 kJ/mol were calculated for Pd, Ir and Ru catalyst-electrodes, which are in good agreement with values reported in literatures [78-81, 83]. Table 5.2 summarizes the activation energy values for the studied three catalyst-electrodes under open circuit and positive and negative potential application conditions. As shown E_{act} in case of Pd is lower than Ir and Ru, while E_{act} increases by negative and decreases by positive potential application, in agreement with EPOC theory.

Table 5.2 Apparent activation energy values for Pd, Ir, and Ru catalyst-electrodes under open circuit and positive and negative potential application conditions. $P_{C_3H_8}$ = 1.2 kPa, P_{O_2} = 10 kPa

Metallic film	E_{act} / kJ/mol		
	opc	+1 V	-1 V
Pd	53	47	58
Ir	80	77	85
Ru	49	44	55

5.3 The role of Mn_xO_y interlayer for Pd catalysts deposited on yttria-stabilized zirconia in the deep propane oxidation

The combination of manganese oxide with Pd deposited on YSZ has been investigated in this present study for deep propane oxidation in order to achieve higher catalytic activity under open and closed circuit conditions.

5.3.1 Catalyst Characterization

(a) **(b)**

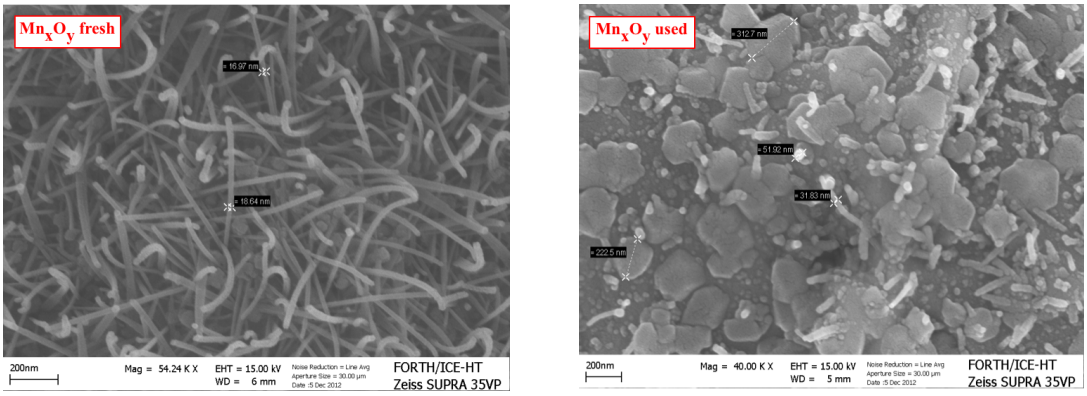

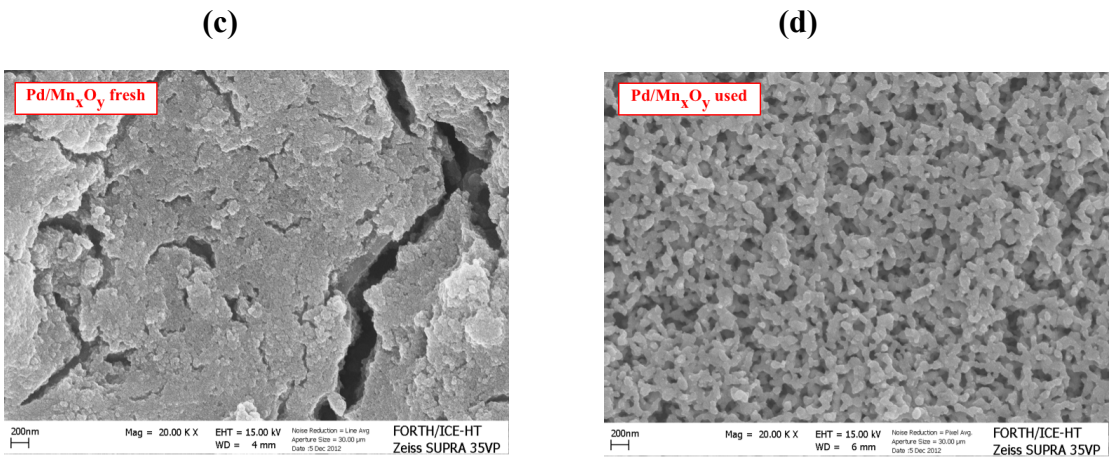

Figure 5.24 SEM micrographs of fresh and used catalyst electrodes; (a) and (b) Mn_xO_y catalyst electrode over YSZ and (c) and (d) Pd/ Mn_xO_y catalyst electrode over YSZ

The catalyst surface morphology for Mn_xO_y and Pd/Mn_xO_y was studied via SEM and XRD techniques after preparation (fresh) and after catalytic activity measurement (used) as show in Figures 5.24a-d. The Mn_xO_y fresh sample exhibits a rough surface with a number of small lines as in Figure 5.24a, while Mn_xO_y is unstable after exposure to the gas mixture. After propane oxidation, a rough surface with less small line and the formation of some crystallize was obtained as shown in Figure 5.24b. In the case of Pd/Mn_xO_y catalyst-electrode is shown in Figures 5.24c and 5.24d for fresh and used catalyst-electrode, respectively. Figures 5.24d shows the main feature of fresh Pd/Mn_xO_y deposited on YSZ. The fresh Pd/Mn_xO_y also exhibits a rough surface with some crack along with the YSZ gain. After the propane oxidation experiment the film had been significantly changed and the formation of cavities and voids was observed, which is most likely due to the unstable of Mn_xO_y phase as mentioned before.

(a)

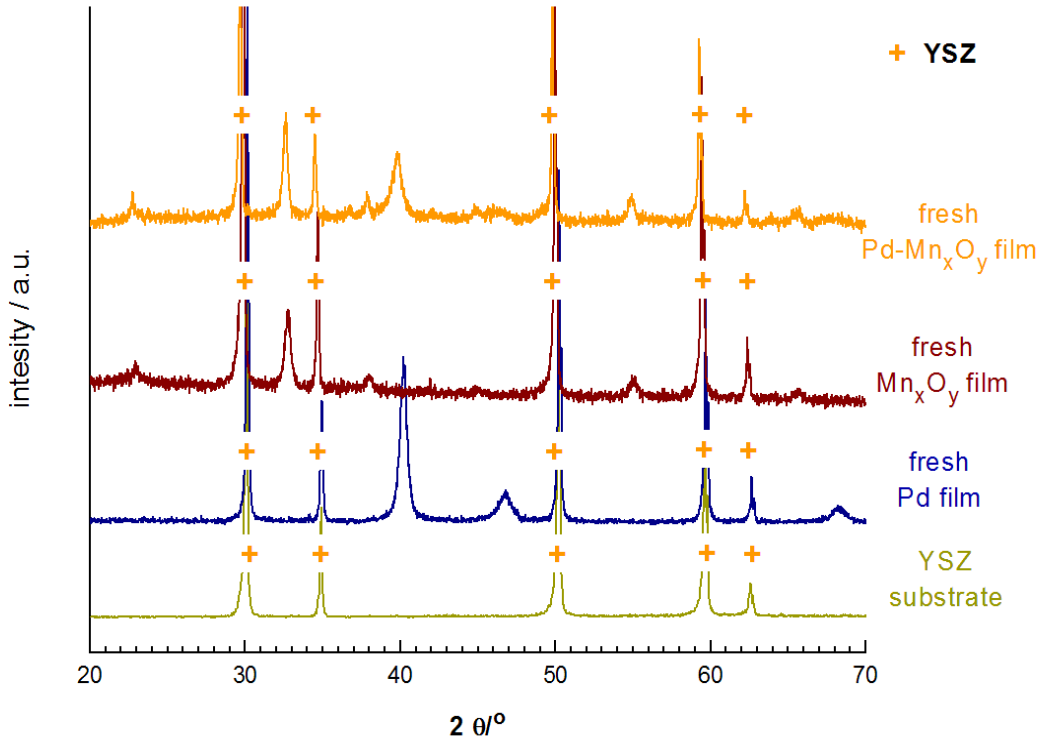
+ YSZ
fresh
Pd-Mn$_x$O$_y$ film
fresh
Mn$_x$O$_y$ film
fresh
Pd film
YSZ
substrate
intesity / a.u.
20
30
40
50
60
70
2 θ/°

(b)

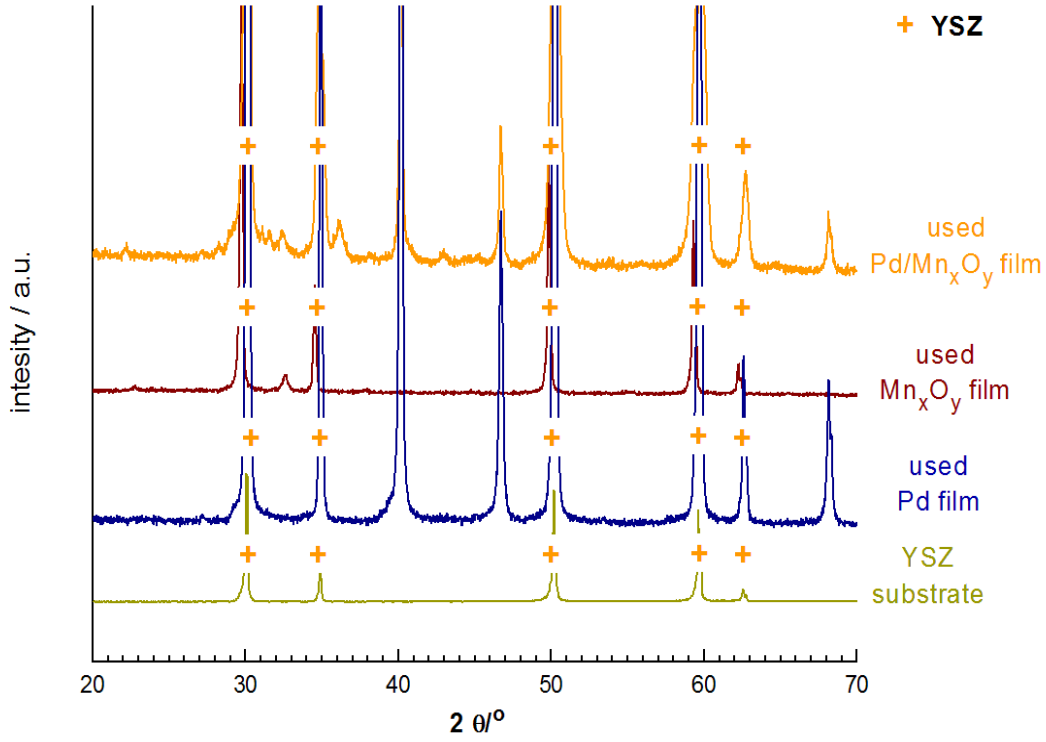

Figure 5.25 XRD spectra for Mn_xO_y /YSZ and Pd/ Mn_xO_y/YSZ catalyst-electrode; (a) fresh and (b) used catalyst electrodes

To identify phase composition of Mn_xO_y, XRD measurement was carried out as shown in Figure 5.25. The XRD patterns of Mn_xO_y samples consist of fresh and used catalyst-electrode. In the case of fresh samples, traces of Mn_3O_4, Mn_2O_3 and mainly $YMnO_3$ were found. In addition, Traces of Mn_3O_4, Mn_2O_3, $Mn_{0.2}Zr_{0.8}O_{1.8}$ and mainly $YMnO_3$ were observed on used samples. This means that even under medium calcination temperatures of 500°C the support may reacts with the interlayer to form $YMnO_3$. According to the strong YSZ reflections, the clear peak of Mn_xO_y interlayer was not observed.

5.3.2 Catalytic activity measurement

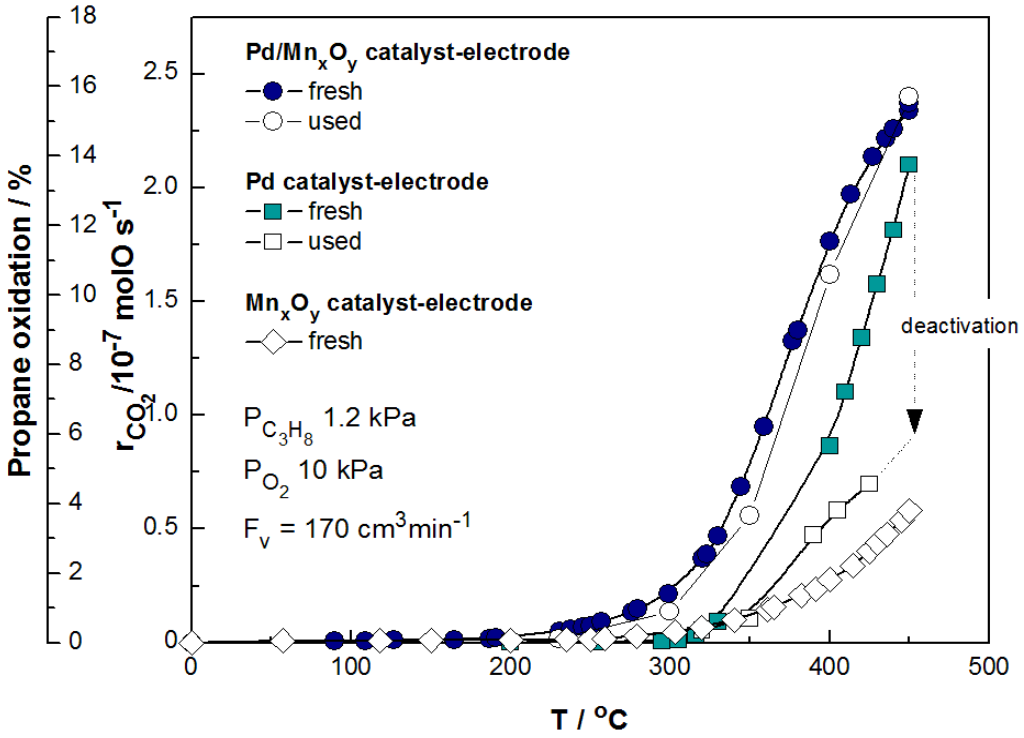

Figure 5.26 Steady-state effect of temperature on the CO_2 formation rate and propane conversion under open circuit condition. Open symbols represent as prepared catalyst results. Closed symbols represent spent catalyst results. Conditions: $P_{C_3H_8}$ = 1.2 kPa, P_{O_2} = 10 kPa, F_v = 170 cm^3min^{-1} (STP)

Figure 5.26 shows the steady-state effect of temperature on the CO_2 formation rate and on propane conversion for different catalyst-electrodes (i.e., Pd, Pd with Mn_xO_y interlayer, and Mn_xO_y) under open circuit (un-promoted) conditions. First, changes in propane conversion were followed by a stepwise increase of the temperature to 450°C, then the three catalysts have been exposed to the reaction mixture at 450°C for 2h, and last catalytic activity was followed during stepwise cooling to 100°C. The sample Pd/Mn_xO_y exhibits best catalytic activity in comparison to the Pd and Mn_xO_y films on YSZ. In the case of only Pd, the conversion dramatically decreases to 4% [82], whereas Pd with an Mn_xO_y interlayer shows no

significant decrease in the conversion in comparison to the fresh sample, which may be because Pd/Mn_xO_y surface is already partially promoted by thermally backspilled over of O^{2-} ion from the solid electrolyte support and the use of high ionic mobility, i.e. Mn_xO_y as interlayer. The promoting ionic from backspillover oxygen species is believed to be responsible for the effect of MSI (metal-support interaction), leading to enhanced catalytic activity for oxidation reaction [95, 125, 126].

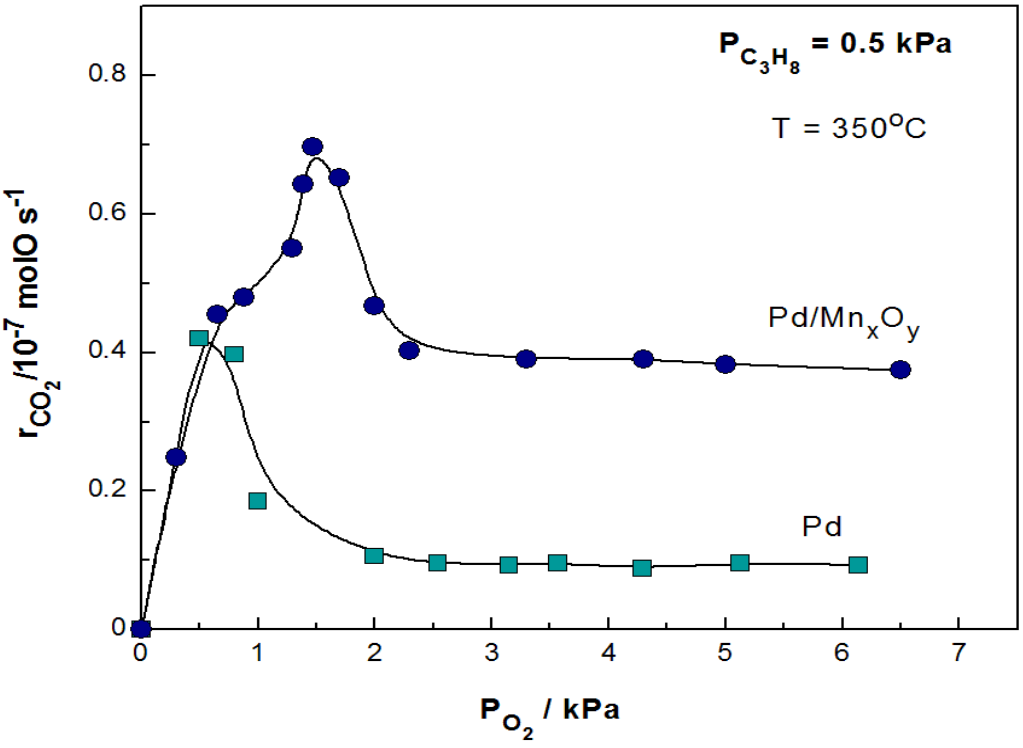

Figure 5.27 Steady-state effect of oxygen partial pressure on the CO_2 formation rate under open circuit condition comparing Pd and Pd/Mn_xO_y catalyst electrodes. Conditions: $P_{C_3H_8}$ = 0.5 kPa, F_v = 170 cm^3min^{-1}(STP)

Figure 5.27 shows the effect of partial pressure of O_2 at fixed $P_{C_3H_8}$ ($P_{C_3H_8}$ = 0.5 kPa) obtained at open circuit (unpromoted) condition and at 350°C in comparing between Pd/Mn_xO_y and Mn_xO_y. It was found that the maximum rate shifts to higher

P_{O_2} if Pd is deposited on an Mn_xO_y interlayer and indicate its better stability in excess of O_2 in agreement with pervious work [127].

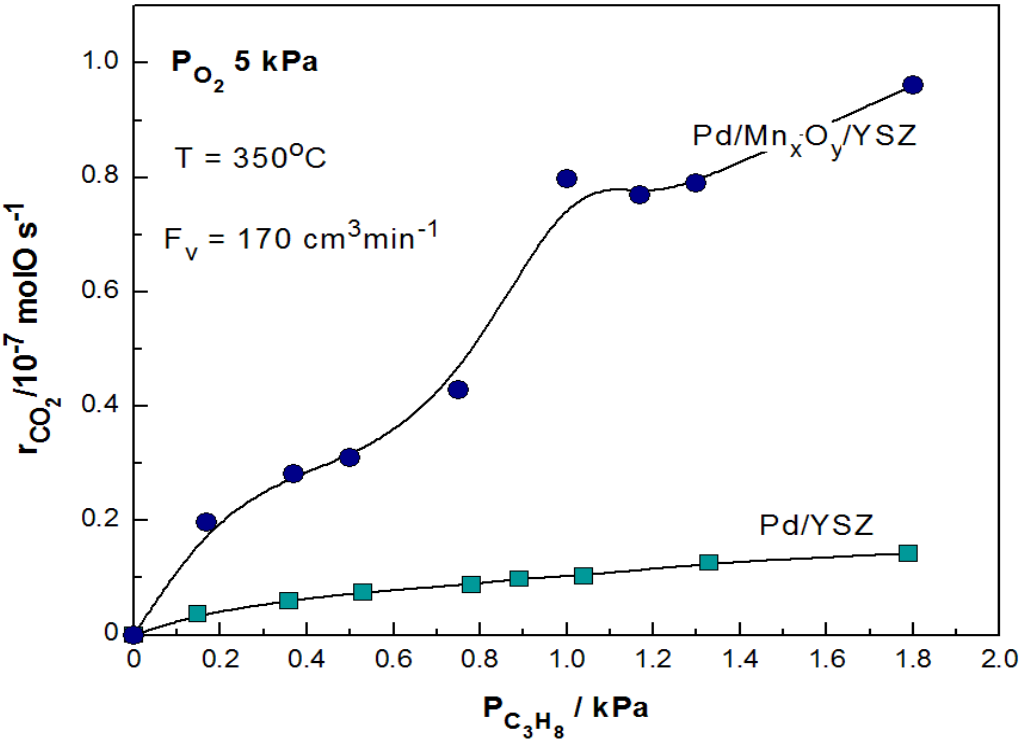

Figure 5.28 Steady-state effect of propane partial pressure on the CO_2 formation rate under open circuit condition comparing Pd and Pd/Mn_xO_y catalyst electrodes. Conditions: P_{O_2} = 5 kPa, F_v = 170 cm^3min^{-1}(STP)

Figure 5.28 shows the effect of partial pressure of C_3H_8 at fixed P_{O_2} (P_{O_2} = 5 kPa) obtained at open circuit or unpormoted condition and at 350°C for Pd/Mn_xO_y and Pd. The observed result indicated that the catalytic rate was positive order in fuel, here for propane in both catalyst-electrodes (i.e., Pd/Mn_xO_y and Mn_xO_y).

(a)

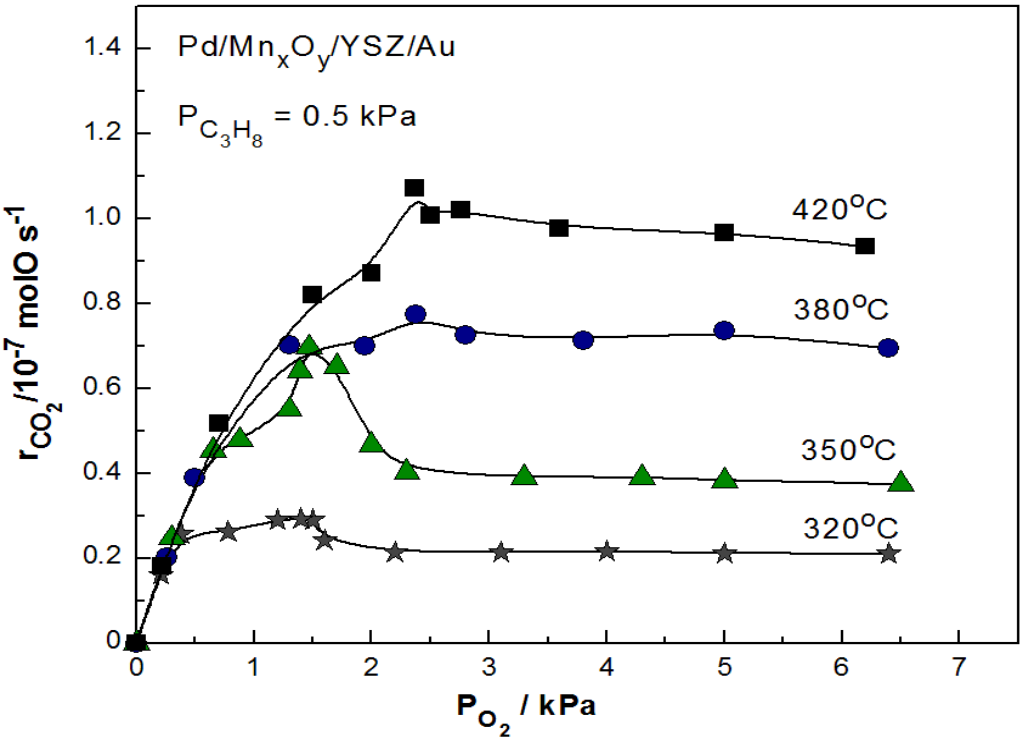
Pd/Mn$_x$O$_y$/YSZ/Au
$P_{C_3H_8}$ = 0.5 kPa
420°C
380°C
350°C
320°C
r_{CO_2} /10^{-7} molO s^{-1}
P_{O_2} / kPa
0
0.2
0.4
0.6
0.8
1.0
1.2
1.4
0
1
2
3
4
5
6
7

(b)

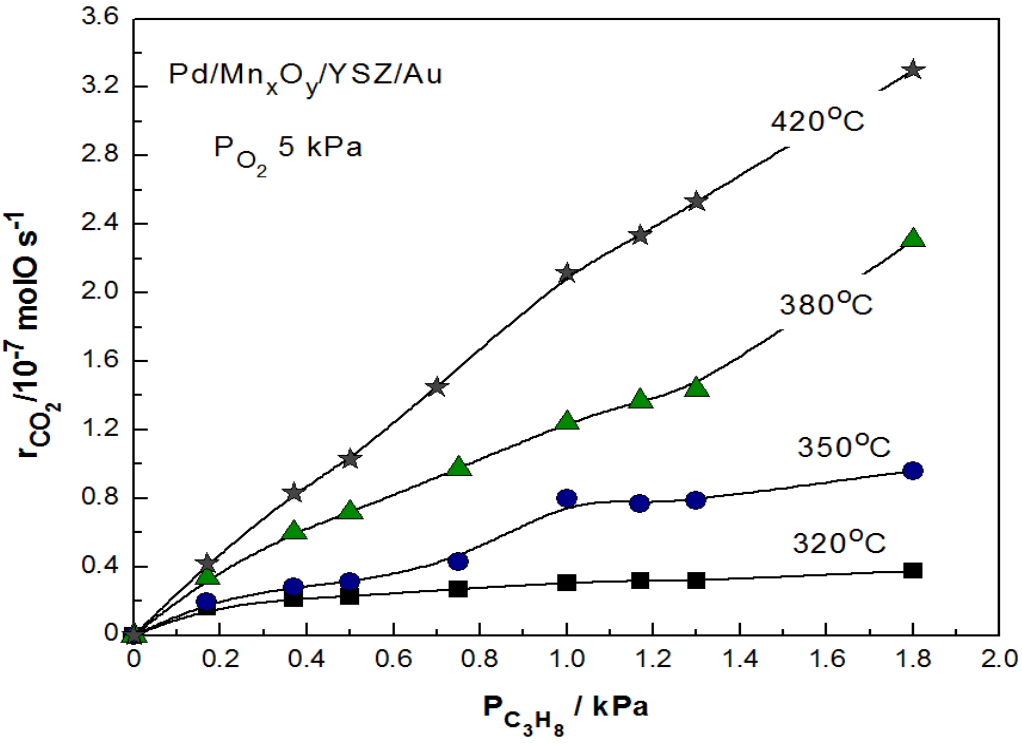

Figure 5.29 Steady-state effect of gas reactant partial pressure on the CO_2 formation rate under open circuit condition for Pd/Mn_xO_y catalyst electrodes upon different temperatures (a) at fixed $P_{C_3H_8}$ = 0.5 kPa, (b) at fixed P_{O_2} = 5 kPa under F_v = 170 cm^3min^{-1}(STP)

Figures 5.29a and b show the dependence of the steady-state and on the partial pressures of O_2 and C_3H_8 under open circuit conditions and at different temperatures (320°C to 420°C). As shown in Figure 5.29a, where the effect of partial pressure of O_2 (at given $P_{C_3H_8}$ = 0.5 kPa) was studied, a Langmuir-Hishelwood kinetic type behaviour was observed more clearly at lower temperatures, indicating the competitive adsorption of C_3H_8 and O_2 over the catalyst surface electrode. The maximum oxygen partial pressure P_{O_2}, here for the maximum catalytic rate is gradually shifted to higher value in together with increasing temperature. This shifting peak indicates a batter stable catalyst-electrode in excess of O_2. On the other hand, Figure 5.29b presents the kinetic study at different values of partial pressure of C_3H_8

(at given P_{O_2} = 5 kPa). The results was observed that the apparent order tends to be positive order in all entire temperature range in agreement with previous study [128].

Under the kinetic experiments in this present work as in Figures 5.27, 5.28, and 5.29, the rate of CO_2 formation is positive order in propane and almost zero order in oxygen under open circuit condition. The observed reaction order implied that catalyst-electrode surface is predominantly with oxygen with a relatively small amount of propane. The comparative co-adsorption of propane and oxygen on the surface catalyst-electrode is preferable on the adsorption of propane [128].

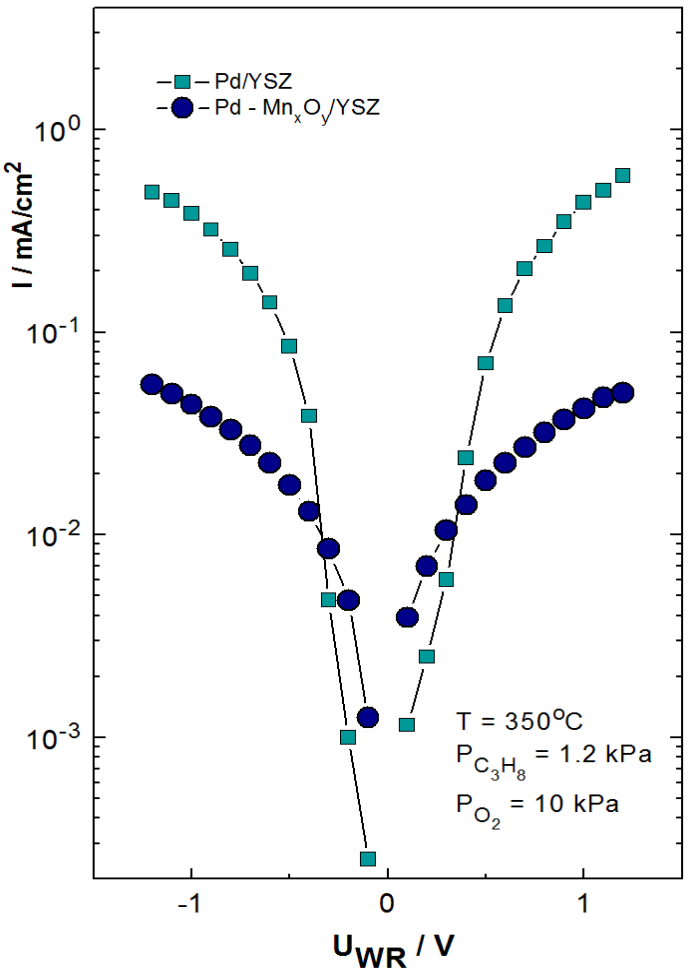

Figure 5.30 Steady-state effect of applied potential as a function of current on Pd and Pd/Mn_xO_y catalyst electrode at 350°C

The effect of the applied potential (U_{WR}) on the steady-state catalytic CO_2 formation rate is shown in Figure 5.30 by comparing between Pd and Pd/Mn_xO_y at

350°C. The exchange current values, i_0, for the positive potential application are found to be 0.06 mA for Pd and 0.01 mA for Pd/Mn_xO_y catalyst-electrodes. A higher exchange current i_0 lead to a faster catalytic rate of reaction but not necessarily higher catalytic activity or the rate of reaction.

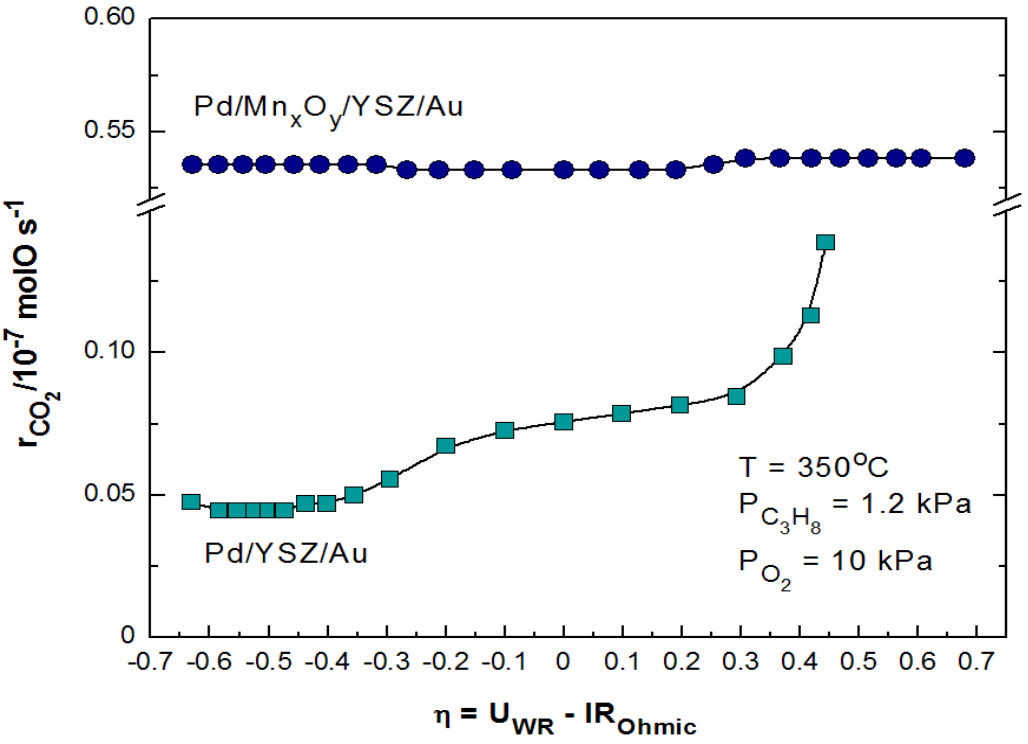

Figure 5.31 Steady-state effect of the applied overpotential on rate of reaction in comparision of Pd and Pd/Mn_xO_y catalyst-electrodes at 350°C under $P_{C_3H_8}$ = 1.2 kPa and P_{O_2} = 10 kPa, flow rate = 170 $cm^3\ min^{-1}$ (STP)

Figure 5.31 shows the steady-state effect of catalyst overpotential on the rate of CO_2 formation at 350°C. The pronounced difference of the rates of CO_2 between two different catalyst-electrodes, i.e Pd and Pd/Mn_xO_y was observed. A significant higher catalytic activity of Pd/Mn_xO_y was obtained under operating conditions. However, Pd with Mn_xO_y interlayer hinders the electrochemical promotion effect, metallic Pd catalyst electrode exhibits the electrophobic behavior with a small value of rate enhancement ratio, ρ, taking value up to 1.6 and a significant Faradaic efficiency value, taking value up to 250 under anodic poralization. The absence of

electrochemical promotion on Pd/Mn_xO_y, it can be the use of high ionic mobility materials; for example, YSZ, CeO_2, TiO_2, Mn_xO_y, and so on. The promoting backspillover species, here for O species backspillover, attribute to enhance the catalytic activity for propane oxidation. Therefore, Pd/Mn_xO_y surface is already promoted due to the thermal backsplillover from this high ionic mobility material as discussed in previous paragraph.

AC impedance spectroscopy has been used to study the Pd and Pd/Mn_xO_y catalyst-electrode under reaction conditions of propane oxidation. Temperature and time of exposure have been varied to investigate the effect of the Mn_xO_y interlayer on the cell resistance, and indirectly on the oxidation resistivity of the Pd and Pd/Mn_xO_y catalyst-electrode.

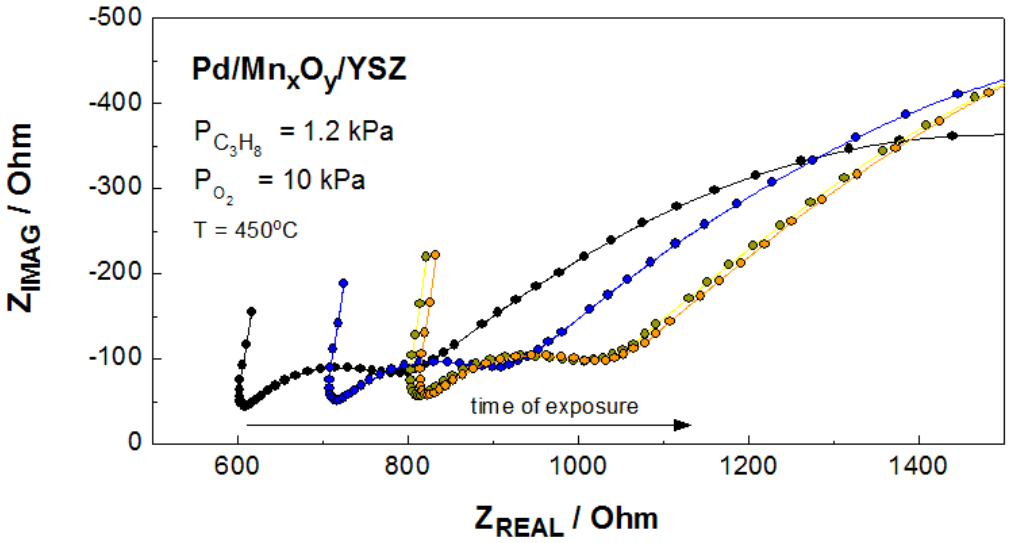

Figure 5.32 Series of AC impedance spectra as a function of time under open circuit condition at T = 450°C, $P_{C_3H_8}$ = 1.2 kPa and P_{O_2} = 10 kPa, volumetric flow rate = 170 $cm^3\ min^{-1}$ (STP)

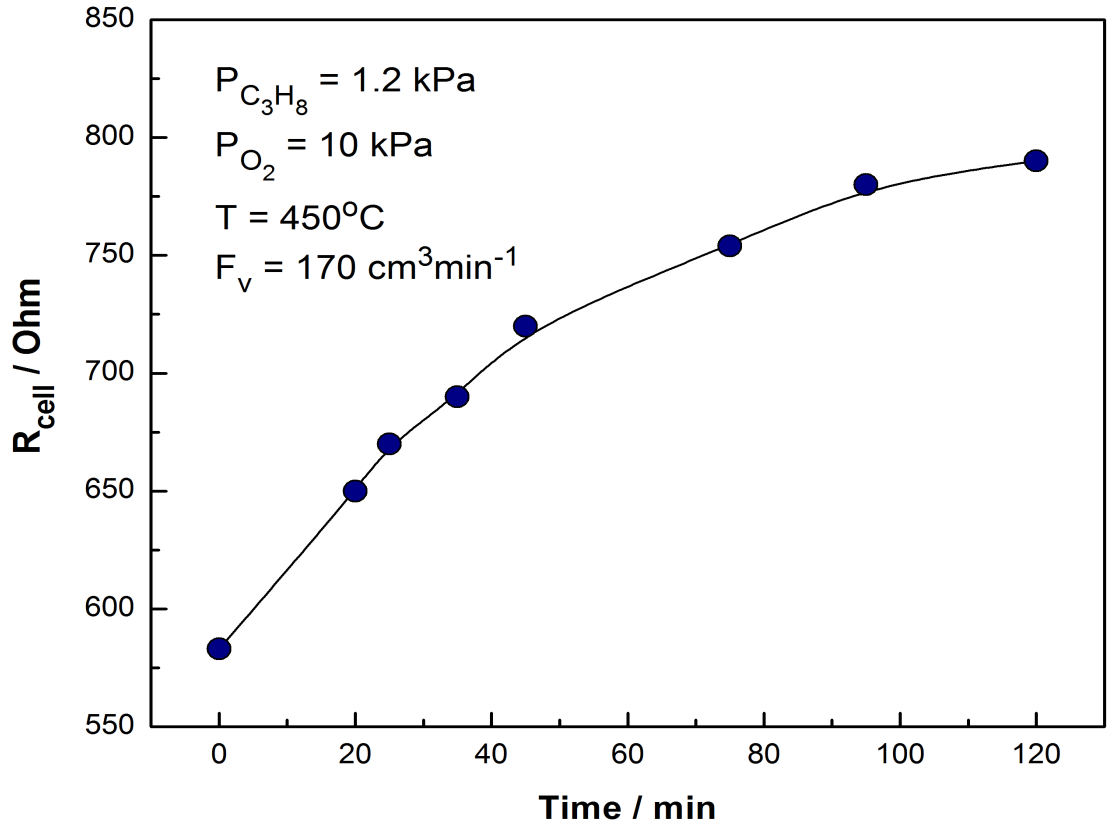

Figure 5.33 High frequency intersect (Ohmic resistance, R_{cell}) as a function of exposure time at 450°C, $P_{C_3H_8}$ = 1.2 kPa and P_{O_2} = 10 kPa, volumetric flow rate = 170 cm^3 min^{-1} (STP) and at open circuit conditions

Figure 5.32 shows the complex impedance spectra (Nyquist plots) with two well-distinguished semicircles: one small semicircle in the range of highest frequencies (10 kHz-10Hz) and a second larger semicircle for frequencies lower than 10 Hz. The spectra are shifted to higher real parts of the impedance with increasing exposure time. The semicircles were fitted with a resistor–capacitor combination as follow: R_{cell}-(R_1C_1)-R_2C_2. The high frequency resistance of the electrolyte and catalyst film (R_{cell}) is found to be 600 Ω at the beginning of the exposure and increase to a stable value of 800 Ohm indicating that Pd/Mn_xO_y has reached a stable oxidation state (Figure 5.33).

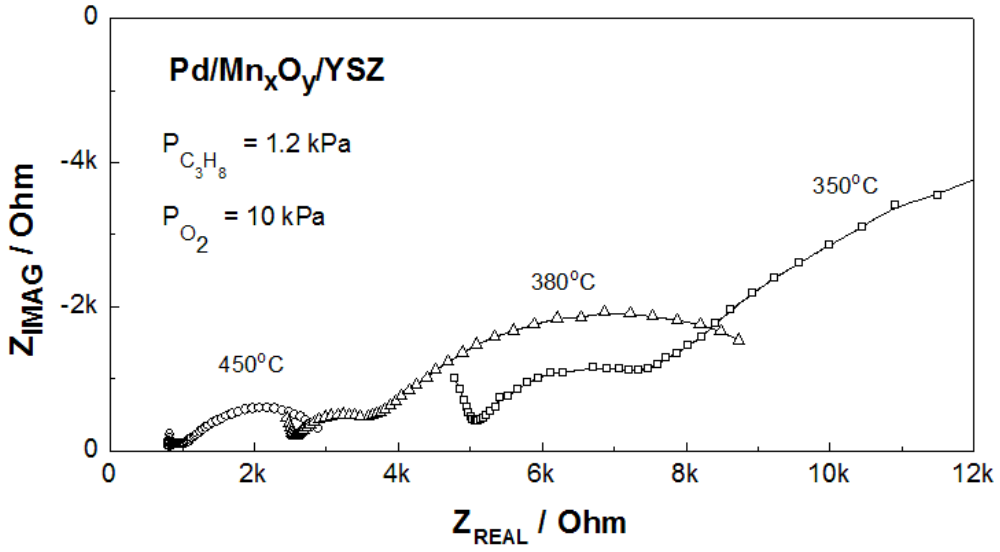

Figure 5.34 Series of AC impedance spectra at open circuit conditions and as a function of temperature. $P_{C_3H_8}$ = 1.2 kPa and P_{O_2} = 10 kPa, volumetric flow rate = 170 cm^3 min^{-1} (STP)

Figure 5.34 also presents the complex impedance spectra with two well-distinguished semicircles same as in Figure 5.32. In this figure shows the AC impedance as a function of temperature. The spectra shifts to higher real parts of the impedance with decreasing temperature indicating Mn_xO_y reaches to a higher the Ohmic resistance at lower temperature.

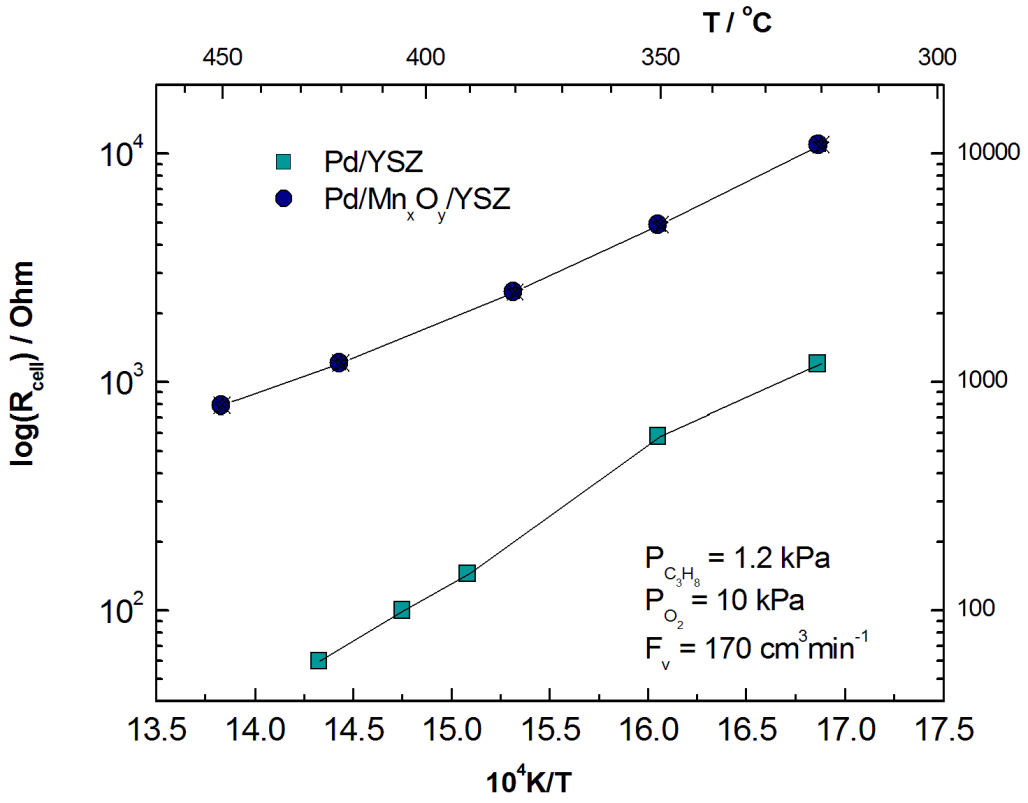

Figure 5.35 Arrhenius plots of R_{cell} for the Pd/YSZ and Pd/Mn_xO_y/YSZ cell under reaction conditions and at open circuit

Figure 5.35 shows that the R_{cell}, the Ohmic resistance, of the Pd/Mn_xO_y catalyst is one order of magnitude higher than the Pd catalyst without interlayer. Since the YSZ electrolyte and the Pd sputter-deposited catalyst for both samples have exactly the same geometry, thickness and chemical composition, the increase in the Ohmic resistance is mainly due to the Mn_xO_y interlayer.

CHAPTER VI

CONCLUSIONS AND RECOMMENDATIONS

This chapter summarizes the works on electrochemical promotion of light hydrocarbon oxidation, i.e. ethylene and propane oxidation on different catalyst electrodes deposited on Ytrria-Stabilized Zirconia under various operating conditions. The recommendation for further study is also provided in this chapter.

6.1 Conclusions

The electrochemical promotion of C_2H_4 oxidation reaction has been investigated under different feed gas compositions and temperatures over a Pt/YSZ catalyst electrode. Under mildly oxidizing conditions the reaction exhibits an electrophobic behavior, i.e. rate increase by positive potential application, while it shifted to electrophilic, i.e. rate increase by negative potential application, under near stoichiometric feed conditions. The observed change in electrochemical promotion behavior by feed gas composition is related to the change in reaction kinetic order with respect to C_2H_4, in total agreement with the rules of electrochemical promotion [10, 52, 53]. It was found that the reaction is positive order in O_2, while it exhibits a maximum with respect to C_2H_4, in the examined range of partial pressure.

The electrochemical promotion of C_3H_8 oxidation has been investigated over Pd, Ir, Ru and Cu catalyst-electrodes sputter-deposited on YSZ disks in the temperature range between 250 and 450^{o}C. Under open circuit conditions the catalytic activity of fresh catalysts was found to decrease in the order Ru>Pd>Ir, while Cu has no significant change. However, at steady-state (used catalysts) the activity order was Pd>Ru>Ir>Cu. This change has been attributed to severe oxidation of Ru and Ir catalyst-electrode surface, as confirmed also by SEM and XRD analyses. Furthermore, an electrophobic type behavior was observed, i.e. rate increase by positive and rate decrease by negative potential application, for all studied catalyst-electrodes. This behavior has been attributed to the potential-induced weakening of the metal-O bond strength due to $O^{\delta-}$ species presence on the catalyst surface, which

results in the formation of a more active O_{ads} species, and also in lower of oxygen coverage of the catalytic surface. In the case of Pd, positive potential application leads to maximum rate enhancement ratio, ρ, values up to 2.6 at 425^{o}C, where apparent Faradaic efficiency, Λ, reaches values up to 130.

In comparison between sputter-deposited Pd and Pd/Mn_xO_y catalyst-electrodes deposited on YSZ using an electrochemical cell had been investigated under variety of operating conditions. Better catalytic performane over the entire temperature range was achieved with Pd/Mn_xO_y and was confirmed in kinetic studies by the shift of the maximum rate to higher oxygen partial pressures.

Open circuit propane oxidation is favored by the metallic Pd phase [82], and can be further increased via the application of a potential or current. Propane oxidation rates are reversibly enhanced by up to a factor 3.

The interlayer of Mn_xO_y hinders the electrochemical promotion of propane oxidation in excess of oxygen.

6.2 Recommendations

In order to further improvement of electrochemical promotion effect, some ideas derived from this dissertation are suggested here for future research:

1. Extent the study Mn_xO_y interlayers to other metals that form stable oxides under oxidative conditions (e.g. Ru, Rh, Cu etc.). It would be interesting to see the effect of Mn_xO_y support on the metal oxide stability and structure (will Ru still form remarkable flowers)

2. Study the effect of Mn_xO_y interlayer in reactions where valuable products are formed (e.g. C_2H_4O formation).

3. Use other interlayer supports that exhibit mixed ionic electronic conductivity, to investigate their effect on EPOC.

4. Use other preparation method for metallic films (i.e. pasted, impregnation method etc.), to investigate the relationship between the competitive adsorption of gas reactant, here for propane and oxygen comparing with different particle size of catalyst-electrode.

REFERENCES

[1] Jiménez-Borja, C., F. Dorado, A. de Lucas-Consuegra, J.M. García-Vargas and J.L. Valverde. Complete oxidation of methane on Pd/YSZ and Pd/CeO_2/YSZ by electrochemical promotion. Catalysis Today 146 (2009): 326-329.

[2] Neyestanaki, A.K., N. Kumar and L.E. Lindfors. Catalytic combustion of propane and natural gas over Cu and Pd modified ZSM zeolite catalysts. Applied Catalysis B: Environmental 7 (1995): 95-111.

[3] Ferrandon, M., Carnö, J., Järas, S., E. Björnbom. Total oxidation catalysts based on manganese or copper oxides and platinum or palladium I: Characterisation. Applied Catalysis A: General 180 (1999): 141-151.

[4] Gèlin, P. and M. Primet. Complete oxidation of methane at low temperature over noble metal based catalysts: a review. Applied Catalysis B: Environmental 39 (2002): 1-37.

[5] Gèlin, P., L. Urfels, M. Primet and E. Tena. Complete oxidation of methane at low temperature over Pt and Pd catalysts for the abatement of lean-burn natural gas fuelled vehicles emissions: influence of water and sulphur containing compounds. Catalysis Today 83 (2003): 45-57.

[6] Papaefthimiou, P., T. Ioannides and X.E. Verykios. Performance of doped Pt/TiO_2 (W^{6+}) catalysts for combustion of volatile organic compounds (VOCs). Applied Catalysis B: Environmental 15 (1998): 75-92.

[7] Yazawa, Y., N. Takagi, H. Yoshida, S.-i. Komai, A. Satsuma, T. Tanaka, et al. The support effect on propane combustion over platinum catalyst: control of the oxidation-resistance of platinum by the acid strength of support materials. Applied Catalysis A: General 233 (2002): 103-112.

[8] Garetto, T.F., E. Rincón and C.R. Apesteguía. Deep oxidation of propane on Pt-supported catalysts: drastic turnover rate enhancement using zeolite supports. Applied Catalysis B: Environmental 48 (2004): 167-174.

[9] C.G. Vayenas, S.B., C. Pliangos, S. Brosda, D. Tsiplakidis. Electrochemical Activation of Catalysis: Promotion, Electrochemical Promotion and Metal-Support Interactions, New York: Kluwer Academic/Plemum Publishers,2001.

[10] Brosda, S. and C.G. Vayenas. Rules and mathematical modeling of electrochemical and classical promotion: 2. Modeling. Journal of Catalysis 208 (2002): 38-53.

[11] Kotsionopoulos, N. and S. Bebelis. Electrochemical promotion of the oxidation of propane on Pt/YSZ and Rh/YSZ catalyst-electrodes. Journal of Applied Electrochemistry 35 (2005): 1253-1264.

[12] Kokkofitis, C., G. Karagiannakis and M. Stoukides. Electrochemical promotion in O^{2-} cells during propane oxidation. Topics in Catalysis 44 (2007): 361-368.

[13] Vernoux, P. Electrochemical Promotion of Propane and Propene Oxidation on Pt/YSZ. Journal of Catalysis 208 (2002): 412-421.

[14] Bebelis, S. and N. Kotsionopoulos. Non-faradaic electrochemical modification of the catalytic activity for propane combustion of Pt/YSZ and Rh/YSZ catalyst-electrodes. Solid State Ionics 177 (2006): 2205-2209.

[15] Kokkofitis, C., G. Karagiannakis, S. Zisekas and M. Stoukides. Catalytic study and electrochemical promotion of propane oxidation on Pt/YSZ. Journal of Catalysis 234 (2005): 476-487.

[16] Lizarraga, L., M. Guth, A. Billard and P. Vernoux. Electrochemical catalysis for propane combustion using nanometric sputtered-deposited Pt films. Catalysis Today 157 (2010): 61-65.

[17] Constantinou, I., I. Bolzonella, C. Pliangos, C. Comninellis and C.G. Vayenas. Electrochemical promotion of RuO_2 catalysts for the combustion of toluene and ethylene. Catalysis Letters 100 (2005): 125-133.

[18] Nicole, J. and C. Comninellis. Electrochemical promotion of IrO_2 catalyst activity for the gas phase combustion of ethylene. Journal of Applied Electrochemistry 28 (1998): 223-226.

[19] Kim, M.H., K.H. Cho, C.H. Shin, S.E. Kang and S.W. Ham. Total oxidation of propane over Cu-Mn mixed oxide catalysts prepared by co-precipitation method. Korean Journal of Chemical Engineering 28 (2011): 1139-1143.

[20] M. C. Álvarez-Galván, V.A.d.l.P.O.S., J. L. G. Fierro and P. L. Arias. Alumina-supported manganese- and manganese–palladium oxide catalysts for VOCs combustion. Catalysis Communications 4 (2003): 223-228.

[21] Craciun, R., B. Nentwick, K. Hadjiivanov and H. Knözinger. Structure and redox properties of MnO_x/Yttrium-stabilized zirconia (YSZ) catalyst and its used in CO and CH4 oxidation. Applied Catalysis A: General 243 (2003): 67-79.

[22] Vayenas, C.G. and C.G. Koutsodontis. Non-Faradaic electrochemical activation of catalysis. The Journal of Chemical Physics 128 (2008): 182506.

[23] Vayenas, C.G. Bridging electrochemistry and heterogeneous catalysis. Journal of Solid State Electrochemistry (2011): 1-11.

[24] Vayenas, C.G. and C.G. Koutsodontis. Non-Faradaic electrochemical activation of catalysis. Journal of Chemical Physics 128 (2008).

[25] Katsaounis, A. Recent developments and trends in the electrochemical promotion of catalysis (EPOC). Journal of Applied Electrochemistry 40 (2010): 885-902.

[26] Baranova, E.A., A. Thursfield, S. Brosda, G. Foti, C. Comninellis and C.G. Vayenas. Electrochemically induced oscillations of C_2H_4 oxidation over thin sputtered Rh catalyst films. Catalysis Letters 105 (2005): 15-21.

[27] Baranova, E.A., A. Thursfield, S. Brosda, G. Foti, C. Comninellis and C.G. Vayenas. Electrochemical promotion of ethylene oxidation over Rh catalyst thin films sputtered on YSZ and TiO_2/YSZ supports. Journal of the Electrochemical Society 152 (2005): E40-E49.

[28] Li, X., F. Gaillard and P. Vernoux. Investigations under real operating conditions of the electrochemical promotion by O_2 temperature programmed desorption measurements. Topics in Catalysis 44 (2007): 391-398.

[29] Cavalca, C.A., G. Larsen, C.G. Vayenas and G.L. Haller. Electrochemical modification of CH_3OH oxidation selectivity and activity on a Pt single-pellet catalytic reactor. Journal of Physical Chemistry 97 (1993): 6115-6119.

[30] Stoukides, M. and C.G. Vayenas. The effect of electrochemical oxygen pumping on the rate and selectivity of ethylene oxidation on polycrystalline silver. Journal of Catalysis 70 (1981): 137-146.

[31] Ladas, S., S. Kennou, S. Bebelis and C.G. Vayenas. Origin of non-Faradaic electrochemical modification of catalytic activity. Journal of Physical Chemistry 97 (1993): 8845-8848.

[32] Harkness, I.R. and R.M. Lambert. Electrochemical Promotion of the NO + Ethylene Reaction over Platinum. Journal of Catalysis 152 (1995): 211-214.

[33] Luerßen, B., S. Günther, H. Marbach, M. Kiskinova, J. Janek and R. Imbihl. Photoelectron spectromicroscopy of electrochemically induced oxygen spillover at the Pt/YSZ interface. Chemical Physics Letters 316 (2000): 331-335.

[34] Arakawa, T., A. Saito and J. Shiokawa. Surface study of a Ag electrode on a solid electrolyte used as oxygen sensor. Applications of Surface Science 16 (1983): 365-372.

[35] Neophytides, S.G. and C.G. Vayenas. TPD and cyclic voltammetric investigation of the origin of electrochemical promotion in catalysis. Journal of Physical Chemistry 99 (1995): 17063-17067.

[36] Neophytides, S.G., D. Tsiplakides and C.G. Vayenas. Temperature-programmed desorption of oxygen from Pt films interfaced with Y_2O_3-Doped ZrO_2. Journal of Catalysis 178 (1998): 414-428.

[37] Tsiplakides, D. and C.G. Vayenas. Temperature programmed desorption of oxygen from Ag films interfaced with Y_2O_3-Doped ZrO_2. Journal of Catalysis 185 (1999): 237-251.

[38] Katsaounis, A., Z. Nikopoulou, X.E. Verykios and C.G. Vayenas. Comparative isotope-aided investigation of electrochemical promotion and metal-support interactions: 2. CO oxidation by $^{18}O_2$ on electropromoted Pt films deposited on YSZ and on nanodispersed Pt/YSZ catalysts. Journal of Catalysis 226 (2004): 197-209.

[39] Katsaounis, A., Z. Nikopoulou, X.E. Verykios and C.G. Vayenas. Comparative isotope-aided investigation of electrochemical promotion and metal-support interactions 1. $^{18}O_2$ TPD of electropromoted Pt films deposited on YSZ and of dispersed Pt/YSZ catalysts. Journal of Catalysis 222 (2004): 192-206.

[40] Luerßen, B., E. Mutoro, H. Fischer, S. Günther, R. Imbihl and J. Janek. In Situ Imaging of Electrochemically Induced Oxygen Spillover on Pt/YSZ Catalysts. Angewandte Chemie International Edition 45 (2006): 1473-1476.

[41] Makri, M., G.G. Vayenas, S. Bebelis, K.H. Besocke and C. Cavalca. Atomic resolution STM imaging of electrochemically controlled reversible promoter dosing of catalysts. Surface Science 369 (1996): 351-359.

[42] Vayenas, C.G., D. Archonta and D. Tsiplakides. Scanning tunneling microscopy observation of the origin of electrochemical promotion and metal-support interactions. Journal of Electroanalytical Chemistry 554-555 (2003): 301-306.

[43] Frantzis, A.D., S. Bebelis and C.G. Vayenas. Electrochemical promotion (NEMCA) of CH_4 and C_2H_4 oxidation on Pd/YSZ and investigation of the origin of NEMCA via AC impedance spectroscopy. Solid State Ionics 136-137 (2000): 863-872.

[44] C.G. Vayenas, S.B., S.Ladas. The Dependence of Catalytic Activity on Catalyst Work Function. Nature 343 (1990): 625-627.

[45] Tsiplakides, D. and C.G. Vayenas. Electrode Work Function and Absolute Potential Scale in Solid-State Electrochemistry. Journal of the Electrochemical Society 148 (2001): E189-E202.

[46] Pacchioni, G., F. Illas, S. Neophytides and C.G. Vayenas. Quantum-chemical study of electrochemical promotion in catalysis. Journal of Physical Chemistry 100 (1996): 16653-16661.

[47] Pacchioni, G., J.R. Lomas and F. Illas. Electric field effects in heterogeneous catalysis. Journal of Molecular Catalysis A: Chemical 119 (1997): 263-273.

[48] Souentie, S., L. Lizarraga, E.I. Papaioannou, C.G. Vayenas and P. Vernoux. Permanent electrochemical promotion of C_3H_8 oxidation over thin sputtered Pt films. Electrochemistry Communications 12 (2010): 1133-1135.

[49] G. Foti, I.B., Ch. Comninellis Modern Aspects of Electrochemistry, ed. B.E.C. C.G. Vayenas, and R.E White. Vol. 36, New York: Kluwer Academic/Plenum Publishers,2003.

[50] Tsiplakides, D. and S. Balomenou. Milestones and perspectives in electrochemically promoted catalysis. Catalysis Today 146 (2009): 312-318.

[51] Mehrer, H., Fast Ion Conductors, in *Diffusion in Solids : Fundamentals, Methods, Materials, Diffusion-Controlled Processes*2007, Springer Berlin Heidelberg. p. 475-490.

[52] Brosda, S., C. Vayenas and J. Wei. Rules of chemical promotion. Applied Catalysis B: Environmental 68 (2006): 109-124.

[53] Vayenas, C.G., S. Brosda and C. Pliangos. Rules and mathematical modeling of electrochemical and chemical promotion: 1. Reaction classification and promotional rules. Journal of Catalysis 203 (2001): 329-350.

[54] Vayenas, C.G., S. Brosda and C. Pliangos. The double-layer approach to promotion, electrocatalysis, electrochemical promotion, and metal-support interactions. Journal of Catalysis 216 (2003): 487-504.

[55] Peng-ont, S., P. Praserthdam, F. Matei, D. Ciuparu, S. Brosda and C.G. Vayenas. Electrochemical Promotion of Propane and Methane Oxidation on Sputtered Pd Catalyst-Electrodes Deposited on YSZ. Catalysis Letters 142 (2012): 1336-1343.

[56] Anastasijevic, N.A. NEMCA—From discovery to technology. Catalysis Today 146 (2009): 308-311.

[57] Bultel, L., P. Vernoux, F. Gaillard, C. Roux and E. Siebert. Electrochemical and catalytic properties of porous Pt-YSZ composites. Solid State Ionics 176 (2005): 793-801.

[58] Glinrun, T., O. Mekasuwandumrong, J. Panpranot, C. Chaisuk and P. Praserthdam. Improvement of propane oxidation activity over Pt/Al_2O_3 by the use of MIXED gamma- and chi-Al_2O_3 supports. Reaction Kinetics Mechanisms and Catalysis 100 (2010): 441-448.

[59] Yazawa, Y., H. Yoshida, N. Takagi, S.I. Komai, A. Satsuma and T. Hattori. Acid strength of support materials as a factor controlling oxidation state of palladium catalyst for propane combustion. Journal of Catalysis 187 (1999): 15-23.

[60] Sarofim, A.F. and R.C. Flagan. NOx control for stationary combustion sources. Progress in Energy and Combustion Science 2 (1976): 1-25.

[61] Lee J.H. and Trimm, D.L. Catalytic combustion of methane. Fuel Processing Technology 42 (1995): 339-359.

[62] Yazawa, Y., H. Yoshida, S.I. Komai and T. Hattori. The additive effect on propane combustion over platinum catalyst: Control of the oxidation-resistance of platinum by the electronegativity of additives. Applied Catalysis A: General 233 (2002): 113-124.

[63] Yoshida, H.Y., Y. and T. Hattori. Effects of support and additive on oxidation state and activity of Pt catalyst in propane combustion. Catalysis Today 87 (2003): 19-28.

[64] Bera, P., K.C. Patil and M.S. Hegde. Oxidation of CH_4 and C_3H_8 over combustion synthesized nanosize metal particles supported on β''-Al_2O_3. Physical Chemistry Chemical Physics 2 (2000): 373-378.

[65] Yazawa, Y., H. Yoshida, N. Takagi, S.I. Komai, A. Satsuma and T. Hattori. Oxidation state of palladium as a factor controlling catalytic activity of Pd/SiO_2-Al_2O_3 in propane combustion. Applied Catalysis B: Environmental 19 (1998): 261-266.

[66] Avila, M.S., C.I. Vignatti, C.R. Apesteguìa, V. Venkat Rao, K. Chary and T.F. Garetto. Effect of V_2O_5 loading on propane combustion over Pt/V_2O_5-Al2O3 catalysts. Catalysis Letters 134 (2010): 118-123.

[67] Lee, A.F., K. Wilson, R.M. Lambert, C.P. Hubbard, R.G. Hurley, R.W. McCabe, et al. The origin of SO_2 promotion of propane oxidation over Pt/Al_2O_3 catalysts. Journal of Catalysis 184 (1999): 491-498.

[68] Hinz, A., M. Skoglundh, E. Fridell and A. Andersson. An investigation of the reaction mechanism for the promotion of propane oxidation over Pt/Al2O3 by SO_2. Journal of Catalysis 201 (2001): 247-257.

[69] Hubbard, C.P., K. Otto, H.S. Gandhi and K.Y.S. Ng. Effects of Support Material and Sulfation on Propane Oxidation Activity over Platinum. Journal of Catalysis 144 (1993): 484-494.

[70] Burch, R., E. Halpin, M. Hayes, K. Ruth and J.A. Sullivan. The nature of activity enhancement for propane oxidation over supported Pt catalysts exposed to sulphur dioxide. Applied Catalysis B: Environmental 19 (1998): 199-207.

[71] Solsona, B., T.E. Davies, T. Garcia, I. V√°zquez, A. Dejoz and S.H. Taylor. Total oxidation of propane using nanocrystalline cobalt oxide and supported cobalt oxide catalysts. Applied Catalysis B: Environmental 84 (2008): 176-184.

[72] Jones, C., K.J. Cole, S.H. Taylor, M.J. Crudace and G.J. Hutchings. Copper manganese oxide catalysts for ambient temperature carbon monoxide oxidation: Effect of calcination on activity. Journal of Molecular Catalysis A: Chemical 305 (2009): 121-124.

[73] Morales, M.a.R., B.P. Barbero and L.E. Cadùs. Total oxidation of ethanol and propane over Mn-Cu mixed oxide catalysts. Applied Catalysis B: Environmental 67 (2006): 229-236.

[74] Lahousse, C., A. Bernier, P. Grange, B. Delmon, P. Papaefthimiou, T. Ioannides, et al. Evaluation of γ -MnO_2as a VOC Removal Catalyst: Comparison with a Noble Metal Catalyst. Journal of Catalysis 178 (1998): 214-225.

[75] Vayenas, C.G. Bridging electrochemistry and heterogeneous catalysis. Journal of Solid State Electrochemistry (2011): 1-11.

[76] Billiard, A. and P. Vernoux. Influence of the thickness of sputter-deposited platinum films on the electrochemical promotion of propane combustion. Ionics 11 (2005): 126-131.

[77] Ackelid, U.O., L.; Petersson, L.G. Ethylene oxidation on polycrystalline platinum over eight orders of magnitude in ethylene pressure: A kinetic study in the viscous pressure regime. Journal of Catalysis 161 (1996): 143-155.

[78] C.G. Vayenas, B.L., J. Michaels. Kinetics, Limit Cycles and Mechanism of Ethylene Oxidation on Pt. Journal of Catalysis 66 (1980): 36-48.

[79] C.G. Vayenas, C.G., J. Michaels and J. Tormo. The role of PtO_x in the isothermal rate and oxygen activity oscillations of the Ethylene Oxidation on Pt. Journal of Catalysis 67 (1981): 348-361.

[80] Bebelis, S. and C.G. Vayenas. Non-faradaic electrochemical modification of catalytic activity. 1. The case of ethylene oxidation on Pt. Journal of Catalysis 118 (1989): 125-146.

[81] Marwood, M. and C.G. Vayenas. Electrochemical promotion of a dispersed platinum catalyst. Journal of Catalysis 178 (1998): 429-440.

[82] Koutsodontis, C., A. Katsaounis, J.C. Figueroa, C. Cavalca, C.J. Pereira and C.G. Vayenas. The effect of catalyst film thickness on the magnitude of the electrochemical promotion of catalytic reactions. Topics in Catalysis 38 (2006): 157-167.

[83] Koutsodontis, C., A. Katsaounis, J.C. Figueroa, C. Cavalca, C. Pereira and C.G. Vayenas. The effect of catalyst film thickness on the electrochemical promotion of ethylene oxidation on Pt. Topics in Catalysis 39 (2006): 97-100.

[84] Athanasiou, C., G. Marnellos, P. Tsiakaras and M. Stoukides. Catalytic and electrocatalytic oxidation of methane on palladium electrodes in a solid electrolyte cell. Ionics 2 (1996): 353-360.

[85] Brosda, S., T. Badas and C.G. Vayenas. Study of the Mechanism of the Electrochemical Promotion of Rh/YSZ Catalysts for C_2H_4 Oxidation Via AC Impedance Spectroscopy. Topics in Catalysis (2011): 1-10.

[86] Tsiplakides, D., S. Neophytides and C.G. Vayenas. Investigation of electrochemical promotion using temperature-programmed desorption and work function measurements. Solid State Ionics 136-137 (2000): 839-847.

[87] Archonta, D., A. Frantzis, D. Tsiplakides and C.G. Vayenas. STM observation of the origin of electrochemical promotion on metal catalyst-electrodes interfaced with YSZ and β''-Al_2O_3. Solid State Ionics 177 (2006): 2221-2225.

[88] Vernoux, P., F. Gaillard, L. Bultel, E. Siebert and M. Primet. Electrochemical promotion of propane and propene oxidation on Pt/YSZ. Journal of Catalysis 208 (2002): 412-421.

[89] Bultel, L., C. Roux, E. Siebert, P. Vernoux and F. Gaillard. Electrochemical characterisation of the Pt/YSZ interface exposed to a reactive gas phase. Solid State Ionics 166 (2004): 183-189.

[90] Kotsionopoulos, N. and S. Bebelis. In situ electrochemical modification of catalytic activity for propane combustion of Pt/β''-Al_2O_3 catalyst-electrodes. Topics in Catalysis 44 (2007): 379-389.

[91] Kotsionopoulos, N. and S. Bebelis. Electrochemical characterization of the Pt/β''-Al_2O_3 system under conditions of in situ electrochemical modification of catalytic activity for propane combustion. Journal of Applied Electrochemistry 40 (2010): 1883-1891.

[92] Souentie, S., C. Xia, C. Falgairette, Y.D. Li and C. Comninellis. Investigation of the "permanent" electrochemical promotion of catalysis (P-EPOC) by electrochemical mass spectrometry (EMS) measurements. Electrochemistry Communications 12 (2010): 323-326.

[93] Falgairette, C., A. Jaccoud, G. Fóti and C. Comninellis. The phenomenon of "permanent" electrochemical promotion of catalysis (P-EPOC). Journal of Applied Electrochemistry 38 (2008): 1075-1082.

[94] Nicole, J. and C. Comninellis. Electrochemical promotion of oxide catalyst for the gas phase combustion of ethylene. Solid State Ionics 136-137 (2000): 687-692.

[95] Papaioannou, E.I., S. Souentie, F.M. Sapountzi, A. Hammad, D. Labou, S. Brosda, et al. The role of TiO_2 layers deposited on YSZ on the electrochemical promotion of C_2H_4 oxidation on Pt. Journal of Applied Electrochemistry 40 (2010): 1859-1865.

[96] Baranova, E.A., G. Foti and C. Comninellis. Current-assisted activation of Rh/TiO_2/YSZ catalyst. Electrochemistry Communications 6 (2004): 389-394.

[97] Poulidi, D. and I.S. Metcalfe. Electrochemical promotion of a metal catalyst supported on a mixed-ionic conductor. Solid State Ionics 177 (2006): 2211-2215.

[98] Makri, M., A. Buekenhoudt, J. Luyten and C.G. Vayenas. Non-faradaic electrochemical modification of the catalytic activity of Pt using a $CaZr_{0.9}In_{0.1}O_{3-a}$ proton conductor. Ionics 2 (1996): 282-288.

[99] Balomenou, S., G. Pitselis, D. Polydoros, A. Giannikos, A. Vradis, A. Frenzel, et al. Electrochemical promotion of Pd, Fe and distributed Pt catalyst-electrodes. Solid State Ionics 136-137 (2000): 857-862.

[100] Gaillard, F. and N. Li. Electrochemical promotion of toluene combustion on an inexpensive metallic catalyst. Catalysis Today 146 (2009): 345-350.

[101] Li, N. and F. Gaillard. Catalytic combustion of toluene over electrochemically promoted Ag catalyst. Applied Catalysis B: Environmental 88 (2009): 152-159.

[102] Yentekakis, I.V. and C.G. Vayenas. The effect of electrochemical oxygen pumping on the steady-state and oscillatory behavior of CO oxidation on polycrystalline Pt. Journal of Catalysis 111 (1988): 170-188.

[103] Karavasilis C., B.S.a.V.C.G. NEMCA: The Oxidation of CO on Ag. Materials Science Forum 76 (1991): 175-178.

[104] Politova T.I., G.v.G.G., Belyaev V.D. and Sobyanin V.A. Non-Faradaic catalysis: the case of CO oxidation over Ag-Pd alloy electrode in a solid oxide electrolyte cell. Catalysis Letters 44 (1997): 75-81.

[105] Pekridis, G., K. Kalimeri, N. Kaklidis, E. Vakouftsi, E.F. Iliopoulou, C. Athanasiou, et al. Study of the reverse water gas shift (RWGS) reaction over Pt in a solid oxide fuel cell (SOFC) operating under open and closed-circuit conditions. Catalysis Today 127 (2007): 337-346.

[106] Karagiannakis, G., S. Zisekas and M. Stoukides. Hydrogenation of carbon dioxide on copper in a H^+ conducting membrane-reactor. Solid State Ionics 162-163 (2003): 313-318.

[107] Bebelis, S., H. Karasali and C.G. Vayenas. Electrochemical promotion of the CO_2 hydrogenation on Pd/YSZ and Pd/ β''-Al_2O_3 catalyst-electrodes. Solid State Ionics 179 (2008): 1391-1395.

[108] Karavasilis, C., S. Bebelis and C.G. Vayenas. In situ controlled promotion of catalyst surfaces via NEMCA: The effect of Na on the Ag-catalyzed ethylene epoxidation in the presence of chlorine moderators. Journal of Catalysis 160 (1996): 205-213.

[109] Karavasilis, C., S. Bebelis and C.G. Vayenas. Non-faradaic electrochemical modification of catalytic activity: X. Ethylene epoxidation on Ag deposited on stabilized ZrO_2 in the presence of chlorine moderators. Journal of Catalysis 160 (1996): 190-204.

[110] Tsiakaras, P.E., S.L. Douvartzides, A.K. Demin and V.A. Sobyanin. The oxidation of ethanol over Pt catalyst-electrodes deposited on ZrO_2 (8 mol% Y_2O_3). Solid State Ionics 152-153 (2002): 721-726.

[111] Pliangos, C., C. Raptis, T. Badas and C.G. Vayenas. Electrochemical promotion of NO reduction by C_3H_6 on Rh/YSZ catalyst-electrodes. Solid State Ionics 136-137 (2000): 767-773.

[112] Pliangos, C., C. Raptis, T. Badas and C.G. Vayenas. Electrochemical promotion of NO reduction by C_3H_6 and CO on Rh/YSZ catalyst-Electrodes. Ionics 6 (2000): 119-126.

[113] Williams, F.J., N. Macleod, M.S. Tikhov and R.M. Lambert. Electrochemical promotion of bimetallic Rh-Ag/YSZ catalysts for the reduction of NO under lean burn conditions. Electrochimica Acta 47 (2002): 1259-1265.

[114] Vernoux, P., F. Gaillard, C. Lopez and E. Siebert. Coupling catalysis to electrochemistry: A solution to selective reduction of nitrogen oxides in lean-burn engine exhausts Journal of Catalysis 217 (2003): 203-208.

[115] Lintanf, A., E. Djurado and P. Vernoux. Pt/YSZ electrochemical catalysts prepared by electrostatic spray deposition for selective catalytic reduction of NO by C_3H_6. Solid State Ionics 178 (2008): 1998-2008.

[116] Dorado, F., A. de Lucas-Consuegra, C. Jiménez and J.L. Valverde. Influence of the reaction temperature on the electrochemical promoted catalytic behaviour of platinum impregnated catalysts for the reduction of nitrogen oxides under lean burn conditions. Applied Catalysis A: General 321 (2007): 86-92.

[117] Dorado, F., A. de Lucas-Consuegra, P. Vernoux and J.L. Valverde. Electrochemical promotion of platinum impregnated catalyst for the selective catalytic reduction of NO by propene in presence of oxygen. Applied Catalysis B: Environmental 73 (2007): 42-50.

[118] de Lucas-Consuegra, A., F. Dorado, C. Jiménez-Borja and J.L. Valverde. Influence of the reaction conditions on the electrochemical promotion by potassium for the selective catalytic reduction of N_2O by C_3H_6 on platinum. Applied Catalysis B: Environmental 78 (2008): 222-231.

[119] Katsaounis, A. Electrochemical promotion of catalysis (EPOC) perspectives for application to gas emissions treatment. Global NEST Journal 10 (2008): 226-236.

[120] Alqahtany, H., P.-H. Chiang, D. Eng, M. Stoukides and A. Robbat, Jr. Electrocatalytic decomposition of hydrogen sulfide. Catalysis Letters 13 (1992): 289-295.

[121] Petrolekas, P.D., S. Brosda and C.G. Vayenas. Electrochemical promotion of Pt catalyst electrodes deposited on $Na_3Zr_2Si_2PO_{12}$ during ethylene oxidation. Journal of the Electrochemical Society 145 (1998): 1469-1477.

[122] Yentekakis, I.V. and S. Bebelis. Study of the NEMCA effect in a single-pellet catalytic reactor. Journal of Catalysis 137 (1992): 278-283.

[123] Brosda, S., C.G. Vayenas and J. Wei. Rules of chemical promotion. Applied Catalysis B: Environmental 68 (2006): 109-124.

[124] Lizarraga, L., S. Souentie, L. Mazri, A. Billard and P. Vernoux. Investigation of the CO oxidation rate oscillations using electrochemical promotion of catalysis over sputtered-Pt films interfaced with YSZ. Electrochemistry Communications 12 (2010): 1310-1313.

[125] Tauster, S.J. Strong metal-support interactions. Accounts of Chemical Research 20 (1987): 389-394.

[126] Nicole, J., D. Tsiplakides, C. Pliangos, X.E. Verykios, C. Comninellis and C.G. Vayenas. Electrochemical Promotion and Metal‚ÄìSupport Interactions. Journal of Catalysis 204 (2001): 23-34.

[127] Schwartz, A., L.L. Holbrook and H. Wise. Catalytic oxidation studies with platinum and palladium. Journal of Catalysis 21 (1971): 199-207.

[128] Yiokari, K. and S. Bebelis. In situ controlled electrochemical promotion of catalyst surfaces: Pd-catalysed ethylene oxidation. Journal of Applied Electrochemistry 30 (2000): 1277-1283.

APPENDICES

APPENDIX A
CALCULATION FOR ETHYLENE AND PROPANE OXIDATION CONVERSION

A1. The overall reaction of ethylene oxidation can be represented by

$$C_2H_4 + 3O_2 \rightarrow 2CO_2 + 2H_2O \quad (A.1)$$

The ethylene conversion corresponding to CO_2 was defined as:

$$C_2H_4 \text{ conversion} = \frac{y^{in}_{C_2H_4} - y^{out}_{C_2H_4}}{y^{in}_{C_2H_4}} \times 100 \quad (A.2)$$

Where $y^{in}_{C_2H_4}$ and $y^{out}_{C_2H_4}$ are the mole fractions of C_2H_4 inlet and outlet, respectively.

Or we can compute by

$$C_2H_4 \text{ conversion} = \frac{2P_{CO_2}}{P_{C_2H_4} - 2P_{CO_2}} \times 100 \quad (A.3)$$

Where P_{CO_2} and $P_{C_2H_4}$ are the partial pressures of CO_2 and C_2H_4, respectively.

A2. The overall reaction of propane oxidation can be represented by

$$C_3H_8 + 5O_2 \rightarrow 3CO_2 + 4H_2O \quad (A.4)$$

The propane conversion corresponding to CO_2 was defined as:

$$C_3H_8 \text{ conversion} = \frac{y^{in}_{C_3H_8} - y^{out}_{C_3H_8}}{y^{in}_{C_3H_8}} \times 100 \quad (A.5)$$

Where $y^{in}_{C_3H_8}$ and $y^{out}_{C_3H_8}$ are representative the mole fractions of C_3H_8 inlet and outlet, respectively.

Or we can compute by

$$C_3H_8 \text{ conversion} = \frac{P_{CO_2}}{P_{CO_2} + 3P_{C_3H_8}} \times 100 \quad (A.6)$$

Where P_{CO_2} and $P_{C_3H_8}$ are the partial pressures of CO_2 and C_3H_8, respectively.

APPENDIX B
RATE OF CO_2 FORMATION CALCUALTION

The rate of CO_2 formation is defined as

$$r_{CO_2}=y_{CO_2}\times G \qquad \text{expressed in mol /s} \tag{B.1}$$

$$G=\frac{F(\,{}^{cm^3}/_{min})}{22400(\,{}^{cm^3}/_{mol})\times 60(\,{}^{s}/_{min})}$$

B1. In the case of ethylene oxidation

The overall reaction of ethylene oxidation can be represented by

$$C_2H_4+ 3O_2 \rightarrow 2CO_2+ 2H_2O \tag{B.3}$$

Therefore, the rate of CO_2 formation, expressed in molO/s, is defined by

$$r_{CO_2}=3 \times y_{CO_2}\times G \qquad \text{expressed in mol O/s} \tag{B.4}$$

B2. In the case of propane oxidation

The overall reaction of propane oxidation can be represented by

$$C_3H_8+ 5O_2 \rightarrow 3CO_2+ 4H_2O \tag{B.5}$$

Therefore, the rate of CO_2 formation, expressed in molO/s, is defined by

$$r_{CO_2}={}^{10}/_{3} \times y_{CO_2}\times G \qquad \text{expressed in mol O/s} \tag{B.6}$$

For example,

In case of propane oxidation

Obtained, CO_2 = 180 ppm under volumetric flow rate = 170 cm^3min^{-1}

So, $y_{CO_2} = 180 / 10^6 = 1.8 \times 10^{-4}$

Substitution all these value into Eq. B.2, gives

$$G=\frac{170(\,{}^{cm^3}/_{min}\,)}{22400(\,{}^{cm^3}/_{mol}\,)\times 60(\,{}^{s}/_{min}\,)}$$

$$G=1.26 \times \cdot 10^{-4}\ mol\cdot s^{-1}$$

From, $r_{CO_2}={}^{10}/_{3} \times y_{CO_2} \times G$ expressed in mol O/s

$r_{CO_2}={}^{10}/_{3} \times 1.8 \times 10^{-4} \times 1.26 \times 10^{-4}$ mol O/s

$r_{CO_2}= 7.56 \times 10^{-8}$ mol O/s

Therefore, the rate of CO_2 formation is 7.56×10^{-8} molO/s

APPENDIX C
OVERPOTENTIAL CALCUALTION

The cell overpotential is defined as,

$$\eta = U_{WR}-U_{OC} -IR_{ohmic} \quad (C.1)$$

Where U_{WR} is applied potential difference

U_{OC} is the open circuit (I=0) value of the potential difference

I is the applied current

R_{ohmic} is a resistance of the electrolyte between the working and counter electrodes.

The ohmic overpotential (IR_{ohmic}) is sometimes also negligible, provided that the catalyst electrode is sufficiently conductive.

Again for the cell over potential is possible to defined as,

$$\eta = U_{WR}-U_{OC} \quad (C.2)$$

Where U_{WR} is the working-reference overpotential

U_{OC} is the open circuit (I=0) value of the potential difference

APPENDIX D
THE RATE ENHANCEMENT RATIO CALCULATION

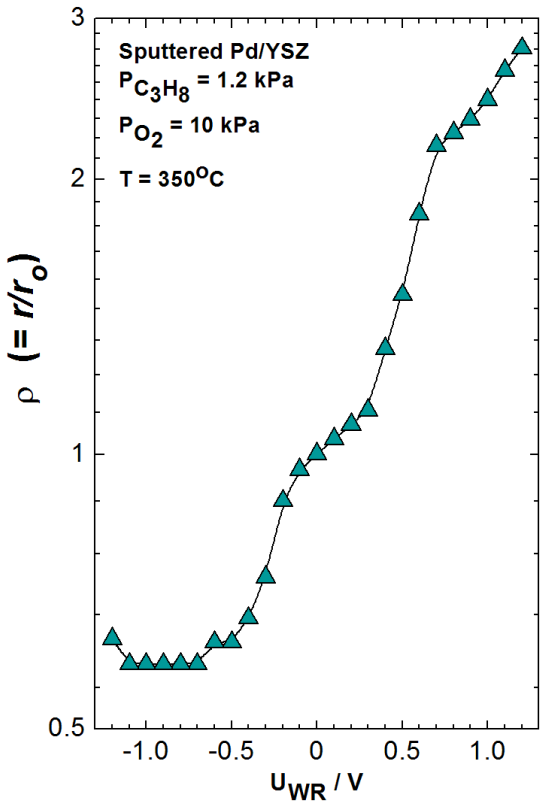

Figure D1 Steady-state effect of applied potential on the electrochemically promoted propane oxidation at 350°C on the rate enhancement ratio, ρ. Operating coditions as shown in figure

The rate enhancement ratio, ρ, is defined as

$$\rho = \frac{r}{r_0} \tag{D.1}$$

Where r_0 is the catalytic rate under open circuit condition (I=0)

r is the catalytic rate under closed circuit condition

For example,

At open circuit, $I = 0$, $r_0 = 7.56 \times 10^{-8}$ molO s^{-1}

At $U_{WR} = 1.2$ V, $r = 2.10 \times 10^{-7}$ molO s^{-1}

The rate enhancement ratio is computed from eq. D.1 as,

$$\text{So,} \quad \rho = \frac{2.1 \times 10^{-7}}{7.56 \times 10^{-8}} \text{ molO} \cdot s^{-1}$$

$$\rho = 2.7$$

Therefore, the rate enhancement ratio, ρ, is 2.7.

APPENDIX E
THE FARADAIC EFFICIENCY CALCULATION

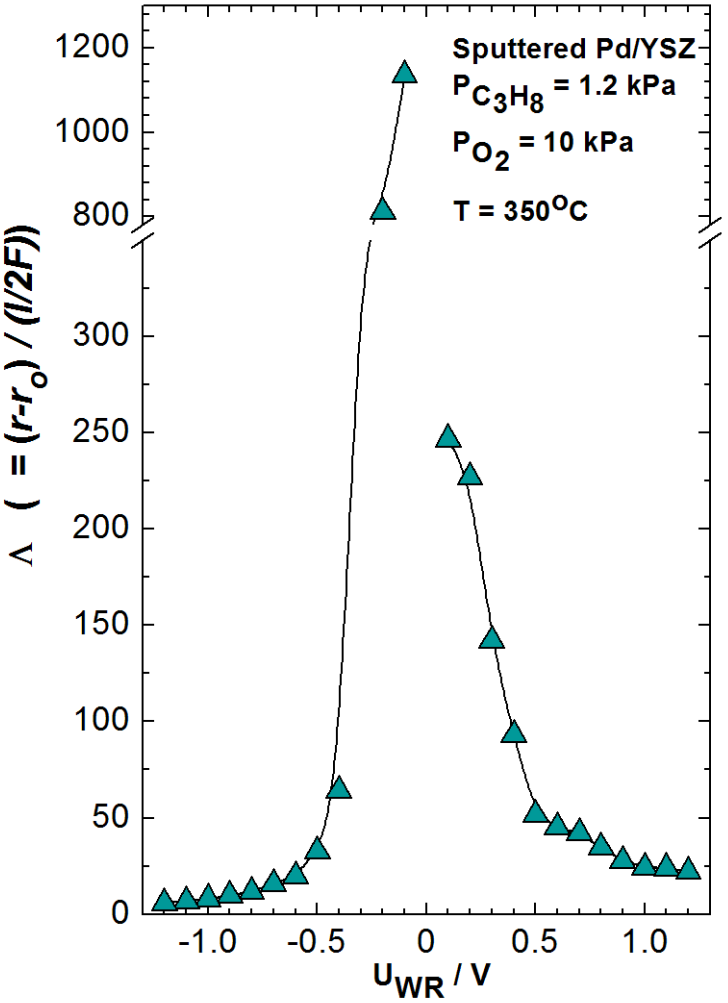

Figure E1 Steady-state effect of applied potential on the electrochemically promoted propane oxidation at 350°C on the Faradaic efficiency, Λ. Operating conditions as shown in figure

The Faradaic efficiency or enhancement factor, Λ, defined as

$$\Lambda = \frac{\Delta r}{I/nF} \qquad \text{(E.1)}$$

Where Δr is the change in Faradaic reaction rate

I is the applied current

n is the ion charge that can be up to 3×10^{5} or down to -10^{4}

F is faraday's constant, 96500 s A / mol

For example,

At open circuit, $I = 0$, $r_0 = 7.56 \times 10^{-8}$ molO s^{-1}

At $U_{WR} = 0.1$ V, $I = 2.3\times 10^{-6}$ A and $r = 7.85 \times 10^{-8}$ molO s^{-1}

The Faradaic efficiency is computed from eq. E.1 as,

$$\Lambda = \frac{\left(7.85 \times 10^{-8}\right) - \left(7.56 \times 10^{-8}\right) \text{molO}\cdot\text{s}^{-1}}{\left(2.3 \times 10^{-6}\right) \text{A} \Big/ 2\times 96500 \text{ s}\cdot\text{A}\cdot\text{mol}^{-1}}$$

$$\Lambda = 246.67$$

Therefore, Faradaic efficiency, Λ, is 246.67.

APPENDIX F
THE SURFACE METAL CATALYST CALCULATION

The relaxation time constant, τ, during galvanostatic transient is defined as

$$\tau = \frac{2FN_G}{I} \qquad \text{(F.1)}$$

Where, the term of $\frac{2FN_G}{I}$ stands for the time required for 63% rate of the steady state value meant the time required to form a monolayer of O on a surface film and N_G is the surface metal catalyst expressed in moles of metal.

For example,

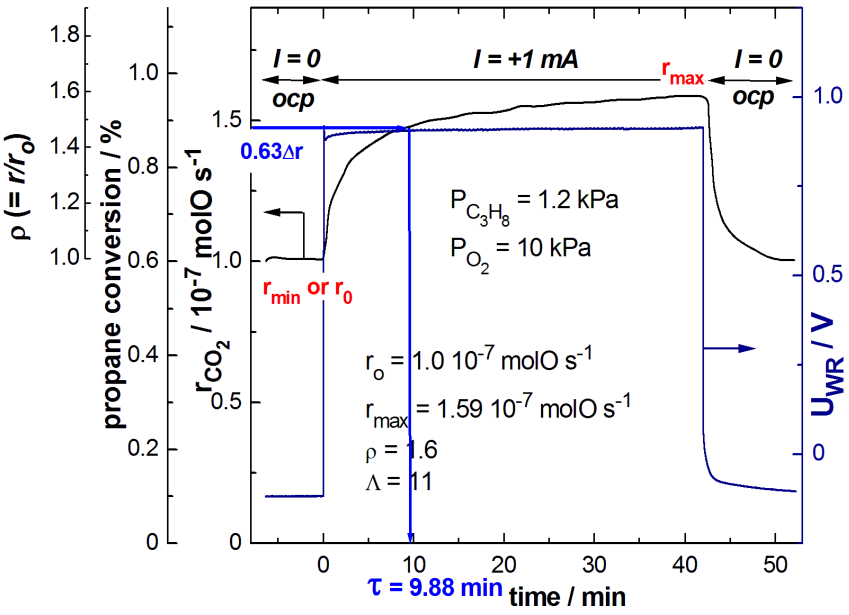

Figure F1 Rate of CO_2 formation, r_{CO_2}, and catalyst potential, U_{WR}, corresponds to in an applied positive current of 1 mA at T = 350°C, (a) $P_{C_3H_8}$ = 1.2 kPa, P_{O_2} = 10 kPa, F_v = 170 cm^3min^{-1} (STP). Catalyst: Sputtered Pd catalyst-electrode deposited on YSZ

From figure F1,

$r_0 = 1.0 \times 10^{-7}$ mol O/s

$r_{max} = 1.58 \times 10^{-7}$ mol O/s

$\Delta r = 0.58 \times 10^{-7}$ mol O/s

$0.63\Delta r = 0.37 \times 10^{-7}$ mol O/s

r at 63%$= \left(1.0 \times 10^{-7}\right) + \left(0.37 \times 10^{-7}\right) = 1.37 \times 10^{-7}$ mol O/s

From 63% rate of the steady state value, one can read the relaxation time constant, τ from this figure, $\tau = 9.88$ min

Substitution of the above terms into eq. F.1 gives,

$$9.88 \times 60 \text{ s} = \frac{2 \times 96485 \text{ s·A·mol} \times N_G}{1 \times 10^{-3} \text{ A}}$$

$$N_G = 1.1 \times 10^{-6} \text{ molO}$$

Assuming a 1:1 surface Pd:O ratio,

The metal active site on surface metal catalyst, N_G, is approximately 1.1×10^{-7} mol Pd.

From $m_{Pd} = 0.8$ mg (weighting)

$MW_{Pd} = 106.42$ g.mol^{-1}

$$\text{mol}_{Pd} = 0.8 \text{ mg} \times {}^{1\text{g}}/_{1000 \text{ mg}} \times {}^{1 \text{ mol}}/_{106.42 \text{ g}}$$

$\text{mol}_{Pd} = 7.52 \times 10^{-6}$ molPd

Therefore, the true surface area is roughly 7.5×10^{-7} mol Pd.

Finally, the percent of Pd dispersion is calculated by

$$\% \text{ dispersion} = \frac{N_G}{\text{True surface area}} \qquad \text{(F.2)}$$

Substitution of those values into this eq. F.2 gives finally,

$$\% \text{ dispersion} = \frac{1.1 \times 10^{-6} \text{ molPd}}{7.52 \times 10^{-6} \text{ molPd}}$$

$$\% \text{ dispersion} \approx 13$$

The percent of Pd dispersion is approximately 13%, which is similar order of magnitude to the previous study [43, 81].

In summary, Pd : N_G, was found to be approximately 1.1×10^{-7} mol Pd.

Ir : N_G was approximately 7.46×10^{-7} mol Ir ($5.58\text{-}8.7 \times 10^{-7}$ mol Ir)

Ru : N_G was approximately 2.86×10^{-6} mol Ru

APPENDIX G
ACTIVATION ENERGY CALCUALTION

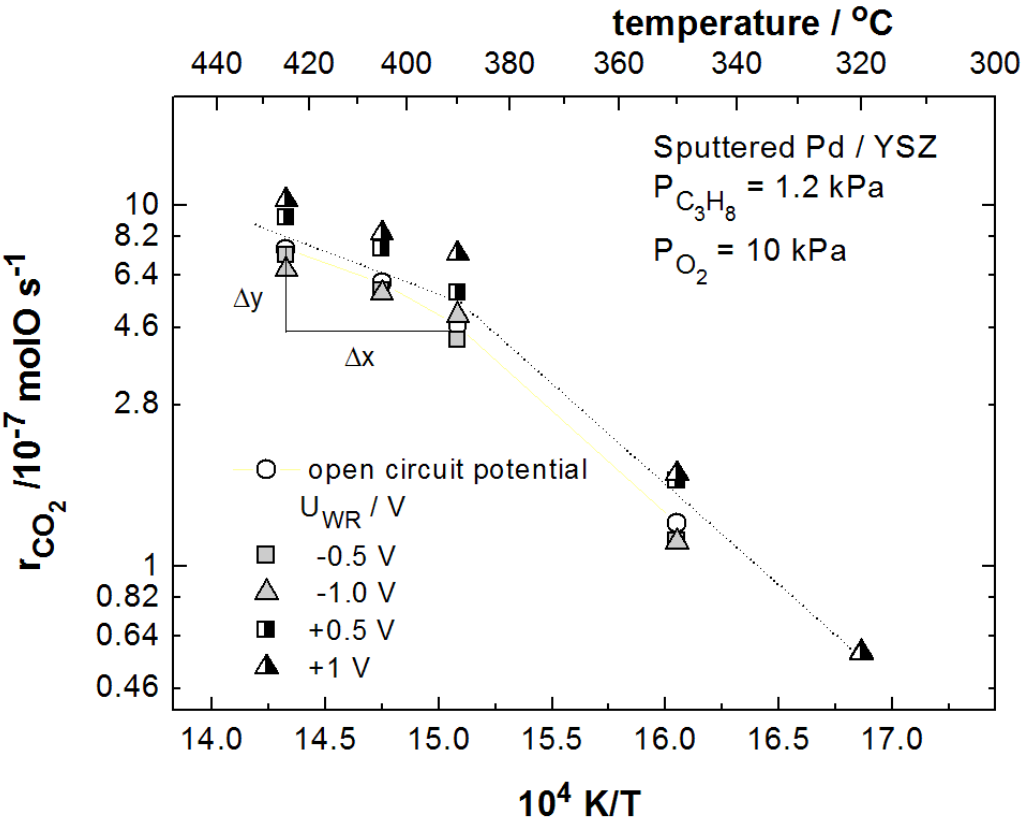

Figure G1 Steady-state effect of temperature on rate of CO_2 formation under closed and open circuit conditions for Pd/YSZ. Condition: $P_{C_3H_8}$ = 1.2 kPa, P_{O_2} = 10 kPa, and F_v = 170 cm^3min^{-1} (STP)

From $-E_A/R$ = slope of r_{CO_2} vesus 1/T (as shown in figure F1)

$= \Delta y/ \Delta x$

Where R is gas constant, R = 8.314 $J\,K^{-1}\,mol^{-1}$

For example,

In the case of Pd/YSZ, as shown in figure F1

First compute the slope in high temperature region,

$$\text{Slope} = \frac{\Delta y}{\Delta x}$$

$$= \frac{\ln(8.01\times10^{-7})-\ln(5.24\times10^{-7})}{(15.09-14.33)\times10^{-4}}$$

$$=-5{,}583.8\ \text{K}$$

So, $$-\frac{E_A}{R} = -5{,}583.8\ \text{K}$$

With $R = 8.314\ \text{J K}^{-1}\ \text{mol}^{-1}$

$$E_A = 5{,}583.8\ \text{K} \times 8.314\ \frac{\text{J}}{\text{mol K}}$$

$$E_A = 46{,}420\ \frac{\text{J}}{\text{mol}}$$

$$E_A = 46.42\ \frac{\text{kJ}}{\text{mol}}$$

Therefore, the apparent activation energy, E_A, as calculated from above procedure is approximately 50 kJ/mol

APPENDIX H
SOLID ELECTROLYTE CONDUCTIVITY CALCULATION

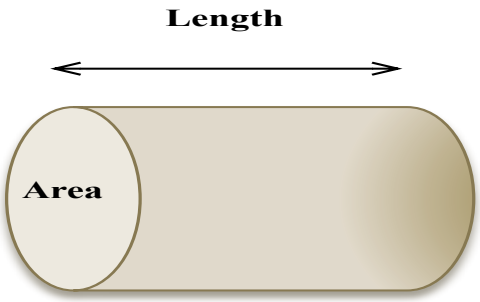

Figure H1 A cylindrical shape

$$R=\frac{\rho L}{A} \quad \text{(H.1)}$$

$$\rho=\frac{RA}{L} \quad \text{(H.2)}$$

$$\sigma=\frac{1}{\rho} \quad \text{(H.3)}$$

Where R is resistance of solid electrolyte between working and counter electrodes, Ω

A is cross section area of sample, cm^2

L is the length of sample, cm

ρ is electrical resistivity, Ω. cm

σ is conductance, Ω^{-1}. cm^{-1}

For example,

Pd/YSZ at 320^{o}C, A = 1.88 cm^{-2}, and L=0.2 cm

From the AC impedance measurement, R = 1200 Ω

According to eq. H.2, the electrical resistivity can compute as,

$$\rho=\frac{1200\ \Omega\times 1.88\ \text{cm}^2}{0.1\ \text{cm}}$$

$$\rho=11280\ \Omega.\text{cm}$$

From eq. H.3, we can now calculate conductivity, σ, as

$$\sigma=\frac{1}{11280}\Omega^{-1}\text{cm}^{-1}$$

$$\sigma=8.9\times 10^{-5}\Omega^{-1}\text{cm}^{-1}$$

Therefore, the conductivity is $8.9 \times 10^{-5}\ \Omega^{-1}.\ \text{cm}^{-1}$.

APPENDIX I
CALCULATION FOR MANGANESE OXIDE PREPARATION

Preparation of Mn_xO_y by impregnation method

Reactant: Manganese(II)nitrate hydrate ($Mn(NO_3)_2.xH_2O$ was used as raw material .

Preparation of manganese oxide solution 150 mM as shown in following,

$$C = \frac{n}{V} \qquad (I.1)$$

Where C is concentration of solution

V is volume

n is mole of substrate

Substitution eq. I.1 with above terms as,

$$150 \times 10^{-3} = n / 30 \times 10^{-3}$$

$$n = 4.5 \times 10^{-3} \text{ mol}$$

From MW of $Mn(NO_3)_2.xH_2O$ = 178.95

We can estimate the used weigh of $Mn(NO_3)_2.xH_2O$ by

1 mol of $Mn(NO_3)_2.xH_2O$ = 178.95 g

4.5×10^{-3} mol $Mn(NO_3)_2.xH_2O$ = 0.8 g

Therefore, the 0.8 g of $Mn(NO_3)_2.xH_2O$ was used in this preparation.

Then, a 30 ml of 2-propanol is served as the solvent for this solution because alcohol is easy to evaporate.

Finally, The 150 mM of Manganese oxide solution is obtained.

APPENDIX J

CONDITION OF GAS CHROMATROGRAPHY

The conditions of Gas Chromatography (GC) analysis for this study are provide as following,

Gas analysis of reactants and products was performed by on-line gas chromatography (Shimadzu 14A with thermal conductivity detector, equipped with a Porapak column for separation of C_2H_4, C_3H_8 and CO_2 and a Molecular sieve for the O_2 detection). He was used as the carrier gas as presented in Table J.1

Table J.1 GC analysis condition for ethylene and propane oxidation

Gas Chromatography	Shimadzu A14A
Detector	TCD (Thermal conductivity detector)
Column	Porapak (C_2H_4, C_3H_8 and CO_2) Molecular sieve (O_2)
Carrier gas	He
TCD temperature (^oC)	150
Injector temperature (^oC)	120
Detector temperature (^oC)	138
Column temperature (^oC)	80
Current (mA)	124

APPENDIX K

LIST OF PUBLICATIONS

K1. International publications

(1) "Electrochemical Promotion of Propane and Methane Oxidation on Sputtered Pd Catalyst-Electrodes Deposited on YSZ", by **S. Peng-Ont**, P. Praserthdam, F. Matei, D. Ciuparu, S. Brosda, C.G. Vayenas, *Cat. Lett.* **142** (2012) 1336. (*Impact Factor*: 2.242 (2011))

(2) "Reaction Kinetic-Induced Changes in the Electrochemically Promoted C_2H_4 Oxidation on Pt/YSZ", by **S. Peng-ont**, S. Souentie, S. Assabumrungrat, P. Praserthdam, S. Brosda, C. G. Vayenas, *Cat. Lett.* (2012) Accepted. (*Impact Factor*: 2.242 (2011))

(3) "Electrochemical Promotion of deep Propane Oxidation on Sputtered Pd, Ir, and Ru Catalyst-Electrodes Deposited on YSZ"**,** by **S. Peng-ont**, S. Souentie, S. Assabumrungrat, P. Praserthdam, S. Brosda, C. G. Vayenas, Cat. Lett. (2013) in preparation. (*Impact Factor*: 2.242 (2011))

K2. International conferences

(1) The 15th International Congress on Catalysis, July 1-6, 2012, Munich, Germany. In the topic of *Electrochemical Promotion of Methane and Propane Oxidation on Sputtered Pd Catalyst-Electrodes Deposited on YSZ* by **S. Peng-ont**, F. Matei, D. Ciuparu, S. Assabumrungrat, P. Praserthdam, C. Jiménez-Borja, F. Dorado, J. L. Valverde, S. Brosda, C. G. Vayenas (Poster Presentation).

(2) The 63rd Annual Meeting of the International Society of Electrochemistry, August 19-24, 2012, Prague, Czech Republic. In the topic of *Reactions Kinetics of the Electrochemically Promoted C_2H_4 Oxidation on Pt/YSZ Catalysts* by S. Brosda, S. Souentie**, S. Peng-ont**, P. Praserthdam, C. G. Vayenas (Oral Presentation).

(3) The 7th International Conference on Environmental Catalysis, September 2-6, 2012, Lyon, France.

3.1 In the topic of *Reaction Kinetics of the Electrochemically Promoted C_2H_4 Oxidation on Pt/YSZ Catalysts* by S. Souentie, S. Brosda, **S. Peng-ont**, P. Praserthdam, C.G. Vayenas (Oral Presentation).

3.2 In the topic of *Electrochemical Promotion of C_3H_8 Oxidation on Pd Catalysts Deposited on Yttria-Stabilized Zirconia* by **S. Peng-ont**, S. Souentie, S. Assabumrungrat, P. Praserthdam, S. Brosda, C. G. Vayenas (Poster Presentation).

(4) The 11th European Congress on Catalysis – EuropaCat-XI, September 1-6, 2013, Lyon, France. In the topic of *The role of Mn_xO_y interlayers for Pd catalysts deposited on yttria-stabilized zirconia in the deep oxidation of C_3H_8* by **S. Peng-ont**, S. Souentie, S. Assabumrungrat, P. Praserthdam, S. Brosda, C. G. Vayenas (Oral presentation and the EFECT PhD student awards).

K3. National conferences

(1) The Royal Golden Jubilee Ph.D. Congress XIV (RGJ-Ph.D. Congress XIV), April 5 -7, 2013, Pattaya, Thailand. In the topic of *Electrochemical Promotion of C_3H_8 Oxidation on Pd Catalysts Deposited on Yttria-Stabilized Zirconia* by **S. Peng-ont,** S. Souentie, S. Assabumrungrat, P. Praserthdam, S. Brosda, C. G. Vayenas (Oral Presentation)

VITA

Miss Saranya Peng-ont was born on April 11, 1987 in Suphanburi, Thailand. She graduated high school from Sa-nguanying School, Suphanburi in 2005. She received Bachelor's Degree in Chemical engineering from King Mongkut's University of Technology Thonburi in 2009. She consequently continued studying Doctoral degree of Chemical Engineering, Chulalongkorn University since May 2009 and received Royal Golden Jubilee PhD program Scholarship from Thailand Research Fund (TRF) and Chulalongkorn University. She had collaborated with Professor C.G.Vayenas and finished parts of her research experiment at Electrochemical Promotion of Catalysis (EPOC) laboratory, Department of Chemical Engineering, Faculty of Engineering, University of Patras, Greece from October 1, 2011-September 26, 2012.